LAPPEENRANTA-LAHTI UNIVERSITY OF TECHNOLOGY LUT
LUT School of Engineering Science
Master's Program in Biorefineries

Santtu Onikki

RECOVERY OF SOFTWOOD LIGNOSULPHONATES AND HEMICELLULOSE SUGARS FROM SPENT ORGANOSOLV LIQUOR

Examiners: Professor, D. Sc (Tech) Mari Kallioinen-Mänttäri
M. Sc (Tech) Marko Maukonen

ABSTRACT

Lappeenranta-Lahti University of Technology LUT
LUT School of Engineering Science
Master's Program in Biorefineries

Santtu Onikki

Recovery of Softwood Lignosulphonates and Hemicellulose Sugars from Spent Organosolv Liquor

Master's Thesis
2022
69 pages, 53 figures, 18 tables and 5 attachments

Examiners: Professor, D. Sc (Tech) Mari Kallioinen-Mänttäri
M. Sc (Tech) Marko Maukonen
Supervisors: Ph. D Timo Leskinen, D. Sc (Tech) Ilkka Malinen, M. Sc (Tech) Jussi Lahti

Keywords: lignosulphonate, hemicellulose sugars, membrane filtration

In this thesis, the effect of pH and temperature into membrane filtration of spent organosolv liquor lignosulphonates (LS) and hemicellulose sugars was studied. The effect of filtration conditions was monitored in terms of membrane permeability, selectivity and fouling. Viability of a membrane process was considered on an industrial point of view according to results of laboratory experiments.

The filtration experiments were carried out by using DSS LabStak® M20-0.72 cross-flow unit with a stack of either three, four or seven membranes. The membranes used in experiments were Alfa Laval's GR95PP (2 kDa, PES), UFX5 pHt (4 kDa, PSU), and RC70PP (10 kDa, RCA), Nadir's NP010 (1.0–1.2 kDa, PES), and UH004P (4 kDa, PES), GE membranes/Suez's GE (1 kDa, CPA) and GK (3.5 kDa, TFC PA), and Synder Filtration's NFG (0.6–0.8 kDa, TFC PA). The filtration temperatures were 32, 45 and 60 °C, pH-values 0.88, 4.59, 4.70 and 6.33, filtration pressures 1–4 and 4–16 bar, and cross-flow velocity was 0.8 m s^{-1}.

Membrane permeability seemed to increase with pH and temperature – with PES membranes being the most promising in terms of pH-response. The permeability of NP010 increased almost tenfold at pH 6.33 compared to pH 0.88. In terms of membrane selectivity, the membrane MWCO seemed to affect the results more than pH and temperature. Overall, the best selectivity was achieved with the tightest membranes.

Overall, membrane filtration of spent organosolv liquor's LS and hemicellulose sugars seemed viable. However, due to the trade-off between membrane permeability and selectivity more experimenting is needed so that the process can be optimized.

TIIVISTELMÄ

Lappeenrannan-Lahden teknillinen yliopisto LUT
LUT School of Engineering Science
Master's Program in Biorefineries

Santtu Onikki

Havupuun lignosulfonaattien ja hemiselluloosasokerien talteenotto organosolv-prosessin jäteliemestä

Diplomityö
2022
69 sivua, 53 kuvaa, 18 taulukkoa and 5 liitettä

Tarkastajat: Professori, D. Sc (Tech) Mari Kallioinen-Mänttäri
M. Sc (Tech) Marko Maukonen
Ohjaajat: Ph. D Timo Leskinen, D. Sc (Tech) Ilkka Malinen, M. Sc (Tech) Jussi Lahti

Hakusanat: lignosulfonaatti, hemiselluloosasokerit, membraanierotus

Tässä työssä tarkasteltiin pH:n ja lämpötilan vaikutuksia kuusi-mäntyhakkeen organosolv-prosessin jäteliemen lignosulfonaattien (LS) ja hemiselluloosasokerien kalvosuodatukseen. Suodatusolosuhteiden vaikutuksia tarkasteltiin havainnoimalla kalvojen läpäisy- ja erottelukykyä sekä likaantumista. Kalvoerotusprosessin mielekkyyttä tarkasteltiin tulosten perusteella teollisen tuotannon perspektiivistä.

Suodatuskokeet tehtiin DSS LabStak® M20-0.72 ristivirtaussuodattimella käyttäen yhtaikaisesti joko kolmea-, neljää- tai seitsemää kalvoparia. Kokeissa käytetyt kalvot olivat Alfa Lavalin GR95PP (2 kDa, PES), UFX5 pHt (4 kDa, PSU) ja RC70PP (10 kDa, RCA), Nadirin NP010 (1,0–1,2 kDa, PES) ja UH004P (4 kDa, PES), GE membranes/Suezin GE (1 kDa, CPA) ja GK (3,5 kDa, TFC PA) sekä Synder Filtrationin NFG (0,6–0,8 kDa, TFC PA). Suodatuslämpötilat olivat 32, 45 ja 60 °C, suodatus-pH:t 0,88, 4,59, 4,70 ja 6,33, suodatuspaineet 1–4 tai 4–16 bar ja ristivirtausnopeus oli 0.8 m $s^{-1.}$

Membraanien permeabiliteetti vaikutti yleisesti ottaen paranevan pH:ta ja lämpötilaa nostettaessa – PES-kalvojen reagoidessa parhaiten pH:n nostoon. NP010:n permeabiliteetti nousi likimain kymmenkertaiseksi, kun pH:ta nostettiin arvosta 0,88 arvoon 6,33. Membraanien erottelukyvyn suhteen kalvon katkaisukoko näytti vaikuttavan tuloksiin enemmän kuin pH ja lämpötila. Parhaat retentiot saavutettiin niillä kalvoilla, joiden katkaisukoot olivat pienimmät.

Kaiken kaikkiaan organosolv-prosessin jäteliemen LS:n ja hemiselluloosasokerien membraanierotus vaikutti toteutuskelpoiselta. Kalvon läpäisy- ja erottelukyvyn välisen vaihtokaupan vuoksi lisää kokeita kuitenkin vaaditaan prosessin optimoimiseksi.

PREFACE

I would like to thank my employer, St1 Oy, for making it possible to combine work and studying, and to take the time needed to finish this thesis. I would also like to express my gratitude to Timo Leskinen and Ilkka Malinen from St1 Oy, and Liisa Puro and Mari Raitavuo from LUT School of Engineering Science for their time and efforts during this interesting, yet challenging journey. I am also thankful to Jussi Lahti for the guidance, and Mari Kallioinen-Mänttäri and Marko Maukonen for their efforts, and of course, my friends and family.

My biggest thanks to my wife for all the patience and support, and my deepest apologies to my children for all the missed moments due to the time away from home when carrying out the laboratory experiments.

Hämeenlinna, May 20th, 2022

TABLE OF CONTENTS

APPENDIXES

TABLE OF FIGURES

LIST OF SYMBOLS AND ABBREVIATIONS

A	Absorbance, - or a.u.
A_m	Membrane surface area, m^2
c	Concentration, g L^{-1}
c_f	Concentration of the component in feed, g L^{-1}
c_p	Concentration of the component in permeate, g L^{-1}
J	Permeate flux, kg m^{-2} h^{-1}
l	Optical path length, cm
MRF	Mass reduction factor, -
m_0	initial feed mass, g
m_R	mass of retentate, g
MWCO	Molecular weight cut-off, Da or kDa
m_p	Mass of the permeate, kg
n	Membrane ordinal number, -
n_{tot}	Total number of membranes plus 1, -
PWF_a	pure water flux after filtration, kg m^{-2} h^{-1}
PWF_b	Pure water flux before filtration, kg m^{-2} h^{-1}
PWF_r	Pure water flux return, %
p	Pressure, bar
p_{in}	Inlet pressure, bar
p_{mean}	Mean pressure, bar
p_{out}	Outlet pressure, bar
R_{obs}	Observed retention, %
T	Temperature, °C
t	Time, h
TMP	Transmembrane pressure, bar
W	Wagner unit, bar °C

ATR-FTIR	Attenuated total reflection fourier transform infrared spectroscopy
CAPEX	Capital expenditures
CPA	Composite polyamide
DM	Dry matter
DDF	Discontinuous diafiltration
NF	Nanofiltration
OPEX	Operating expenses
PES	Polyethersulphone
PSU	Polysulphone
RCA	Regenerated cellulose acetate
TFC PA	Thin-film composite polyamide
TOC	Total organic carbon
UF	Ultrafiltration
UV-Vis	Ultraviolet-visible absorption

ε	Extinction coefficient, L g^{-1} cm^{-1}

1 INTRODUCTION

In biorefining, where biomass is turned into bioenergy and biobased products, one of the many feedstocks is inedible lignocellulosic biomass, which consists mainly of cellulose, hemicellulose, and lignin. In commercial biorefining processes, the focus has been mainly in deriving high-value products such as bioethanol and viscose from cellulose whereas lignin has been seen merely as a by-product. (Løhre et al., 2017)

Organosolv pulping aims to liberate cellulose fibers from the complex of lignin and hemicelluloses whereas organosolv fractionating pretreatment takes focus on improving digestibility of cellulose (Zhao et al., 2017). Organosolv process can be catalyzed by using organic or inorganic acid (Shui et al. 2016; Sun and Cheng 2002), e.g., sulphur dioxide (SO_2), which reacts with lignin forming water-soluble lignosulphonates (Iakovlev et al., 2020; Pylkkänen et al., 2015). Membrane separation of the spent organosolv liquor stream could provide means to improve the biorefining process by providing hemicellulose-sugar-rich fraction for e.g., fermentation, and water-soluble lignin. Recovering and valorization of lignin could improve the profitability (especially if sold as a raw material for e.g., chemical industry) and environmental sustainability of both cellulose processing and – more widely – biorefining. Hence, in an industrial point of view there is a clear incentive in finding ways to effectively separate the lignin fraction from the lignocellulosic feedstock. (Olsson, 2006; Gillgren et al. 2017)

In this thesis, membrane filtration of spent organosolv liquor (pretreated using organosolv pretreatment) lignosulphonates and hemicellulose sugars is studied with an aim to gain understanding on the effects of operating conditions (pH and temperature) into membrane permeability and selectivity. Membrane permeability is calculated from the corresponding permeate fluxes monitored, whereas membrane selectivity is monitored by retention factors (R_{obs}) for lignosulphonates, sugars, total organic carbon (TOC) and conductivity. Membrane fouling is monitored by pure water flux return (PWF_r), and by attenuated total reflection fourier transform infrared spectroscopy (ATR-FTIR).

This research is carried out in two steps: literature part and experimental part. Literature part introduces background for the biorefining of lignocellulosic biomass accompanied by an introduction of organosolv process and aspects related to membrane technology. The experimental part, on the other hand, consists of filtration experiments with an aim to: (1) find out the effect of spent liquor pH on membrane separation, (2) find out the effect of spent liquor temperature on the membrane separation, and (3) find out whether further concentration of lignosulphonates seems reasonable or not. By answering these three research questions the viability of membrane filtration of spent organosolv liquor can be assessed in an industrial point of view.

LITERATURE PART

2 LIGNOCELLULOSIC BIOMASS

Lignocellulosic biomass is a non-food feedstock of plant origin that provides a sustainable raw material for advanced biofuel production as opposed to e.g., sugarcane and corn kernels used in first generation biofuel production. The problem with sugarcane and corn kernels is irrigation, fertilizers and pesticides causing ecological problems (Bordonal et al., 2018). Also, the competition with other crops causes inflation in food prices. (Sathitsuksanoh et al., 2010; Agrimi et al., 2012)

Lignocellulosic biomass consists mainly of cellulose, hemicellulose, and lignin with the composition (Table 1) varying by the plant species, age, and stage of growth. In addition to the main building blocks, there is a minor fraction of extractives e.g., waxes, fatty acids, gums, resins, clorophyll, terpenoids and a variety of phenolic substances present in lignocellulosic biomass, acting as metabolic intermediates or energy reserve. (Bajpai, 2016; Mussatto and Dragone, 2016).

Table 1. Chemical composition of some lignocellulosic biomass sources on dry matter basis (modified from Mussatto and Dragone, 2016, p. 6)

Biomass classification	Lignocellulosic biomass type	Celluloce content (%)	Hemicellulose content (%)	Lignin content (%)
Hardwood	Eucalyptus	46.6–50.3	12.7–14.4	26.9–28.2
	Willow	42.4–45.3	20.6–22.9	16.9–18.9
	Oak	40.4	35.9	24.1
Softwood	Pine	42.0–50.0	24.0–27.0	20.0
	Spruce	45.5	22.9	27.9
Agricultural residues	Sugarcane bagasse	31.9–43.4	12.2–25.5	23.1–27.6
	Rice straw	29.2–34.7	23.0–25.9	17.0–19.0
	Wheat straw	25.0–39.0	23.0–33.0	12.0–16.0
	Barley straw	36.0–43.0	24.0–33.0	6.3–9.8
	Barley hull	34.0	36.0	13.8–19.0
	Ray straw	36.0–47.0	19.0–24.5	9.9–24.0
Other	Cellulose sludge	31.4	9.8	15.3
	Waste papers from chemical pulps	60.0–70.0	10.0–20.0	5.0–10.0
	Solid cattle manure	1.6–4.7	1.4–3.3	2.7–5.7

2.1 Cellulose

Cellulose (Figure 1) is the most abundant renewable polymer resource on earth. It is a homopolysaccharide consisting of a chain of cellobioses i.e., two anhydroglucose units linked via β-(1,4)-glycosidic bonds and is found in both crystalline and amorphous forms. (Bajpai, 2016; Fengel and Wegener, 1989) By estimation, an amount of 10^{11}–10^{12} tons of cellulose is synthesized annually by plants via photosynthesis (Heinze et al., 2018).

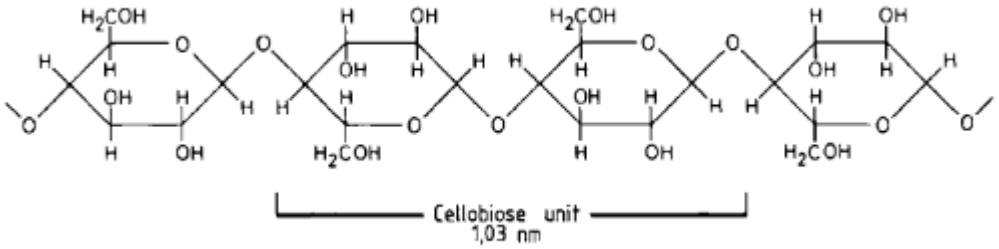

Figure 1. Structure of cellulose and cellobiose (Fengel and Wegener, 1989, p. 68)

The structure of cellulose is strong due to the hydrogen bonds and van der Waal's forces, which cause anhydroglucose units to form elementary fibrils that form further microfibrils (Sathitsuksanoh et al., 2010). Each cellulose molecule comprises of 5,000–10,000 anhydroglucose units, i.e., the degree of polymerization is 5,000–10,000 (Mussatto and Dragone, 2016).

2.2 Hemicellulose

Hemicellulose (Figure 2) is the second most abundant polysaccharide in nature with a degree of polymerization from 100 up to 200 (Heinze et al., 2018). Unlike cellulose, hemicelluloses are chemically heterogenous consisting of varying combinations of pentoses (xylose and arabinose), hexoses (mannose, galactose, and glucose), and sugar acids (Bajpai, 2016). The main hemicelluloses in softwood, are galactoglucomannans and arabinoglucoronoxylans whereas hardwood hemicelluloses consist mainly of glucuronoxylan. (Saha, 2003; Ragauskas and Huang, 2013) The polysaccharides are cleaved into monosaccharides via enzymatic hydrolysis (Arato et al., 2005).

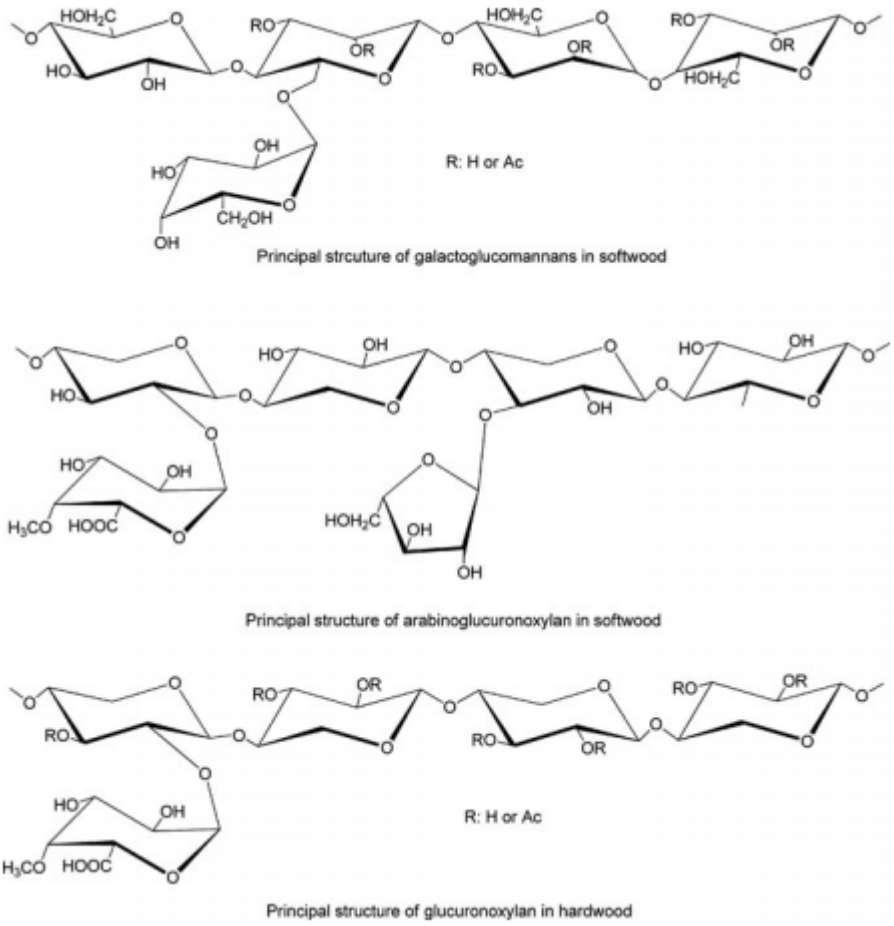

Figure 2. Structure of hemicellulose polysaccharides present in hardwood and softwood (Ragauskas and Huang, 2013, p. 156)

The main chain of hemicellulose is formed by either a homopolymer or a heteropolymer with short branches most often linked by β-(1,4)-glycosidic bonds. The molecular weight of hemicelluloses is lower compared to cellulose and its function within plant cell wall is to coat the cellulose fibrils. In bioprocessing, removal of majority of the thermo-chemically sensitive hemicellulose increases the digestibility of cellulose significantly. Some hemicellulose degradation products e.g., furfurals and hydroxymethylfurfurals, act as inhibitors in fermentation process and formation of such products should be kept at minimum. (Bajpai, 2016)

2.3 Lignin

Lignin, the second most abundant renewable polymer after cellulose (Xu and Ferdosian, 2017), is a three-dimensional, amorphous, and highly complex mainly aromatic polymer with a degree of polymerization up to 10,000 (Cao et al., 2019). In lignocellulosic biomass lignin coats cellulose and hemicellulose and is responsible for the recalcitrance to enzymatic treatment. (Rowell et al., 2005; Mussatto and Dragone, 2016).

Lignin is formed by radical coupling polymerization of three monolignols (Figure 3): *p*-coumaryl alcohol, coniferyl alcohol and sinapyl alcohol with the corresponding monomers being identified as *p*-hydroxyphenyl (H), guaiacyl (G) and syringyl (S) units, respectively (Mussatto and Dragone, 2016; Xu and Ferdosian, 2017). These phenyl-propanols are linked mainly by ether linkages e.g., α-*O*-4, 5-*O*-4 and β-*O*-4, and condensed linkages such as 5-5, β-β, β-5 and β-1. Out of condensed linkages the β-*O*-4 linkage is the predominant one. The composition of lignin varies by the source: softwood lignins are polymerization products of coniferyl alcohol (guaiacyl lignin), hardwood lignins consist mostly of syringyl and guaiacyl units (Rowell et al., 2005), and grass lignin consists of all the three (Mussatto and Dragone, 2016).

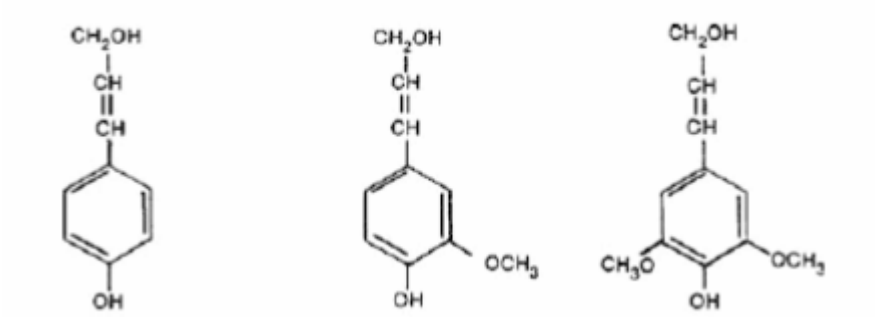

Figure 3. Chemical structures of lignin monomers *p*-coumaryl alcohol, coniferyl alcohol and sinapyl alcohol, respectively (Rowell et al., 2005, p. 44)

Lignin is a by-product in both pulping and lignocellulosic ethanol processes with applications limited mainly for heat and power generation. But lignin, due to its great availability, various functional groups, and other promising characteristics such as biodegradability and antioxidant capability, is also a potential feedstock for the industries producing e.g., chemicals, bio-based materials, and biopolymers. Utilization of lignin could take place in, e.g., the production of bioaromatic chemicals such as vanillin and phenol, carbon fibers or bio-based polymeric materials. Due to the separation method dependent partial degradation of lignin causing changes in molecular weight and polydispersity, different processing (Figure 4) yields different kind of lignin as a product. The technical lignin is conventionally named after the separation or extraction method as either lignosulfonate, Kraft, organosolv or soda lignin. Lignin isolated by insoluble methods, on the other hand, is called Klason or hydrolysis lignin. Lignin can be separated either by dissolution of lignin into a solution or by separating lignin as an insoluble residue after hydrolysis. (Xu and Ferdosian, 2017)

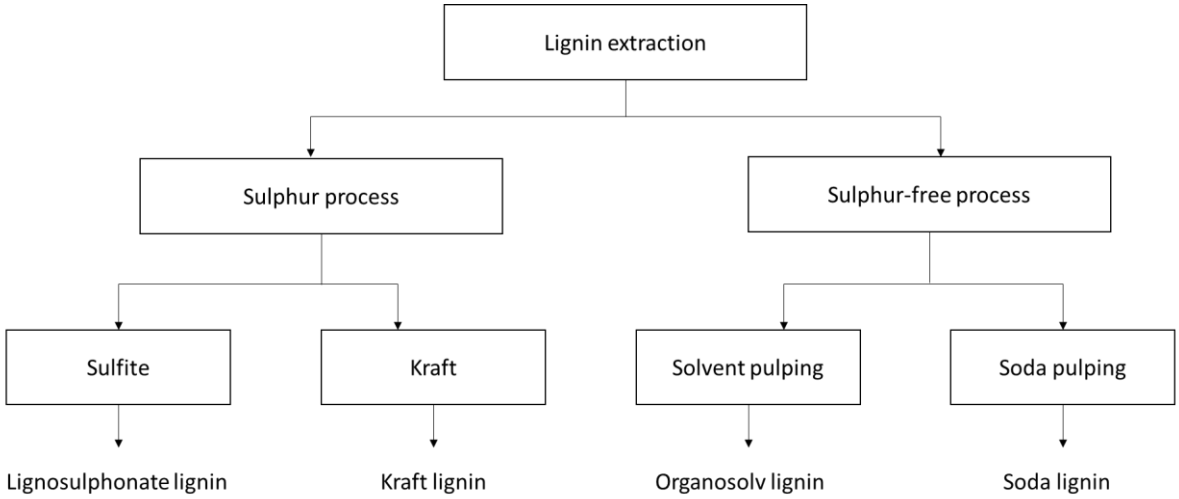

Figure 4. Lignin extraction and corresponding products (modified from Laurichesse and Avérous, 2014, p. 1272)

Valorization of lignin, accounting 15–40 % dry weight in most plants, followed by targeted upgrading could provide a way to improve both economic- and environmental sustainability in biorefineries using lignocellulosic material as a feedstock. Lignin sold as a biofuel does not, according to Olsson et al., (2006), necessarily improve the economics of a biorefinery, but when sold as a raw material for chemical industry lignin could provide a financially meaningful co-product. Utilization of membrane technology could provide means to not only recover lignin but also improve water circulation and decrease chemical consumption if water and chemicals recovered with the membranes were returned to the process (Lipnizki, 2006).

A major challenge for lignin-conversion technologies lays in the complexity and irregularity of the lignin structure and the fact that different fractionation methods provide lignin with different structures and applications (Figure 5). (Cao et al., 2019) For instance, the molecular weight of lignin obtained by soda and Kraft pulping is in the range of 1,000–3,000 Da and 1,000–15,000 Da, respectively, whereas the molecular weight of organosolv lignin is usually in the range of 500–5,000 Da. (Galkin and Samec, 2016).

From an environmental point of view, the organosolv lignin seems preferrable over e.g., Kraft lignin since the organosolv process generates less acid or base waste streams. (Cao et al., 2019) Organosolv lignin can be used as, for example, a phenol substitute whereas lignosulphonates can find a use in e.g., binders and dispersants (Basma et al., 2016; Hongzhang, 2015).

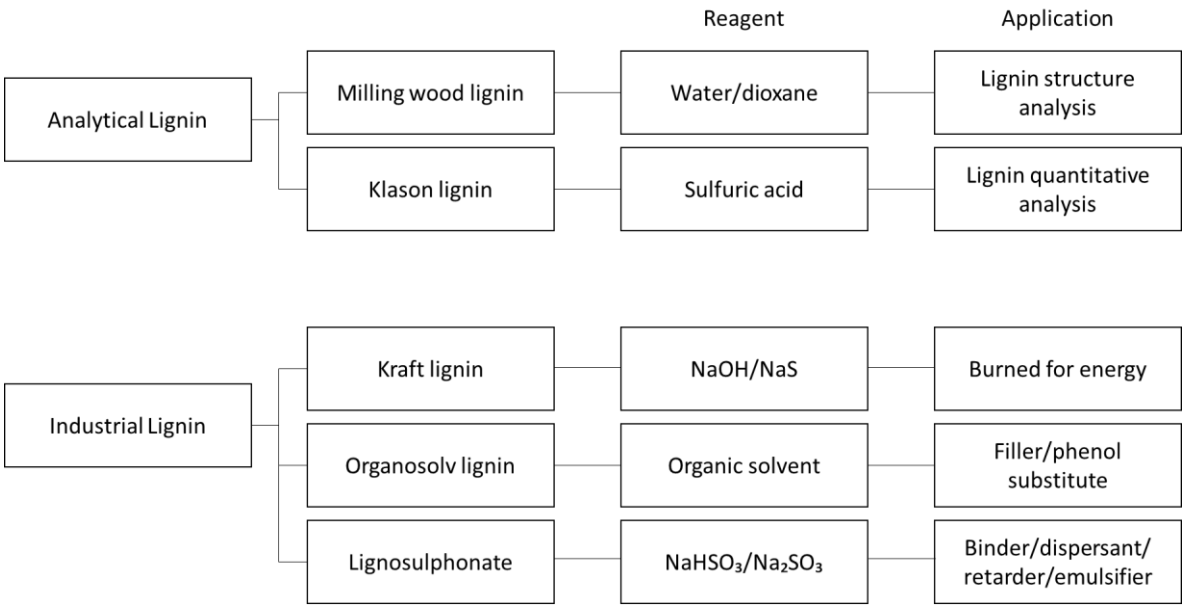

Figure 5. Lignin types, separation reagents and applications (modified from Hongzhang, 2015, p. 77)

2.4 Lignosulphonate

Lignosulphonates or sulphonated lignins are water-soluble polymers with a hydrophobic aromatic structure combined with hydrophilic sulphonate groups. Lignosulphonates are formed in e.g., spent sulfite pulping- and sulphur dioxide utilizing ethanol organosolv process. The pulping processes, depending on the bases used, produce various types of lignosulphonates, such as calcium-, sodium-, magnesium- and ammonium lignosulphonate. (Iakovlev and Heiningen, 2012; Xu and Ferdosian, 2017)

Sulfonated kraft lignins are used in applications similarly to lignosulphonates, but the chemical properties between these two are different: the sulfonic acid groups in kraft lignins are in the aromatic ring whereas in lignosulphonates they are found in the side alkyl chains. Lignosulphonates and sulfomethylated lignins have been commercialized by e.g., Borregaard, MeadWestvaco and Tembec in applications such as binders, dispersants, crystal growth modifiers and emulsion stabilizers (Borregaard, n.d.).

Reaction condition related degradation of lignin takes place when sulphonated lignin is transformed from solid phase into solution leading into high variance in the molecular mass of lignosulphonates. (De Wild et al., 2014) Weight averaged molar weights (M_w) of lignosulphonate in the range of 5,400–152,000 (Hong and Qiu, 2020), 1,000–150,000 (Aro and Fatehi, 2017) and 1,700–21,000 g mol^{-1} (Zhou et al., 2013) have been reported. Utilization of membrane technologies seems attractive in lignosulphonate separation due to the vast variance of the lignosulphonate molecular weights. By choosing the membranes carefully it is possible to recover the specific, or multiple different lignosulphonate fractions. Lignosulphonate recovery via membrane separation has been well demonstrated by e.g., Domsjö. (Joensson et al., 2016)

3 ORGANOSOLV PROCESS

The organosolv process, first developed and patented by Kleinert and Tayenthal in the 1930s (Lai, 2017) and further developed by the University of Pennsylvania and the General Electric Company in the 1970s (Pan et al., 2005), can be divided into two main methods: organosolv pulping and organosolv fractionating pretreatment. The objective of organosolv pulping is to liberate cellulose fibers from the complex of lignin and hemicelluloses whereas organosolv fractionating pretreatment takes focus on improving digestibility of cellulose. (Zhao et al., 2017) These two methods could also be categorized by the degree of delignification, which is higher in organosolv pulping compared to organosolv fractionating pretreatment. (Brosse et al., 2017)

Organosolv pretreatment process can be catalyzed by using organic or inorganic acid (Shui et al. 2016; Sun and Cheng 2002). In its core, the process using involves treating lignocellulosic biomass in an aqueous solution with organic solvents present. The process temperature ranges from 100 to 250 degrees Celsius, and the reaction time depends on the preferred outcome. The pretreatment process aims to solubilize both lignin and hemicellulose leading into three separate fractions: (1) a fraction of dry and solid lignin – after precipitating with water, as stated by Zhao et al., (2017) – (2) a fraction of solid cellulose and (3) an aqueous fraction containing hemicellulose. Should the process be catalyzed by a sulphur-based catalyst, the aqueous fraction (3) includes water-soluble lignosulphonates also. Ethanol is one of the most frequently used solvents in the process because it is easily recovered by distillation to be reused in the following organosolv pretreatment batches. (Gillgren et al., 2017; Matsakas et al., 2018)

The chemical hydrolysis reactions occurring in the cooking step of organosolv process consist of partial hydrolysis of cellulose into smaller yet insoluble (in the liquor) fragments, and hydrolysis of polysaccharides. Most of the polysaccharides are hydrolyzed into monosaccharides, acetyl groups are hydrolyzed into acetic acid, and an operating condition related amount of pentose sugars are dehydrated into furfural. Low pH value, high temperature and high cooking time increase the sugar dehydration and vice versa. (Arato et al., 2005)

In organosolv pretreatment, the lignin breakdown is reached via cleavage of aryl ether bonds, from which the α-*O*-aryl ether bonds are cleaved more easily whereas the cleavage of β-*O*-aryl ether bonds require more severe conditions. A major concern within acidic conditions is lignin condensation, which is counter-productive to organosolv delignification. Lignin condensation occurs when the benzylic carbocation intermediate (i.e., α-carbon in lignin side chain) interacts with the neighboring lignin unit possessing an electron-rich carbon atom. These reactions – resulting into highly condensed and insoluble, high molecular weight lignin – can be prevented by using e.g., phenolic solvents. Another option in preventing lignin condensation is combinative pretreatment with the use of organic scavengers such as 2-naphthol in pre-hydrolysis to scavenge the carbonium ion intermediate. Cleavage of β-*O*-aryl bonds with elimination of formaldehyde and formation of Hibbert's ketones are presented in Figure 6. (Brosse et al., 2017)

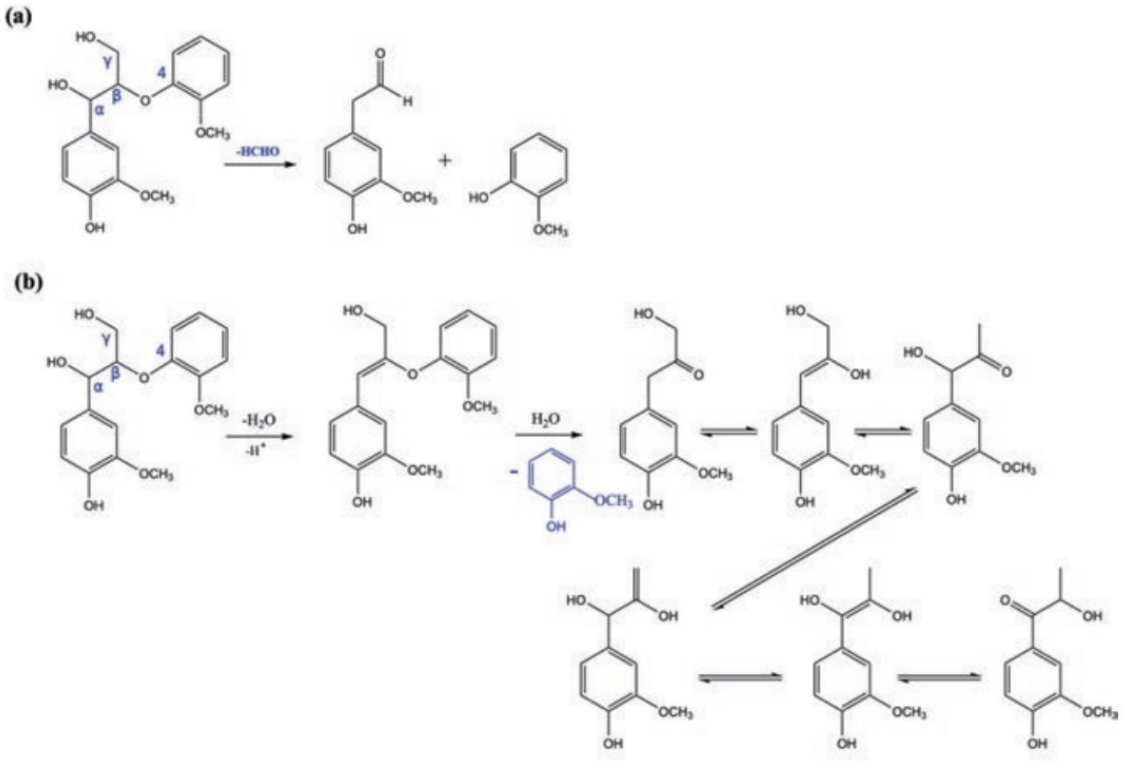

Figure 6. (a) solvolytic cleavage of β-*O*-aryl bonds with the elimination of formaldehyde and (b) solvolytic cleavage of β-*O*-aryl bonds to form Hibbert's ketones (Zhou et al., 2021, p. 31)

Several companies have developed their own variations of organosolv pulping and organosolv fractionating pretreatment processes with each utilizing different chemicals, cooking temperatures and times. The Alcell Process and the CIMV (compagnie industrielle de la matière végétale) process represent the former, and the Lignol process and AVAP (American value added pulping) process represent the latter. (Pan et al., 2005).

4 MEMBRANE TECHNOLOGY AND MEMBRANE MATERIALS

Membranes are semipermeable barriers between two phases, which separate components and molecules from each other due to the differences in the ability of the components to move through the membrane. The history of the membrane science traces back to 1748 but until microfiltration became an important application in manufacturing of biological products and pharmaceuticals in the 1960s and 1970s the use of membranes was limited merely to laboratories and industrial applications of small-scale. Since then, the use of membrane technology has been extensive especially in seawater desalination and the treatment of water and wastewater, and after the exponential growth of membrane applications starting in the 1990s, the use of membrane technologies has become widespread in various other separation processes also. (Zhang et al., 2012)

In membrane separation of lignosulphonates pressure is used as the driving force in the most common membrane systems (Rudolph, 2021). These systems are classified according to the operating principle in cross-flow and dead-end filtration. The operation of the former includes recirculation of the feed producing two different product streams i.e., retentate and permeate. The operation of the latter, instead, resolves around driving the feed through a filter media (or membrane). (Bhave, 2014) The differences of cross-flow and dead-end filtration processes are illustrated in Figure 7.

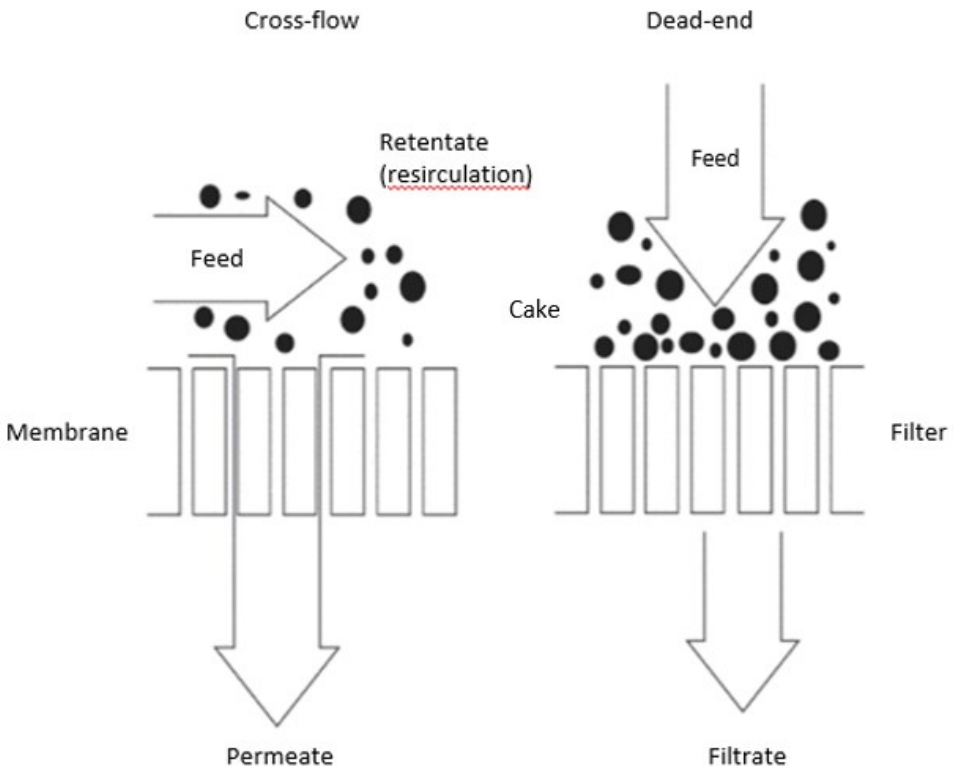

Figure 7. The principle of cross-flow and dead-end filtration (adapted from Bhave, 2014, p. 151)

The two major types of operational units i.e., modules, which for the membranes are engineered are spiral-wound and hollow fiber (Figure 8) (Wenten and Ganesha, 1996). Tubular modules are also an option, when the feed contains e.g., high dissolved solids, but their high CAPEX and OPEX might be an issue in an industrial point of view (Synder Filtration n.d.a; n.d.b & n.d.c). The spiral-wound elements constitute of membrane envelopes wrapped around a permeate pipe allowing a big membrane area to be fitted in a rather small and tight package. The feed flow enters the module through feed channel spacers and a portion of the feed flow permeates through the membrane and, due to the permeate collection material, spirals down to exit the system through the permeate pipe. (McKeen, 2012) Hollow fiber module, instead, is filled with hundreds of tubes with tiny pores in their walls. The feed enters the system from one end, a portion of the feed permeates through the pores while particles larger than the pore size continue their way out of the module. (MSR, 2021)

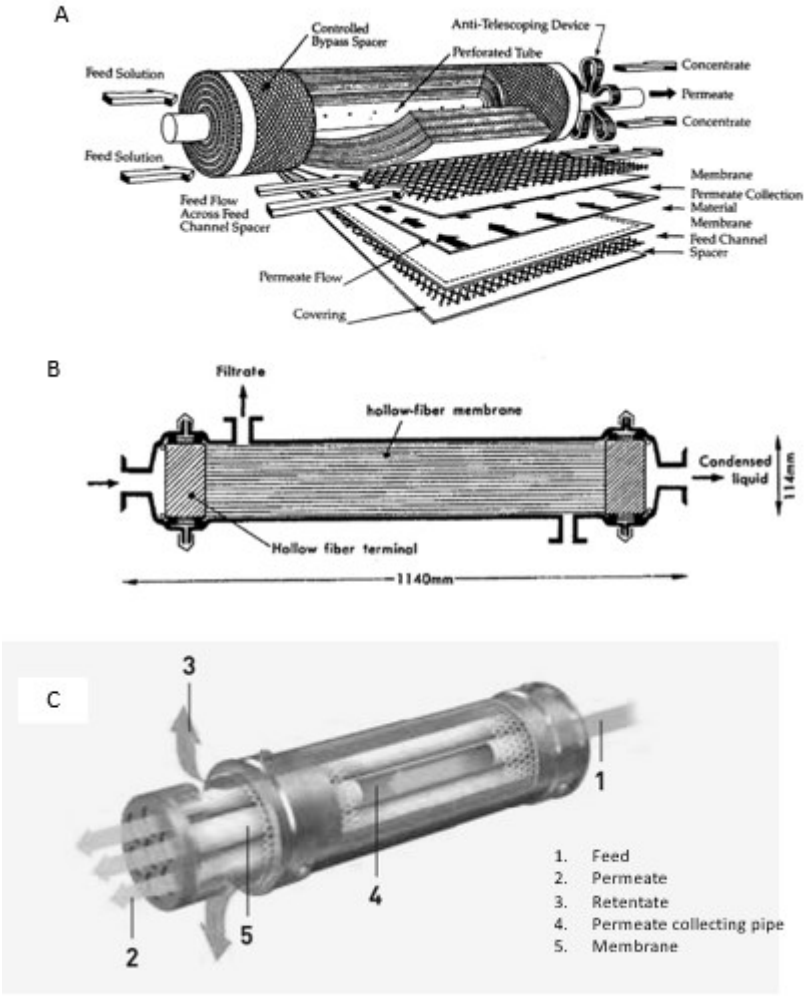

Figure 8. Spiral-wound (A), hollow fiber (B), and tubular (C) modules (Porter, 1990, p. 205, 213; Lehmann&Voss&Co, n.d.)

According to Cheryan and Kuo (1984), spiral-wound and hollow fiber modules are the least energy intensive options when compared to other ultrafiltration systems and are hence promising options for industrial ultrafiltration processes. The disadvantage of hollow fiber modules is their irreversible fouling and fiber breakage combined with moderate capital costs (CAPEX) and high operating costs (OPEX). Spiral-wound, instead, is less prone to fouling, has a low risk of membrane breakage and both the CAPEX and OPEX are low. A comparison of some of the properties of these setups are presented in Table 2.

Table 2. A comparison of some of the properties of spiral-wound, hollow fiber and tubular membrane setups (Synder Filtration n.d.a; n.d.b & n.d.c)

	Spiral-wound	**Hollow fiber**	**Tubular**
Fouling tendency	Moderate	High (irreversible)	Moderate
Packing density	Moderate/High	High	Low
Cleaning	CIP	Backflush	Backflush/Mechanical
Risk of membrane breakage	Low	Moderate/High	Low
CAPEX	Low	Moderate	High
OPEX	Low	High	High

The development of economically viable membrane-based processes is based on understanding the factors responsible of membrane performance. Such factors are, for example: membrane materials, formation, pore size distribution and interactions between the membrane and the feed components. The deployment of membrane process in relevance to the other unit operations of the process chain is also a factor requiring attention and hence, the selection of the membrane material (Table 3) is strictly in relation with the entire chain of processes. (Kumar, 2012)

Table 3. Examples of membrane materials used in different membrane processes (modified from Kumar, 2012, p. 76; Wagner, 2001, p. 10)

Process	Membrane Materials
Reverse Osmosis	Cellulose acetate, polyamide, thin film composite on polysulfones
Nanofiltration	Polyacronitrile, polyvinyl alcohol, silicone
Ultrafiltration	Cellulose acetate, ceramic, polyacronitrile, polyethersulfone, polyvinyl alcohol, polyvinylidene fluoride, regenerated cellulose, thin-film composite
Microfiltration	Carbon composite, cellulose nitrate, modified polyethylene and polypropylene, polycarbonate, stainless steel coated with ceramic

Membranes must be chemically resistant to not only the feed but also to the cleaning fluids. Membranes must also have mechanical and thermal stability to withstand the stress caused by particle collision and heat, and they must have high permeability and selectivity combined with long lifetime and the ability to withstand high transmembrane pressures characteristic for the membrane processes (Sparks and Chase, 2016). A simplified guide in membrane selection is presented in Table 4.

Table 4. Examples of membrane properties and membrane selection (Wagner, 2001, p. 10)

Membrane	Advantages	Disadvantages
Cellulose acetate (CA)	Cheap and hydrophilic, not very prone to fouling	Limitations with respect to pH, temperature and microorganisms
Polyether- and polyarylethersulfone (PSU/PSO/PES)	Exceptional resistance to pH and temperature	Intolerant to oil, grease, fat and polar solvents
Polyvinylidenefluoride (PVDF)	Highly resistant to hydrocarbons and oxidizing environments	Difficult to produce
Thin-film composite (TFC, TFM)	Highly resistant to pH and temperature	Intolerant to oxidizing environments

Membrane technologies are applied in various industrial fields e.g., automobile-, the electronics- and the pharmaceutical industry, due to the two advantages making membrane filtration an ideal method for separation: the use of pressure difference as driving force leading into separation being not accompanied by a phase change, and low-energy consumption combined with the fact that the target to be separated becomes scarcely denatured or decomposed. Membranes can be divided in four categories depending on the pore size (Figure 9) from the smallest to the largest: reverse osmosis (RO), nanofiltration (NF), ultrafiltration (UF) and microfiltration (MF). (Kubota et al. 2008)

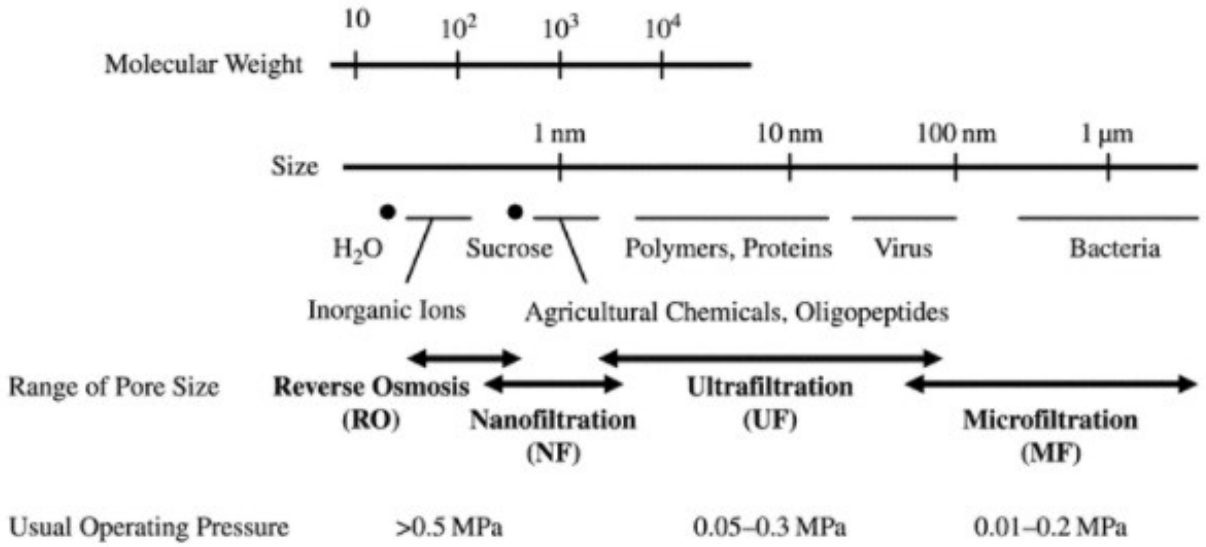

Figure 9. Membrane pore size range in relevance to molecular weight, particle size and operating pressure (Kubota et al., 2008, p. 102)

Concentration polarization is an issue with any pressure-driven membrane separation process. Concentration polarization is caused by the accumulation of molecules near the surface of the membrane. The layer of high concentration exerts a force in the opposite direction to the mass transfer creating resistance. Such a flux-decline causing phenomenon cannot be avoided but can be controlled via process variable optimization and membrane selection. (Bhattacharya et al., 2005; Mulder, 1996)

4.1 Microfiltration and ultrafiltration

Microfiltration and ultrafiltration are technologies used for separation of polymers/low-molecular weight compounds, respectively. The use of MF and UF resolves around retention and concentration, and permeation and purification of valuable compounds. (Kubota et al., 2008) The membranes used in MF and UF are microporous which remove the particulate matter via sieving mechanism (Bergman, 2007; Kumar, 2012).

In ultrafiltration, it is necessary to select the proper membrane material among the various polymer materials due to the material playing a vital role in the membrane performance (Bing et al., 2016). The membrane selection is best done experimentally due to the diffuse nature of membranes, molecular charge and interactions between the membrane surface and the components in the feed. The experimental selection involves measuring the rejection rates of the components at the selected operating conditions acknowledging that, for most components, the rejection value increases by the time. The rejection or retention factor R_{obs} (%) can be calculated with Equation (1):

$$R_{obs} = \frac{(c_F - c_p)}{c_F} * 100\%, \quad (1)$$

Where c_F is the concentration of the component in the feed (e.g., g L^{-1}) and c_p is the concentration of the component in permeate. The rejection rates are in the range of 0–1, where a value of zero implicates that the component is freely permeating and a value of one implicates that the component is fully retained by the membrane. (Lewis, 1996)

Membrane manufacturers use different solutes e.g., polyethylene glycol and dextrans, to characterize and rate the membranes based on the sieving. In the procedure, solutes of varying molecular weight are filtrated at constant pressure constructing a sieving curve to estimate the nominal molecular weight cut-off (MWCO) of the membrane. For example, in the sieving curve (Figure 10), values of 650 and 500 Dalton are determined for the curves presented with solid squares and crosses, respectively, corresponding a rejection rate higher than 90 % (w/w). (Kumar, 2012)

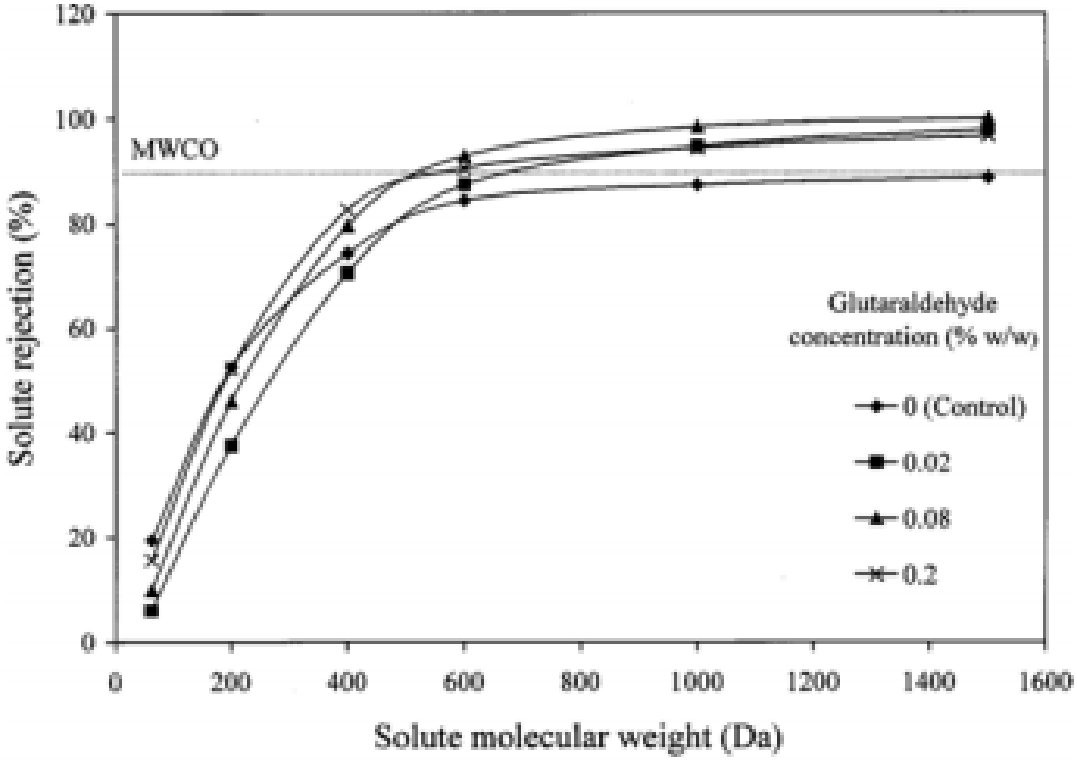

Figure 10. Solute sieving curves (Musale and Kumar, 2000, cited in Kumar, 2012, p. 80)

MWCO is one of the most useful tools for pre-screening UF membranes to be used in chosen application. The pre-screening by using MWCO comes in handy due to the macromolecules to be retained being characterized by their molecular weights and MWCO describing the molecular weight at which 90 % of the macromolecules are rejected by the membrane. The use of MWCO, however, has limitations. For example, there is variance in the size and form of UF membrane pores and different solutions have different retentions due to interactions between membrane and solute e.g., adsorption of macromolecules on the membrane surface and inside the pores. The membrane adsorption is controlled by, for example, altering the solute concentration, pH, ionic strength, and temperature. Another limitation with MWCO is that polymers of the same molecular mass differ in molecular size i.e., the macromolecule to be retained may or may not be spherical. Also, the differences in the shapes of retention- and molecular weight curves makes it hard to pick the exact point at which 90 % of the macromolecules are retained. As a rule of thumb, good separation is reached when the molecular mass between two solutes to be separated differs by a factor to ten and the MWCO rating of the membrane is half or less of the molecular weight of the particles to be retained. (Singh, 2014)

4.2 Nanofiltration and reverse osmosis

Nanofiltration and reverse osmosis are – similarly to MF and UF – pressure-driven processes. However, the primary target of RO and NF is the removal of dissolved contaminants via

diffusion through semipermeable membranes. The primary materials for RO and NF membranes are cellulose acetate (and its derivatives) and various polyamides. (Bergman, 2007)

Osmosis is a natural process where concentrations of two solutions, divided by a semipermeable membrane, are equalized by water and some ions passing through the membrane from the solution with a lower concentration to the solution with a higher concentration. In reverse osmosis, high pressure is applied on the solution with higher concentration causing the water to move from the solution of higher concentration towards the solution of lower concentration leading into purification or demineralization of the water. The difference between osmosis and reverse osmosis is shown in Figure 11. (Kucera, 2015)

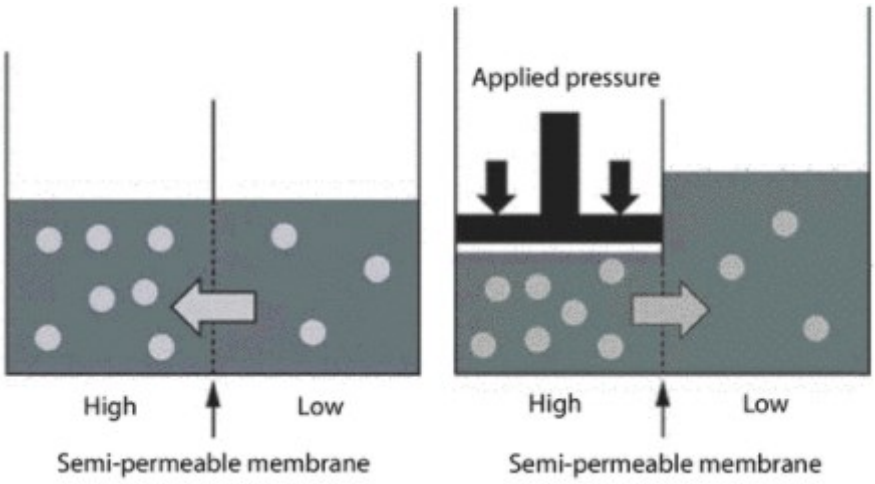

Figure 11. Osmosis and reverse osmosis (Kucera, 2015, pp. 20–21)

4.3 Diafiltration

Diafiltration, as a term, means using dilution in combination with filtration with an aim to remove most of the smaller molecular weight compounds from the solution. This is achieved by diluting the solution with e.g., water, through filtration cycles to make up the water lost in permeate and to keep the concentration of target products (compounds to be concentrated) constant. (Lenntech, n.d.) Diafiltration can be operated either in a continuous- (CDF, continuous diafiltration) or discontinuous (DDF, discontinuous diafiltration) manner. In the former, water is added constantly at a rate that equals the rate of permeate volume while in the latter the water addition is done between the filtration cycles. (Lewis, 1996)

4.4 Membrane structure

The membranes can be manufactured out of a variety of materials, and the choosing of the right material for the given application depends on the membrane structure and the separation problem. Based on the separation principles and structure, two basic types of membranes can be distinguished (Figure 12): porous and nonporous membranes. The porous membranes are

used for micro- and ultrafiltration, and nonporous for gas separation, pervaporation, and dialysis. (Mulder, 1996)

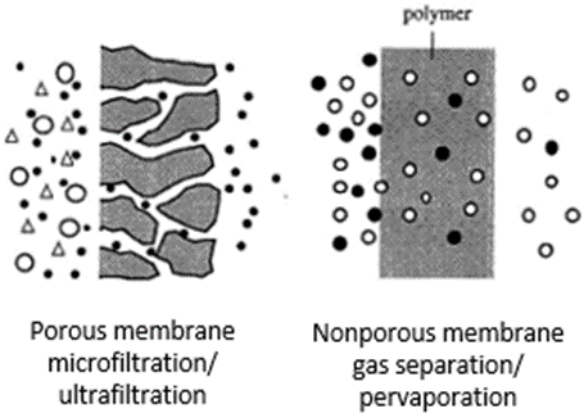

Figure 12. Two basic membrane types, a schematic drawing (Mulder, 1996, p. 71)

4.5 Membrane fouling

Membrane fouling, i.e., the permeate flux reduction as a function of time (Ochando-Pulido and Stoller, 2015), is a major an unavoidable drawback in the implementation of membrane technologies. Fouling (Figure 13) is caused by the accumulation of colloids, soluble organic compounds, and microorganisms on both the membrane surface and its pores. Fouling is also caused by pore blocking and gel layer formation (Rudolph, 2021), and it can be either reversible, semi-reversible or irreversible in nature, meaning that cleaning procedures are either effective or ineffective – if the latter, the process faces a technical failure before long. (Pulido, 2017)

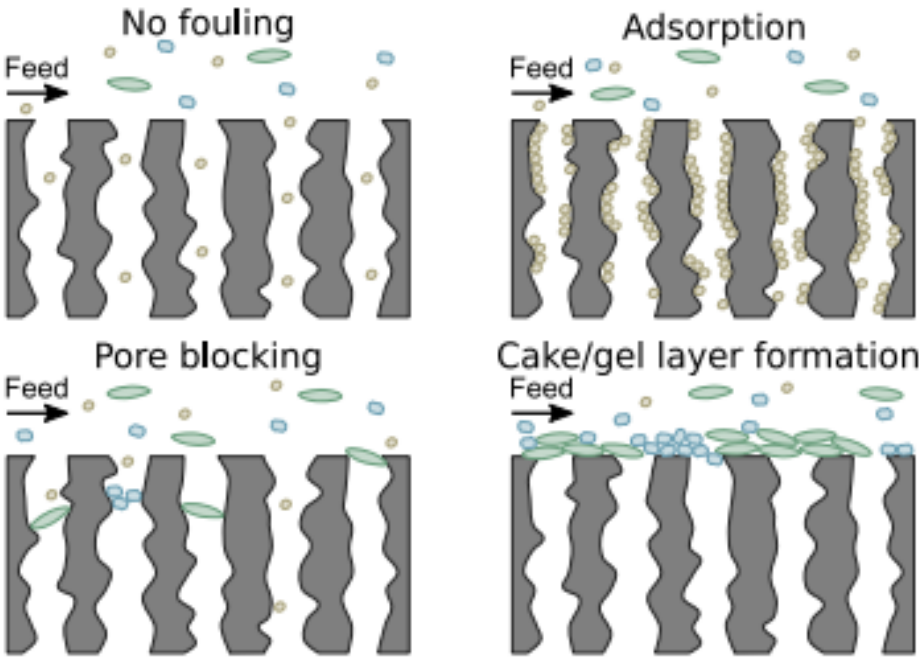

Figure 13. Different fouling phenomena in membrane filtration (Rudolph, 2021, p. 8)

When optimizing a system in regards of e.g., membrane lifetime and the interval of washings, a use of critical flux hypothesis is proposed. The hypothesis is that on start-up there exists a hydrodynamic – and probably other variant dependent – flux below which membrane fouling does not occur and, on the other hand, above that flux the fouling is observable. This means, that by selecting a hydrodynamics related critical and generally low transmembrane pressure (*TMP*) – which is strongly dependent on the given membrane resistance – below which constant flux operating can be reached, little or no irreversible fouling should be present. (Field et al., 1995)

The critical flux theory identifies three regimes (Figure 14) during a membrane filtration process. The subcritical regime (I) is the first stage of the filtration and has an optimal membrane selectivity. Variations in flux and *TMP* are linear and reversible, the capacity of permeation is increased by employing a high cross-flow velocity and, at the end of the first regime, the critical pressure is achieved. At the second regime, the critical regime (II), the flux is independent of *TMP*, and the process is at equilibrium: the particle transportation towards the membrane is balanced with the particle transportation towards the bulk flow. At high *TMP* the permeate flux is not notably affected by the increases in pressure because the materials deposited due to the mass transport on the membrane are removed by the wall shear force. The final regime, decline regime (III), is the endpoint of membrane filtration process, where the membrane fouling reaches a point where the accumulated and compacted material must be removed before the process can be continued. The critical flux is identified experimentally: the flux is increased until the *TMP* reaches a point of reduced stability. (Muro et al., 2012)

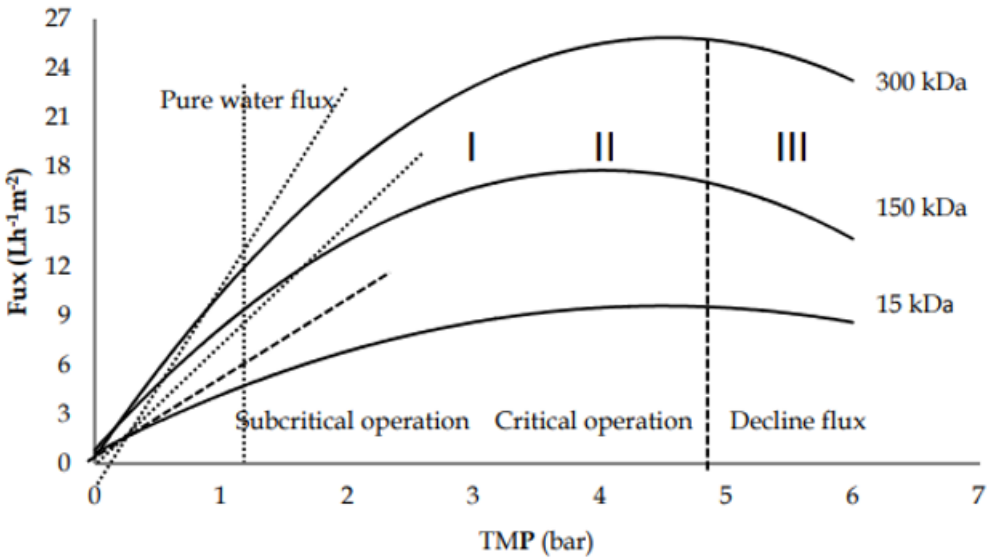

Figure 14. Critical flux regimes with 300, 150 and 15 kDa membranes: (I) Subcritical-, (II) Critical- and (III) Decline flux (Muro et al., 2012, p. 265)

4.6 The effect of pH, temperature, and pressure into membrane separation

The effect of solution pH in membrane separation must be acknowledged when selecting optimum operation conditions due to pH affecting membrane fouling among with membrane material and operating variables (Marson et al., 2021). Membrane lifetime, properties of the feed solution and the filtration outcome are all affected by pH. When it comes to membrane lifetime, commercial membranes can have pH recommendations in the range of e.g., 1–13 (Alfa Laval, n.d.a) or 0–14 (Mann+Hummel, 2021a), but the extremities will most likely take a toll.

The variance of the effect of solution pH into membrane separation is demonstrated by e.g., Marson et al., 2021, who suggested that the effect of pH on the peptide retention in UF of spent brewer's yeast protein hydrolysate on polymeric membranes is within the margin of experimental error. Butylina (2007), on the other hand, showed more feasible NF of whey UF permeates in alkaline- than in acid conditions emphasizing on the importance of feed properties and membrane material characteristics.

When it comes to temperature, an increase of 1 °C in operating temperature leads into an increase of 1–3 % in flux depending on the characteristics of the feed – the greatest increase is achieved on pure water. The flux increase is due to viscosity decreasing when the temperature rises (Wang et al., 2007). Hence operating the filtration process with as high a temperature as possible is recommended flux-wise but the resulting chemical and bacteriological phenomena must be acknowledged. High operating temperatures are truly advantageous with viscous liquids only. (Wagner, 2001)

Pressure-related membrane compaction (Stade et al. 2013), that reduces the membrane MWCO due to a decline in pore size, tends to increase retention and is also be affected by an increase in temperature. Compaction may also lead into changes in the pore geometry causing, overall,

reduction of the flux. Compaction can be either reversible or irreversible by nature and plays major role in the efficiency of the ultrafiltration unit (Stade et al. 2015). According to Wagner (2001), the compaction causing stress caused by pressure and temperature can be estimated by using Equation (2):

$$W = pT, \tag{2}$$

where W is Wagner unit (bar °C), p is pressure (bar), and T is temperature (°C). A Wagner unit under 1200 is considered safe for standard membrane elements, while 1200–2000 W requires special element design.

4.7 Lignosulphonate fractionation via membrane separation

Lignosulphonate fractionation via membrane separation provides means to improve the fermentation process by concentrating the sugar fraction (permeate) and the lignosulphonate fraction (retentate) improving the feasibility of a lignocellulosic feedstock using biorefinery. The feasibility is improved by providing valuable, purified lignosulphonates, that can be sold to be used as a raw material in applications such as industrial detergents, concrete additives, glue, and adhesives. According to Gillgren et al., (2017), lignosulphonate derivatives could also find a use in a form of oxygen scavengers in food packaging. (Restolho et al., 2009)

In membrane selection, it must be assured that the permeation of sugars and the retention of lignosulfonates is maximal. While the molecular weight of lignosulphonates can vary from 1,000 to 150,000 Da (Aro and Fatehi, 2017), the molecular weight of hemicellulose sugars ranges from 150 Da (xylose and arabinose) to 180 Da (mannose) (Weng et al., 2010). When considering the rule of thumb in membrane selection (Singh, 2014) the molecular weight of sugars and the lightest lignosulphonates can become an issue due to being rather close to the same. The best result in separation might be achieved by using a combination of membrane technologies in series. (Restolho et al., 2009)

Membrane separation of lignosulphonates and sugars (Table 5) out of process liquors of e.g., acid sulphite pulping, hot water pretreatment and ethanol organosolv pretreatment, have been studied widely. Some of the most promising results by the means of separation efficiency of lignosulphonates from sugar have been obtained using e.g., Microdyn Nadir UP010 (Restolho et al., 2009).

Fernández-Rodríguez et al., (2015), suggested a use of membranes of different MWCOs in series, should the aim be in maximizing the yield of both lignosulphonates and sugars (MWCO of 15 kDa offered the best permeate flux, while MWCO of 5 kDa offered the best lignosulphonate rejection and MWCO of 1 kDa showed the lowest loss of sugars). Alriols et al., (2010) supported this approach by using four membranes of different MWCO in series to obtain different lignin fractions out of organosolv liquor.

Table 5. Membranes used in various operating conditions according to literature

Membrane	Material	T (°C)	pH	P (MPa)	MWCO (kDa)	Process	Reference
Alfa Laval, UFX5&10 pHt	Polysulphone hydrophilic	25	3.0–3.7	0.1–0.5	5, 10	Acid sulphite pulping	(Restolho et al., 2009)
Microdyn Nadir, UP010	Polyethersulphone	25	3.0–3.7	0.1–0.5	10	Acid sulphite pulping	(Restolho et al., 2009)
Industrial Biotech Membranes	Ceramic TiO2	20	3,3	0.18–0.2	1, 5, 15	Acid sulphite pulping	(Fernández-Rodríguez et al., 2015)
Nitto Denko corp., RS50	Polyvinylidene Fluoride	25	3.7 or 4.4	0.4 or 2.8	1	Hot water pretreatment	(Sasaki et al., 2014)
Atech innovations, GmbH	Ceramic TiO2	25	4	0.05, 0.2, 0.4, 0.6	3	Sulfite pulping	(Ebrahimi et al., 2021)
Alfa Laval, GR	Polyethersulphone	n.d.	8,5	0,69	10, 20, 25, 50, 100	Sulfite pulping	(Bhattacharya et al., 2005)
Industrial Biotech Membranes	Tubular Ceramic	60	n.d.	0,3	5–15	Ethanol organosolv	(Alriols et al., 2010)

When it comes to selection of the membranes to be used in filtration of lignosulphonate containing liquors, Carlsson et al. (1998) have pointed out that, overall, hydrophilic membranes should be selected over hydrophobic membranes due to the lignosulphonates adsorbing onto the membrane surface of the latter causing serious fouling. As for the membrane characteristics, regenerated cellulose and polysulfone are within the best of options. The relative hydrophilicity/hydrophobicity of membranes is presented in Table 6.

Table 6. Relative hydrophilicity/hydrophobicity of membranes (Pearce, 2007, p. 36)

Hydrophilicity/-phobicity	Membrane material	Characteristics
Hydrophilic	CA	Naturally hdrophilic
	PES	Naturally hydrophobic but can be modified into moderately hydrophobic
	PAN	
	PVDF/PS	
Hydrophobic	PE, PP	Difficult to modify

EXPERIMENTAL PART

5 MATERIALS AND METHODS

This section covers the materials and methods used in the laboratory experiments that took place between September 2021 and January 2022 at Lappeenranta. Here, the aim was to gain knowledge of: (1) the effect of spent liquor pH on membrane filtration, (2) the effect of spent liquor temperature on membrane filtration, and (3) whether further concentration of lignosulphonates seem reasonable or not. Membrane performance was monitored in terms of permeability and selectivity – the latter monitored in terms of retention factors for lignosulphonates, total sugars, total organic carbon (TOC), and conductivity. Membrane fouling, playing a vital role in membrane separation, was monitored in terms of pure water flux return (PWF_r) and ATR-FTIR. With the understanding gathered via measurements, analysis and calculations, conclusion on whether membrane separation of spent organosolv liquor seems viable in an industrial point of view could be drawn.

5.1 Raw material and experimental setup

Spent organosolv liquor produced by SO_2-catalysed pretreatment of pine- and spruce chips (4:1) was obtained from St1 company. The SO_2 had been removed by nitrogen bubbling, ethanol by evaporation and insoluble lignin by precipitation and filtration. The liquor was stored in a refrigerator and additional nitrogen bubbling was performed prior to experiments due to SO_2 being still present in vapors to some extent.

5.1.1 Cross-flow filtration

In filtration experiments, DSS LabStak® M20-0.72 cross-flow test unit (Alfa Laval, Denmark) capable of operating up to 20 different membranes simultaneously, was used (Figure 15). The unit consisted of a frequency converter attached to a gear pump (Wanner Hydra-Cell), feed tank equipped with a heating jacket for automatic temperature control (Lauda Proline RP855) and a membrane stack consisting of support and spacer plates. The membrane area ranged from a minimum of 0.036 m^2 to a maximum of 0.72 m^2. The outlet pressure (p_{out}) was controlled manually by adjusting a pressure valve and the pressures (p_{out} and p_{mean}) were monitored via Pixsys ATR401 digital multifunction controller. The cross-flow velocity was monitored with a rotameter.

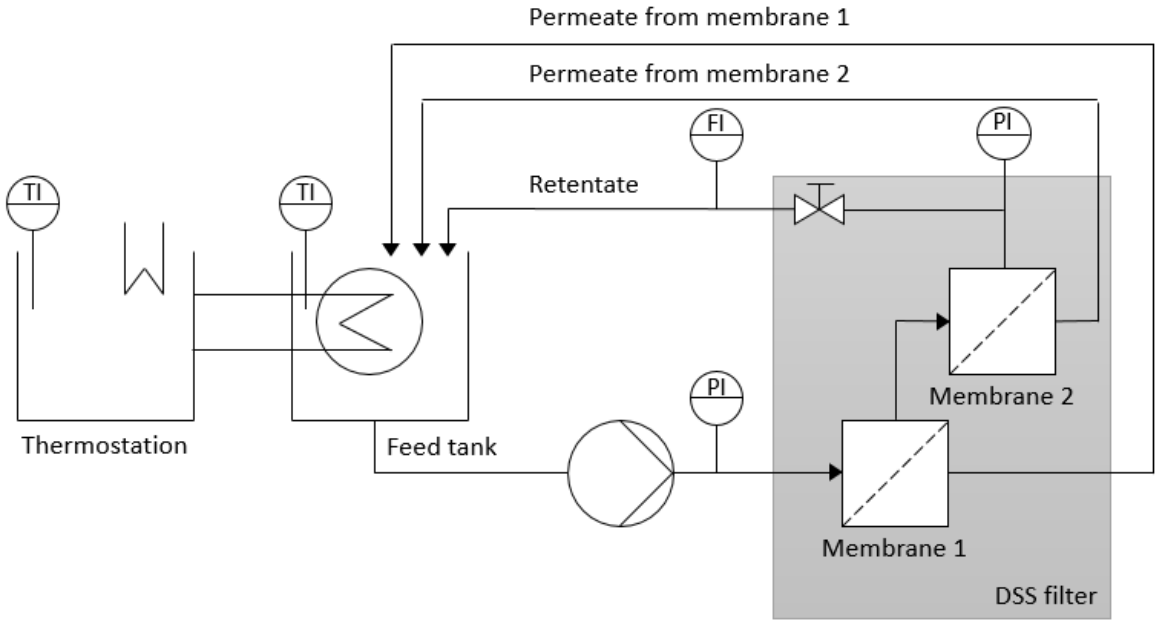

Figure 15. DSS LabStak® M20-0.72 flow chart (modified from Lahti, 2009, p. 37) with two membrane pairs i.e., two support plates with two pieces of a membrane each, and three spacer plates

Even though the membranes were in practice set up in series the setup could, according to Lahti (2009), be considered as if the membranes were set up in parallel. This was due to the retentate flow being so high in relation to permeate flow. An illustration of the membrane stack is shown in Figure 16: the inlet reaches the first membrane pair through a spacer plate with only a small fraction of the inlet permeating through the membrane while most of the inlet continues towards the second spacer plate through a hole in the middle of the support plate (to which two pieces of a membrane are attached with plastic locking rings, one piece of the membrane each side). The inlet passes through the whole membrane stack on a similar manner.

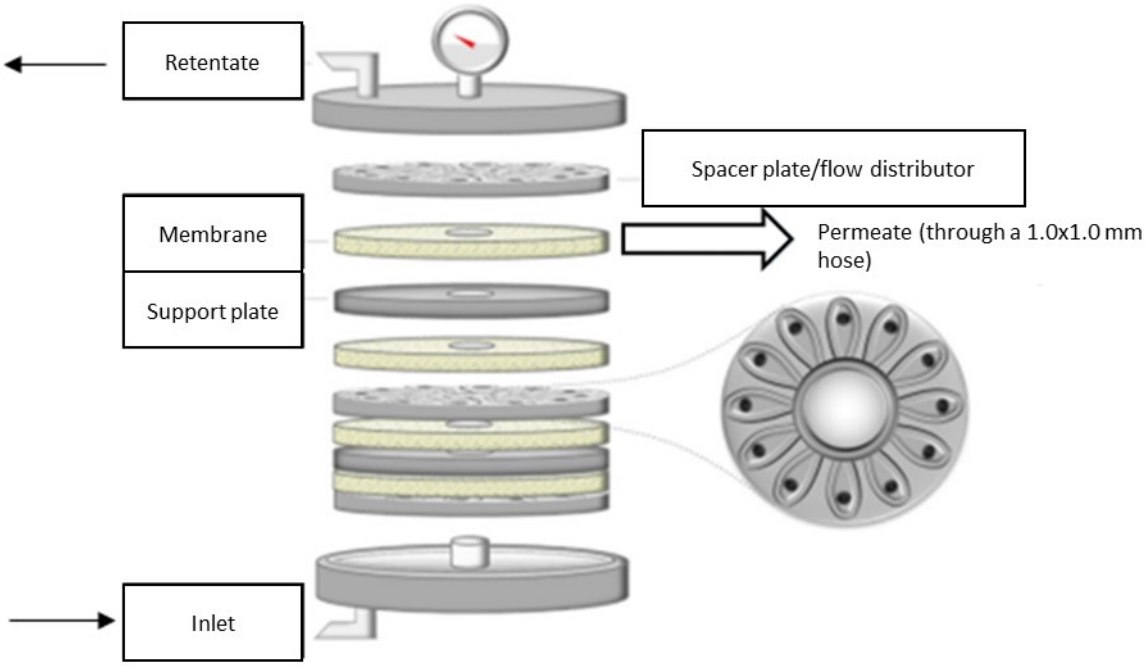

Figure 16. DSS LabStak® M20-0.72 membrane stack (modified from Ajo et al., 2018, p. 9)

Several membranes chosen according to the molecular weight of lignosulphonates (Aro and Fatehi 2017; Hong and Qiu, 2020; Zhou et al., 2013) and the molecular weight of hemicellulose sugars (Weng et al., 2010) were used. The membrane manufacturers were Alfa Laval, Microdyn-Nadir, GE Membranes/Suez, and Synder Filtration, and the membrane models and molecular weight cut-offs (MWCO) (Table 7) were: Alfa Laval GR95PP (2 kDa), UFX5 pHt (5 kDa) and RC70PP (10 kDa), Microdyn-Nadir NP010 (1–1.2 kDa), UH004P (4 kDa), GE Membranes/Suez were GK (3 kDa) and GE (1 kDa), and Synder Filtration NFG (0.6–0.8 kDa). DuPont's NF270 was used in dead-end filtration experiment.

Table 7. Membrane selection: manufacturer, membrane model, suggested operating conditions in terms of pH, temperature and pressure, membrane material and contact angles according to literature.

		pH	T (°C)	p (bar)	MWCO	Support material	Membrane material	Reference	Contact angle	Reference (contact angle)
Alfa Laval	GR95PP	1–13	5–75	1–10	2000	PP*	Polyethersulphone	(Alfa Laval, n.d.b)	60°	Yammine et al., 2019
	UFX5 pHt	1–13	0–75	1–15	5000	PP*	Polysulphone	(Alfa Laval, n.d.c)	(A) 52°, (B) 74°	(A) Rudolph-Schöpping et al., (2022); (B) Koivula et al., (2011)
	RC70PP	1–11	5–60	1–10	10000	PP*	Regenerated cellulose acetate	(Alfa Laval, n.d.d)	(A) 13°, (B) 20°	(A) Koivula et al., (2011); (B) Damar et al., (2020)
Nadir	NP010	0–14	n.d.	≤40	1000–1200	PP*	Polyethersulfone	(Mann+ Hummel, 2021a)	70°	Nicolini et al., (2016)
	UH004P	0–14	n.d.	n.d.	4000	PP*	Polyethersulfone	(Mann+ Hummel, 2021b)	68°	Strand (2016)
GE membranes/Suez	GK	1–11	n.d.	n.d.	3000	n.d.	Polyamide-TFC	(Sterlitech, n.d.a)	71°	Tres et al., (2010)
	GE	1–11	n.d.	n.d.	1000	n.d.	Composite polyamide	(Sterlitech, n.d.a)	(A) 66°, (B) 73°	(A) Yammine et al., 2019; (B) Tres et al., (2010)
Synder Filtration	NFG	4–9	50 (max.)	30 (T>35°C)	600–800	n.d.	Polyamide-TFC	(Synder Filtration, n.d. & Sterlitech n.d.b)	40°	Cheng et al., (2018)
DuPont	NF270	3–10	45 (max.)	41	Salt rejection >97 %		Polypiperazine-TFC	DuPont (2021)	30°	Mänttäri et al., (2004)
						PP* = polypropylene			0° –90° = hydrophobic 90°–180° = hydrophilic	

Prior to beginning of filtration experiments, the membranes were flushed with cool water (approx. 27–32 °C) for 10 minutes with a cross-flow velocity of 0.8 m s^{-1}. Membranes were then washed by circulating alkaline washing fluid (0.1 % Ultrasil 110) for 10 minutes with a cross-flow velocity of 0.1 m s^{-1} at 32 °C. The alkaline washing-fluid remains were flushed out of the system with cool water (approx. 27–32 °C). The flushing was continued for 5–10 minutes (or until the permeate pH matched the pH of water) with a cross-flow velocity of 0.8 m s^{-1}. The membranes were then pressurized (depending on the pressures used in the filtration) at 4.0 or 16.0 bar (p_{out}) and 32 °C for 30 minutes with cross-flow velocity of 0.8 m s^{-1} to reduce the effect of membrane compaction (Stade et al. 2013 & 2015) into measurements.

Additional flushing with pure water was performed after each filtration to remove excessive foulants from the membrane surfaces. The flush time was 10 minutes, and it was performed in a temperature of 32 °C with a cross-flow velocity of 0.8 m s^{-1}. Pure water flux was measured before and after filtration at 32 °C with a cross-flow velocity of 0.8 m s^{-1} to monitor membrane fouling. Pressures of 1.0, 2.0, 3.0, and 4.0 bar (±0.02) or 4.0, 8.0, 12.0, and 16.0 bar (±0.20) were used in both the pure water flux determination and the actual filtration experiments. All the flux measurements were carried out on weight basis by collecting the permeate from each of the membranes in plastic beakers for two minutes (Future Sport professional stopwatch)

followed by weighing of the beakers with Precisa 8200D balance. All the flux measurements were done in duplicate, and averages were used in calculations.

The spent liquor pH was adjusted by using 10 M NaOH. The precise amount of 10 M NaOH needed was interpolated based on the data collected while titrating 100 g of the spent liquor with 1 M NaOH (Appendix II). Interpolation was done by using the functions provided by Excel off the Grid (2020).

Samples from the feed tank, the combined retentate flow, and each of the permeate flows were taken for analysis. Duplicate samples were taken, stored in a freezer, and brought to St1 Oy laboratory for sugar analysis. Both the retentate and the permeate (excluding the taking of the samples) were circulated back to the feed tank to avoid unnecessary concentration of the liquor.

In each of the filtration experiments, the membrane with the lowest MWCO was put on bottom of the stack and the membrane with the highest MWCO on top. Due to the flow direction being from bottom to top of the membrane stack this setup allowed highest pressures for the tightest membranes and vice versa.

5.1.2 Discontinuous diafiltration

Spent liquor lignosulphonate concentration was increased (in retentate) by discontinuous diafiltration (DDF). Here, a stack of three NP010 membranes were used, and the temperature was kept constant at 60 °C. The experiments were carried out for as long as it was possible to maintain a stable pressure of 16 bar and a cross-flow velocity of 0.8 m s^{-1}. The permeate mass was weighed and a matching amount of water was added to the feed tank. The DDF procedure was carried out twice.

5.2 Analytical methods

From each of the samples pH, conductivity, dry matter (DM), brix, TOC, and ultraviolet-visible absorption (UV-Vis) were measured. All the analyses were carried out at room temperature (approx. 22 °C).

The measurement of pH was carried out by Metrohm 744 pH meter and conductivity by Consort 304 conductometer. Dry matter content was determined by freeze drying with Christ Alpha 2-4 LD plus freeze-dryer and weighing with Precisa H225SM-FR balance. For the sample profiles (Table 10–Table 15, p. 49–52) the DM was determined by drying the samples at 105 °C. Brix was determined by Atago PAL-1 Pocket refractometer. A negligible concentration (1 ppm) of inorganic carbon was measured from an unprocessed sample which is why TOC was measured via total carbon (TC) program (Shimadzu TOC-L). For TOC analysis, the samples were diluted 2000 times.

UV-Vis spectra were acquired using Jasco V-670 Spectrophotometer with quartz cuvettes and the samples diluted 4000 times. The spectra were collected using fixed wavelengths of 287, 280, 270, 237, 225 and 212 nm, as suggested by Lee et al., (2013), except for the first set of samples, which with UV spectra between 400–190 nm with 0.1 nm data intervals and scan speed of 100 nm min^{-1} was gathered.

Attenuated total reflection fourier transform infrared (ATR-FTIR) spectrometer (Perkin-Elmer Frontier FT-IR) was used to analyze the foulants on the membranes. Spectra in the range of 4000–400 cm^{-1} were collected with a resolution of 4 cm^{-1} and data interval of 1 cm^{-1} using four accumulations. The samples were scanned twice or thrice depending on the variance between the spectra of the first two scans. The results were averaged and corrected for ATR and base line. The spectra were then slightly moved to set the starting absorbance into zero and normalized by min-max normalization (Gautam et al., 2015) – a method used with FTIR spectrometry of lignosulphonates by e.g., Magina et al., (2021). For the FTIR, the used membranes from filtration experiments were dried and pieces of pristine but similarly preconditioned membranes were prepared for comparison. Preconditioning of the pristine membranes was done in beakers and consisted of rinsing, washing, and flushing the membranes following the procedure introduced with DSS. The preconditioned membranes were then dried in in 40 °C and put in desiccator until cooling down to room temperature. For comparison, spectra of dried liquor sample were collected also.

5.3 Preparation of solutions for UV-Vis calibration curve

To determine the lignosulphonate concentration with UV-Vis, a calibration curve was made. The calibration solutions were prepared, with some deviations, applying the method of Lee et al., (2013). The spent liquor pH close to zero with concentrated sulphuric acid and the solution was left overnight to precipitate. The precipitation was followed by centrifuging the liquor with Multifuge 3 L for 30 minutes at 3500 rpm, and freeze-drying. The freeze-dried samples were put in desiccator to settle until reaching room temperature and weighed with Radwag AS 220/X balance. The samples were then dissolved in both water and 0.035 M NaOH (for comparison) and diluted with water or 0.035M NaOH, respectively. Adsorptions at 212, 225, 237, 270, 280 and 287 nm were obtained and used for concentration determination. The calibration curves are presented in Figure 17.

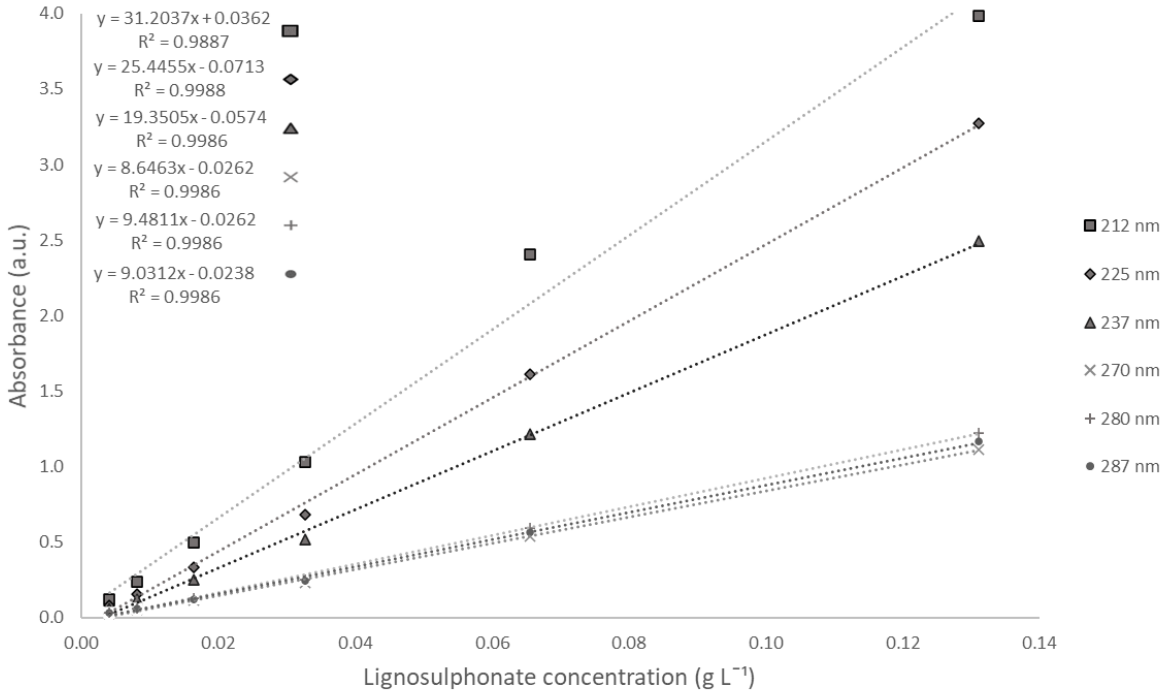

Figure 17. UV-Vis calibration curves with wavelengths of 212, 225, 237, 270, 280 and 287 nm

The extinction coefficients ε_{280} of 6.38, 6.76 (Appendix I) and 9.48 L g^{-1} cm^{-1} (Fig. 18) calculated from the slopes of the curves were notably lower than the extinction coefficients of 17.5 L g^{-1} cm^{-1} (Sjostrom and Haglund, 1964, cited in Iakovlev and Heiningen, 2011) and 19 L g^{-1} cm^{-1} (Iakovlev and Heiningen, 2011). According to sample profiles (Table 10–Table 15, p. 49–52), though, ε_{280} of 9.48 L g^{-1} cm^{-1} seemed to give rather reliable results.

Due to the dilutions being made by a robot using purified water instead of a buffered solution, pH related error margin (Figure 18) was determined. The determination was done simply by comparing the UV absorbances of 122 mg L^{-1} lignosulphonate solution with different pH values. Due to the samples being either acidic or close to neutral, the difference in absorbances between pH 2.92 and 7.09 was deducted as being the most reasonable range for the error margin determination. With these pH values, the absorbance difference was 0.02731 absorbance units which translated into an error margin of ±2.88 mg L^{-1} in lignosulphonate concentration. The effect of furanic compounds and furfural, with an impact from 2.26 up to 8.45 % (Iakovlev and Heiningen, 2011; Tikka and Virkola, 1986) into lignosulphonate concentration was not considered.

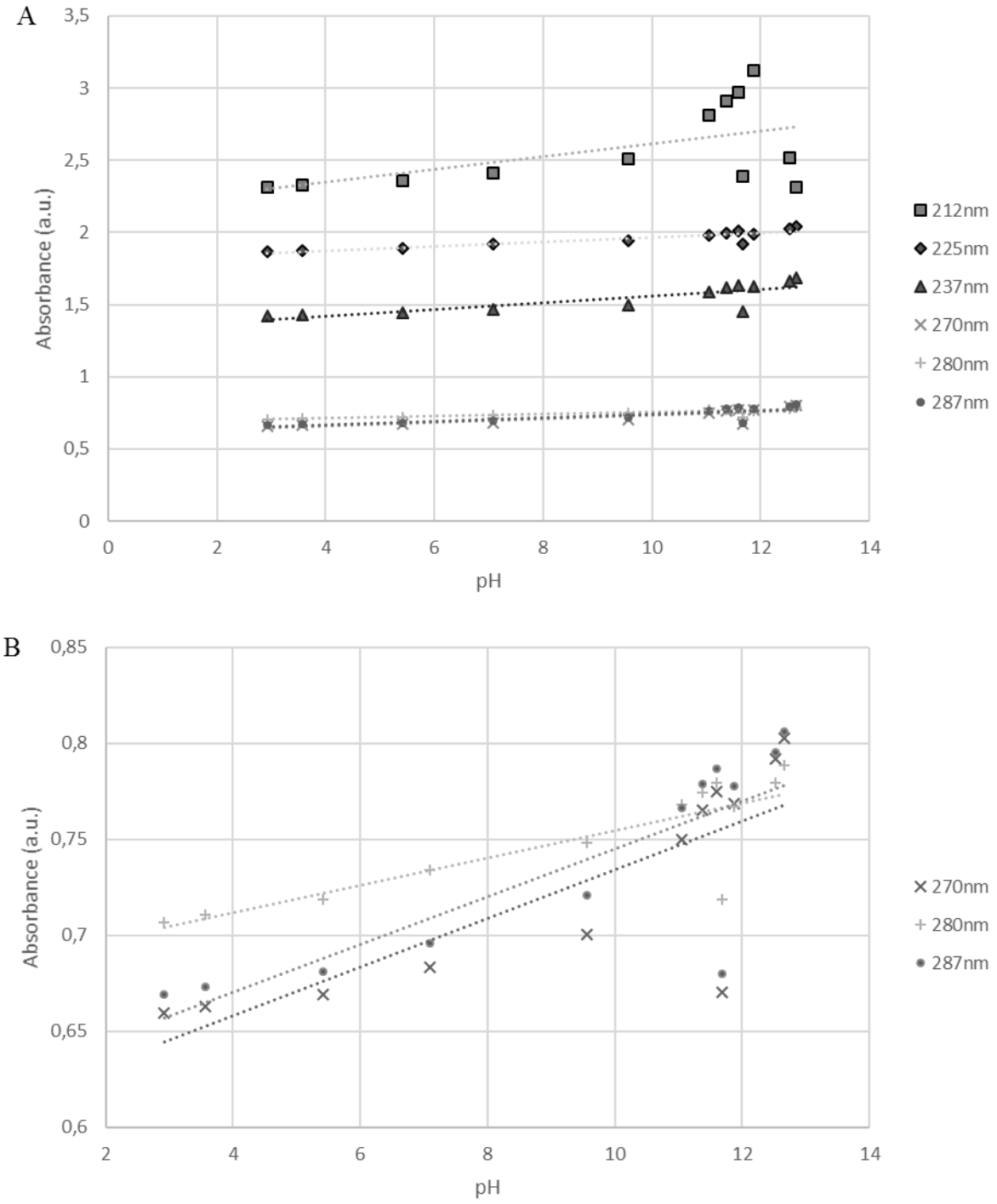

Figure 18. The effect of pH to absorbance in UV/Vis with 122 mg L^{-1} lignosulphonate, (A) with wavelengths of 212, 225, 237, 270, 280 and 287 nm, and (B) with wavelengths of 270, 280 and 287 nm

5.4 Equations used in calculations

The permeate flux was calculated in accordance with the permeate weighing with Equation (3):

$$J = \frac{m_P}{A_m t}, \quad (3)$$

Where

J	permeate flux, kg m^{-2} h^{-1}
m_p	mass of the permeate, kg
A_m	membrane surface area, m^2, and
t	time, h.

When operating the DSS system with multiple membranes, Equation (4) was used to calculate the transmembrane pressures (*TMP*) for each of the membranes separately (Lahti, 2009) assuming that the pressure drop is equal on each of the membranes:

$$TMP = p_{out} + \left(n - \frac{1}{2}\right) * \frac{p_{in} - p_{out}}{n_{tot}}, \quad (4)$$

Where

TMP	transmembrane pressure per each membrane, bar
p_{in}	inlet pressure, bar
p_{out}	outlet pressure, bar
n	membrane ordinal number, the last membrane being No. 1, -, and
n_{tot}	total number of the membranes plus 1 which equals the number of the spacer plates in the membrane stack, -.

Membrane fouling was monitored by comparing the pre- and post-filtration pure water fluxes by using Equation (5):

$$PWF_r = \left(\frac{PWF_b - PWF_a}{PWF_b}\right) * 100\%, \quad (5)$$

Where

PWF_r	pure water flux return, %
PWF_b	pure water flux before filtration, kg m^{-2} h^{-1}, and
PWF_a	pure water flux after filtration, kg m^{-2} h^{-1}.

In UV-Vis analysis, the extinction coefficient ε for calibration curves and the concentration c of a substance (lignosulphonate) was calculated with Equation (6), Beer-Lambert law:

$$A = \varepsilon l c, \tag{6}$$

Where

A	absorbance, -
ε	extinction coefficient, L g^{-1} cm^{-1}
l	optical path length, cm, and
c	concentration, g L^{-1}.

In production of concentrated lignosulphonate and -sugar fractions mass reduction factor was calculated by using Equation (7):

$$MRF = \frac{m_0}{m_0 - m_R}, \tag{7}$$

Where

MRF	mass reduction factor, -
m_0	initial feed mass, g, and
m_R	mass of retentate, g.

6 RESULTS AND DISCUSSION

The performance of a membrane process is determined by both membrane permeability and membrane selectivity, which are affected by characteristics (Butylina, 2007, Marson et al., 2021), feed temperature and operating pressure (Wagner, 2001). Membrane permeability can be determined from the slope when the measured flux is plotted against *TMP*, whereas membrane selectivity is determined by calculating corresponding retention factors (Equation 1). This chapter covers the results of the filtration experiments. Full data can be found in the Appendixes III and IV.

6.1 The effect of pH into membrane permeability

Membrane permeability was monitored by measuring the permeate fluxes and calculating permeabilities from the slopes with Microsoft Excel's slope-function. Due to the rather big variance in the membrane MWCO (from 1 to 10 kDa), rather low filtration pressures were used. The low pressures were also due to the willingness to operate within the boundaries set by regimen (I) of the critical flux theory (Muro et al., 2012) described in literature part.

The test pressures of 1–4 bar in the filtrations at 32 °C with pH 0.88 and 6.33 were too low for the tighter membranes and hence no too far-fetching conclusions could be drawn based on the fluxes. It should be noted that due to the lack of standardization in how the manufacturers determine the membrane MWCO the given cut-offs should always be taken as directional and not exact when comparing membrane properties. The spent liquor permeate-fluxes at pH 0.88 and 6.33, 32 °C, 1–4 bar, and 0.8 m s^{-1} are shown in Figure 19–Figure 21.

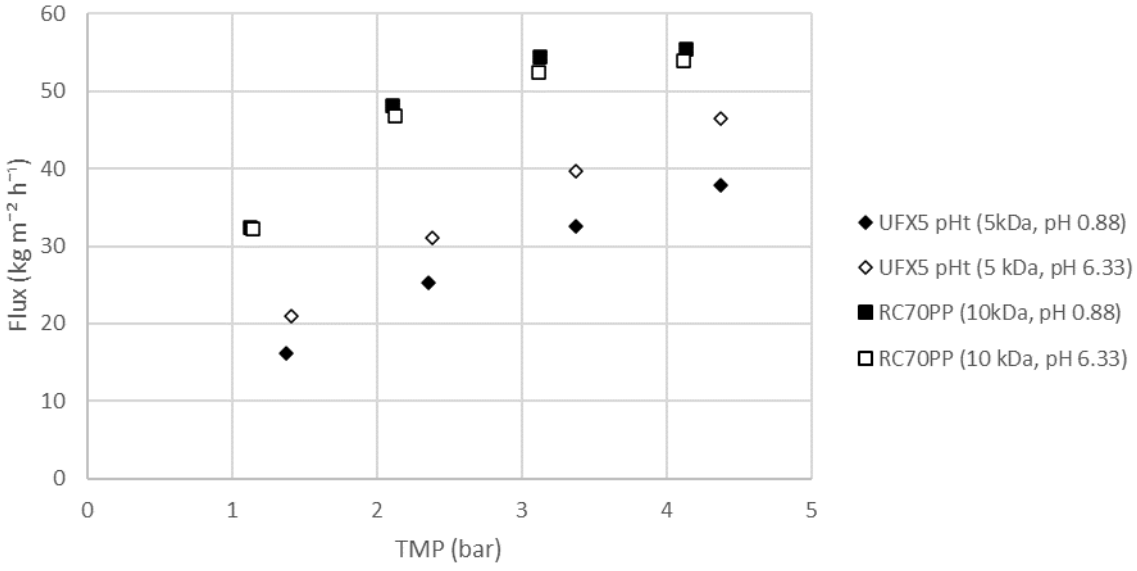

Figure 19. Spent liquor permeate flux with (UFX5 pHt and RC70PP, pH = 0.88 and 6.33, T = 32 °C, p = 1–4 bar, v = 0.8 m s^{-1})

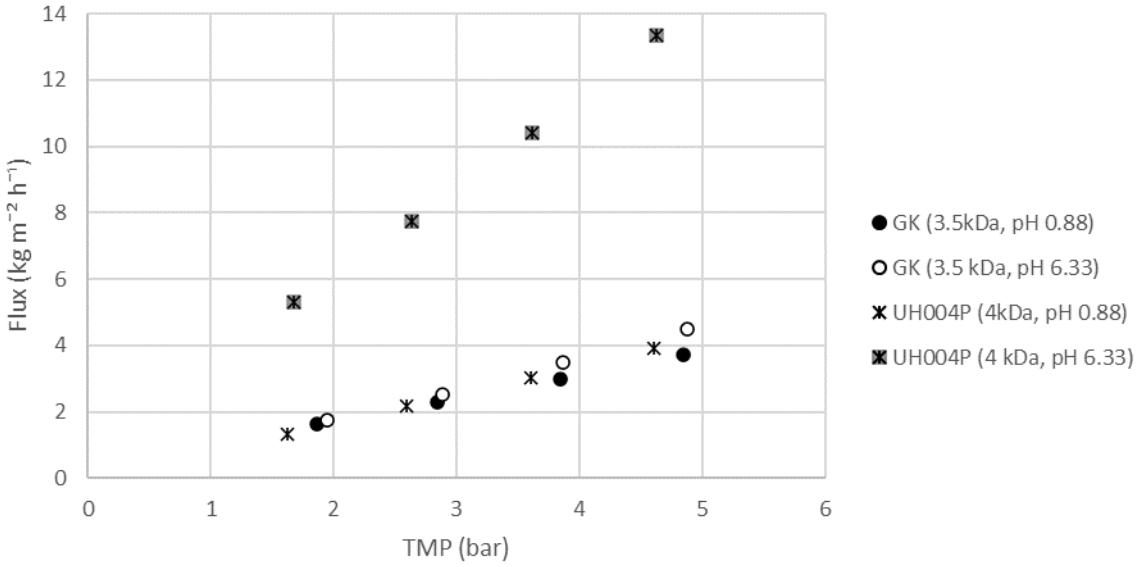

Figure 20. Spent liquor permeate flux with (GK and UH004P, pH = 0.88 and 6.33, T = 32 °C, p = 1–4 bar, v = 0.8 m s^{-1})

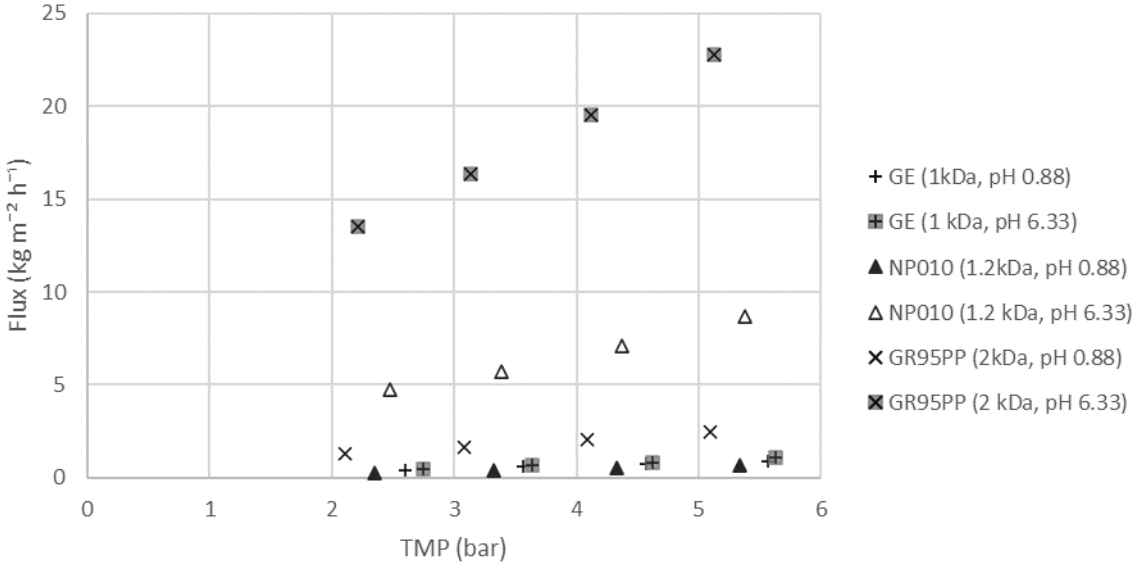

Figure 21. Spent liquor permeate flux with (GE, NP010 and GR95PP, pH = 0.88 and 6.33, T = 32 °C, p = 1–4 bar, v = 0.8 m s^{-1})

As shown in Figure 19–Figure 21, the variations in flux and *TMP* were linear (and most likely reversible), with RC70PP and UFx5 pHt being exception, and hence it could be concluded that the operation of all but these two was well within the boundaries of critical flux theory's regimen (I). An increase in pH seemed to be favorable in terms of permeate flux (Table 8) for all but the loosest membrane, RC70PP. Besides the differences in membrane materials this could have been due to reversible or irreversible membrane compaction (Stade et al. 2013) also.

Table 8. The effect of pH into permeate flux, kg m^{-2} h^{-1}, (pH = 0.88 and 6.33, T = 32 °C, p = 4 bar, v = 0.8 m s^{-1})

pH	GE (1kDa)	NP010P (1.2kDa)	GR95PP (2kDa)	GK (3.5kDa)	UH004P (4kDa)	UFX5 pHt (5kDa)	RC70PP (10kDa)
0,88	0,92	0,67	2,50	3,71	3,92	37,88	55,46
6,33	1,08	8,67	22,75	4,50	13,33	46,54	53,88

Change in spent liquor- and pure water permeabilities in pH 4.70, temperatures of 45 and 60 °C, 1–4 bar, and 0.8 m s^{-1} is shown in Figure 22. The plot elucidates the scale of the pH-related change into permeability. A change in pH had a rather significant impact (up to approx. 1000 % with NP010) on permeabilities. The phenomenon could be at least partly explained by the changes in the membrane surface charges (Childress and Elimelech, 1996). Overall, operating the membrane process with an elevated pH seemed to be well justified. The fact that pH 0.88 is a very extreme pH for all the membranes used in the experiments was also something to keep in mind.

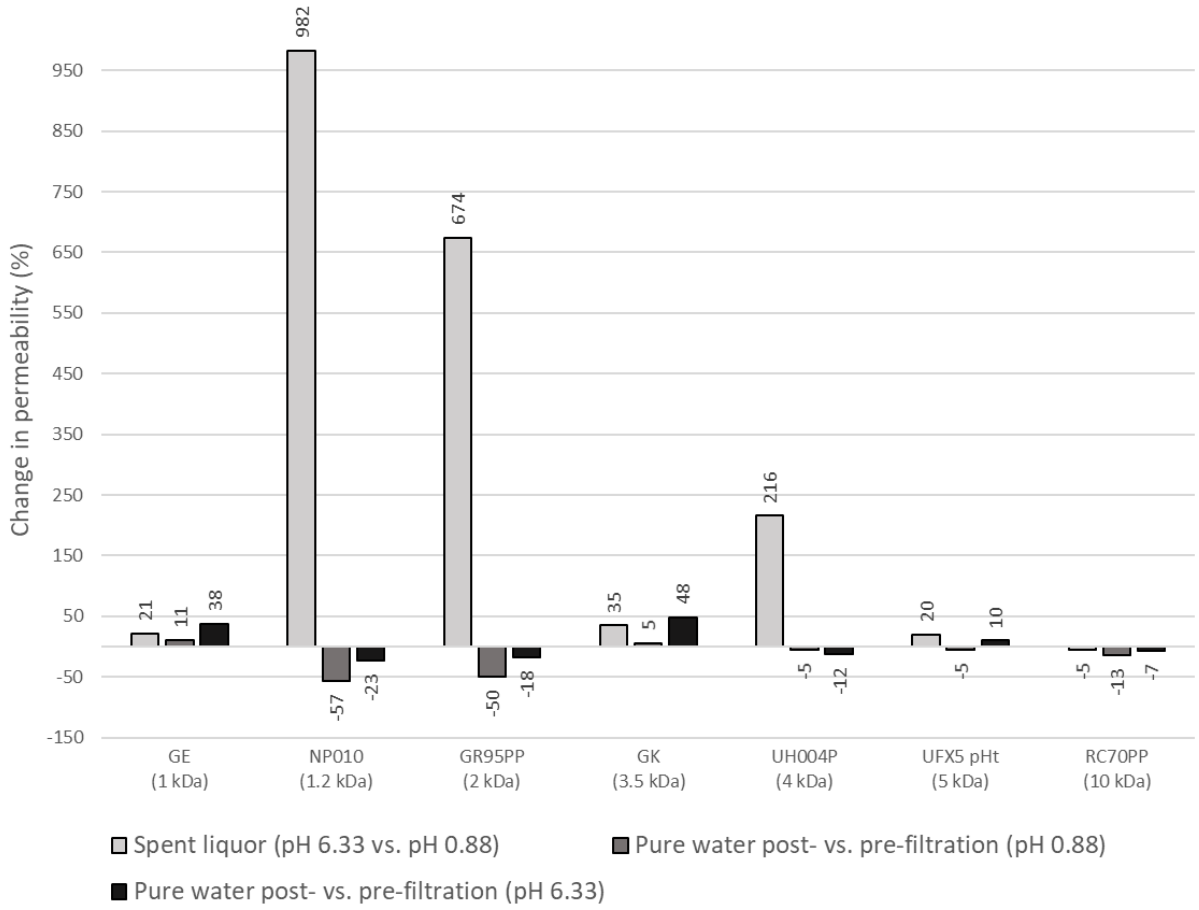

Figure 22. Change of spent liquor- and pure water permeability in percentages (pH = 0.88 and 6.33, T = 32 °C, p = 1–4 bar, v = 0.8 m s^{-1})

6.2 The effect of temperature into membrane permeability

To overcome the problems due to the wide range of MWCO and to better monitor membrane performance, subsequent filtrations were performed using in the same experiment only the membranes with MWCO closer to each other. Here, the filtration experiment was carried out in pH 4.70, temperatures of 45 and 60 °C, 1–4 bar, and 0.8 m s^{-1}. As shown in Figure 23, permeate flux was improved with all the three membranes with increasing temperature (UH004P, UFx5 pHt and RC70PP), which is well in line with (Wang et al., 2007 and Wagner 2001). Here, again, the permeate flux increase of RC70PP wasn't linear with *TMP* most likely due to membrane compaction caused by the test pressures being too high for such a membrane.

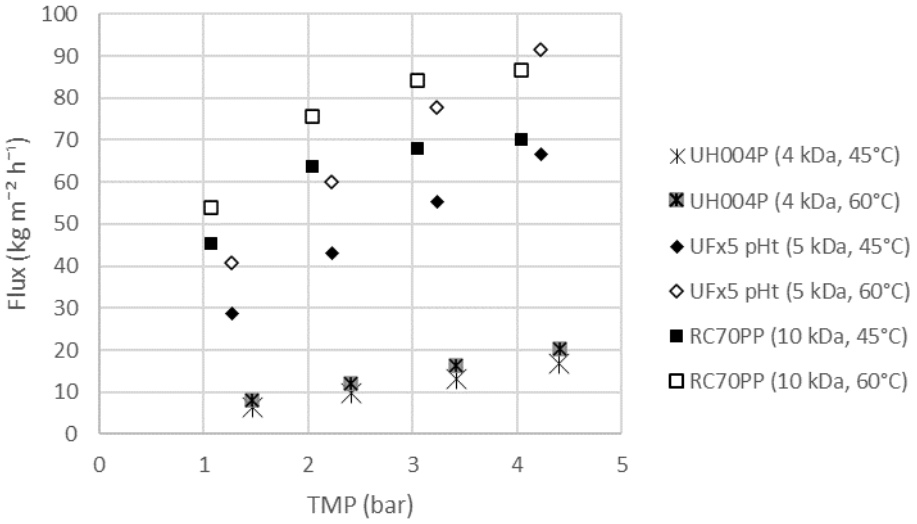

Figure 23. Spent liquor permeate flux with a stack of three membranes (MWCO = 4, 5 and 10 kDa, pH = 4.70, T = 45 and 60 °C, p = 1–4 bar, v = 0.8 m s^{-1})

Filtration experiment with the tighter membranes (NFG, GE and NP010) was performed with higher pressures to better monitor the membrane potential. The filtration experiment was carried out at pH 4.70, temperatures of 45 and 60 °C, 4–16 bar, and 0.8 m s^{-1}. As shown in Figure 24, the experiment gave inconsistent results: the flux of NP010 seemed to be rather unaffected by temperature whereas the flux of NFG showed major improvement. This could be at least partially explained by membrane compaction caused by temperature and pressure Wagner (2001), but a more probable cause might have been membrane fouling (Figure 43, p. 55).

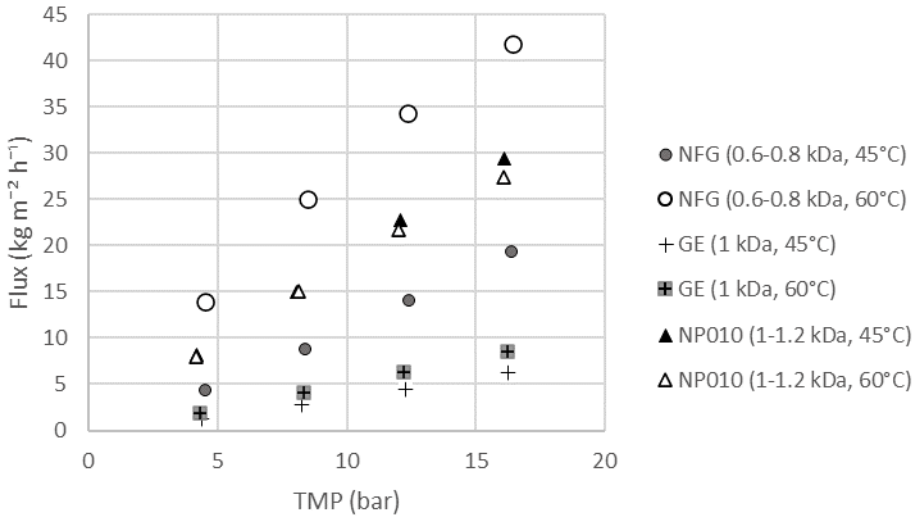

Figure 24. Spent liquor permeate flux with a stack of three membranes (MWCO = 0.6–0.8, 1 and 1–1.2 kDa, pH = 4.70, T = 45 and 60 °C, p = 4–16 bar, v = 0.8 m s^{-1})

To weigh the probability of membrane compaction into permeate fluxes, a plot of filtration pressure against the Wagner units calculated by using Equation (2) was drawn (Figure 25). The plot reveals that each of the filtration experiments took place on a zone of under 1200 Wagner units which, according to Wagner (2001), is held as safe i.e., not causing notable compaction. That is why it could be concluded that membrane compaction most likely was not an issue (at least not a major one) with the filtration experiments. It should be noted that estimating membrane compaction causing stress with Wagner units was rather unsuitable for RC70PP due to the compaction being clearly present, as was seen with e.g., pure water and permeate fluxes.

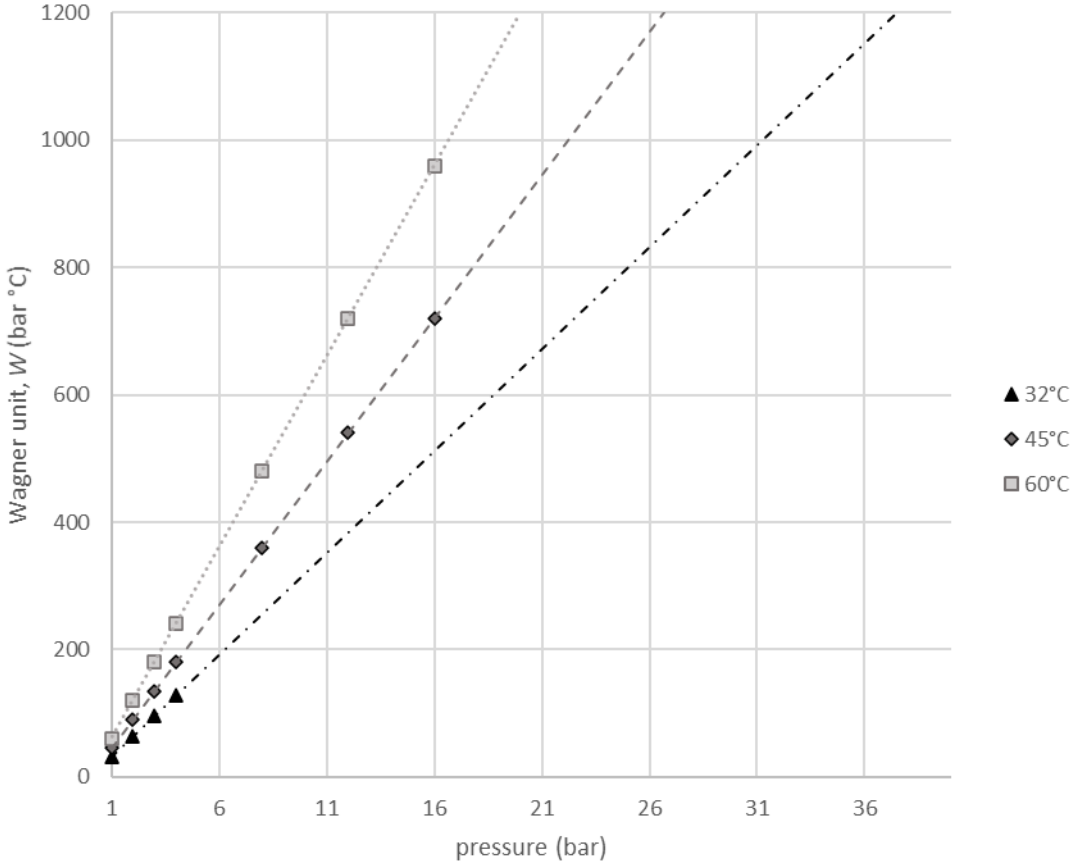

Figure 25. Membrane compaction causing stress estimated with Wagner units (T = 32, 45 and 60 °C, p = 1–16 bar)

Change in spent liquor- and pure water permeabilities in pH 4.70, temperatures of 45 and 60 °C, 4–16 bar, and 0.8 m s^{-1} is shown in Figure 26. The plot elucidates the effects of temperature into permeability. An increase in spent liquor temperature was clearly positive with all but NP010 although the impact was of a minor scale. It should be noted that the permeability decrease with NP010 was probably within a range of experimental error.

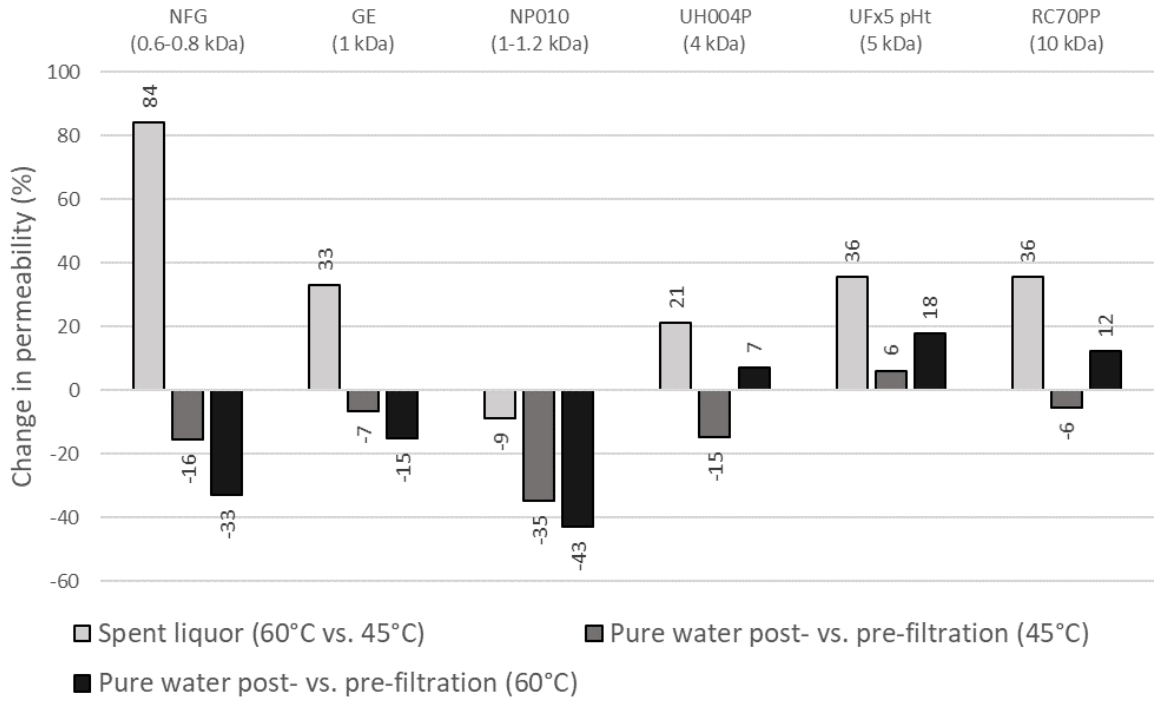

Figure 26. Change of spent liquor- and pure water permeability in percentages (pH = 4.70, T = 45 and 60 °C, p = 1–4 (RC70PP, UFx5 pHt and UH004P) and 4–16 bar (NP010, GE and NFG), v = 0.8 m s^{-1})

As stated by Wagner (2001), an increase of 1–3 % in flux per an increase of 1 °C in temperature can be presumed. As shown in Table 9, the flux increase was within the range of 1–3 % when comparing the filtrations at 45 and 32 °C, and 60 and 45 °C with all but NP010 which showed a decrease of 0.4 and 0.3 %/1 °C in the permeate flux. The flux increase due to increased temperature can probably be explained by a decline in spent liquor viscosity. The flux decline with NP010 could be at least partially explained by differences in membrane characteristics and fouling. Overall, operating the membrane process with as high a temperature as possible seemed to be well justified in terms of permeability.

Table 9. Spent organosolv liquor flux and permeate flux increase (%/1 °C) in various conditions

	UH004P (4 kDa)	UFx5 pHt (5 kDa)	RC70PP (10 kDa)
Flux, liquor, kg m^{-2} h^{-1}, (32°C, pH 6.33, 4 bar)	13,3	46,5	53,9
Flux, liquor, kg m^{-2} h^{-1}, (45°C, pH 4.70, 4 bar)	16,7	66,6	70,0
Flux, liquor, kg m^{-2} h^{-1}, (60°C, pH 4.70, 4 bar)	20,5	91,6	86,6
Flux increase 45°C vs. 32°C (%/1°C)	1,9	3,3	2,3
Flux increase 60°C vs. 45°C (%/1°C)	1,5	2,5	1,6

	NFG (0.6-0.8 kDa)	GE (1 kDa)	NP010 (1-1.2 kDa)
Flux, liquor, kg m^{-2} h^{-1}, (32°C, pH 6.33, 4 bar)	-	1,1	8,7
Flux, liquor, kg m^{-2} h^{-1}, (45°C, pH 4.70, 4 bar)	4,3	1,3	8,3
Flux, liquor, kg m^{-2} h^{-1}, (60°C, pH 4.70, 4 bar)	14,0	1,9	7,9
Flux increase 45°C vs. 32°C (%/1°C)	-	1,5	-0,4
Flux increase 60°C vs. 45°C (%/1°C)	15,3	3,2	-0,3

6.3 Membrane selectivity

Contributing to membrane performance, membrane selectivity is a vital factor in membrane processes also. Membrane selectivity was monitored by analyzing the samples (feed, retentate and permeate) for lignosulphonates, total sugars, TOC, and conductivity. Corresponding retention factors (from here on R=R_{obs}) were calculated by using Equation (1). The retention factors for lignosulphonates and total sugars were calculated to monitor the membrane selectivity. The retention factors for TOC and conductivity were calculated to monitor the removal of organic compounds and salts, respectively.

6.3.1 Analysis

The effect of pH into spent liquor could also be seen by eye i.e., the sample color changed with pH (Figure 27). This was most likely due to an increase in pH leading into better lignosulphonate solubility, as demonstrated by e.g., Zhang et al., (2017). All the samples were analyzed for lignosulphonates, total sugars, pH, conductivity, and DM. Brix, on the other hand, turned out to be anything but suitable for measuring the sugar content of the samples since it was in a very good correlation with DM in the membrane filtration experiments (Figure 28, A) i.e., brix acted as an indicator of DM instead of sugar content.

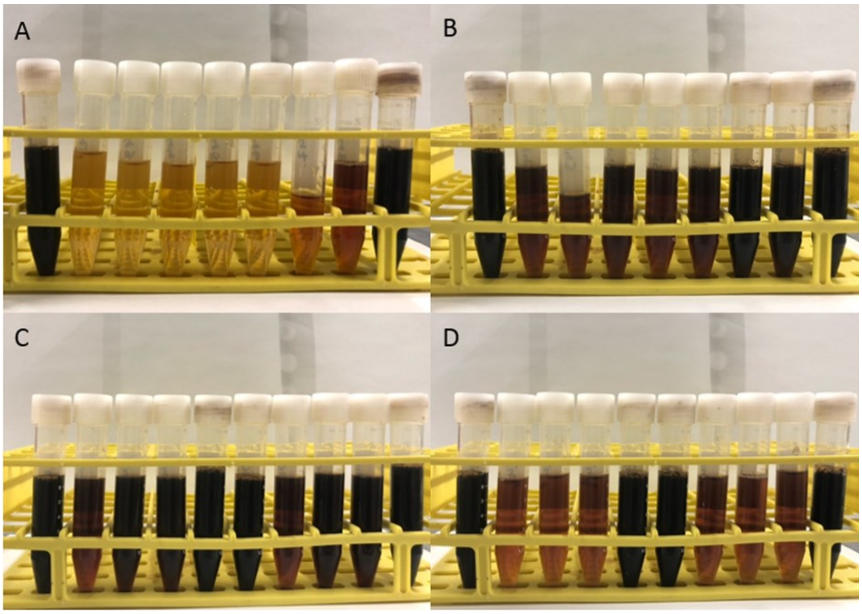

Figure 27. Filtration samples: (A), pH 0.88 at 32 °C; (B), pH 6.33 at 32 °C; (C), pH 4.70 at 45 and 60 °C (4, 5 and 10 kDa); and (D), pH 4.70 at 45 and 60 °C (0.6–0.8, 1 and 1–1.2 kDa)

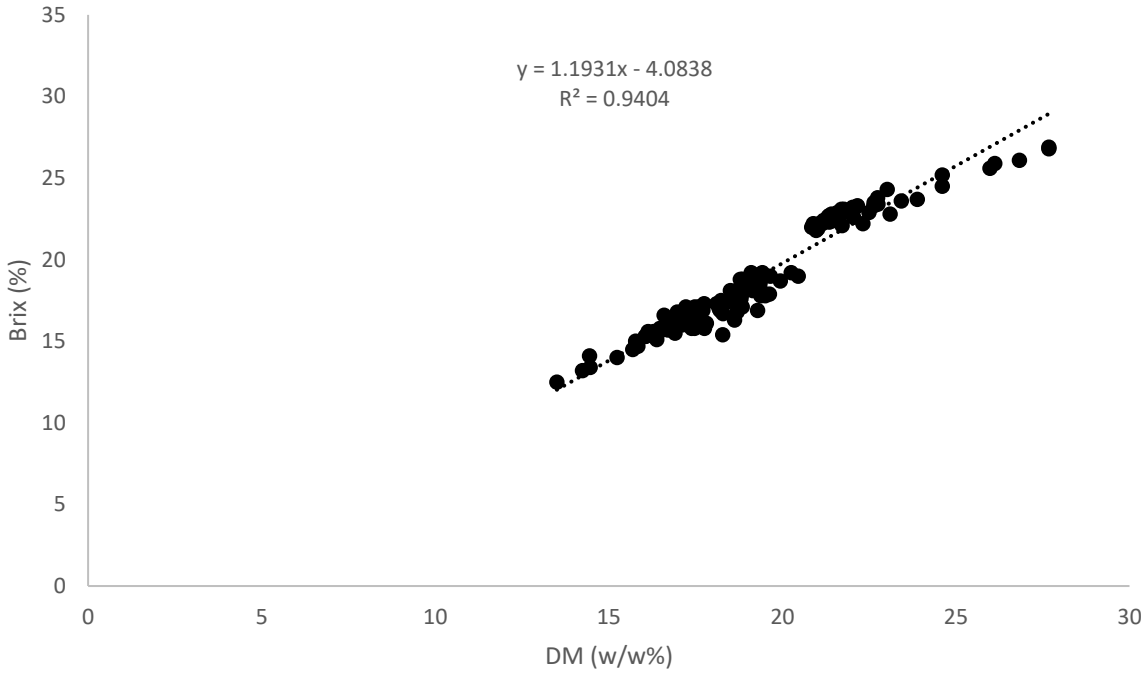

Figure 28. Correlation between dry matter (w/w%) and brix (%) (A) in filtration experiments, and (B) in production of lignosulphonate fraction from the extract with membrane filtration and discontinuous diafiltration

6.3.2 Lignosulphonate retention

The retention factors for lignosulphonates calculated with Equation (1) are shown in Figure 29–Figure 31. As could be expected, the membranes with higher MWCO showed lower retention for lignosulphonates as opposed to the tighter membranes. This was most likely due to the molecular weight of lignosulphonates being smaller than the membrane MWCO to a great extent. As shown in (Figure 29) the differences in lignosulphonate retention in relation to pH seemed rather negligible. It could be concluded that spent liquor pH had no effect on membrane selectivity in terms of lignosulphonate.

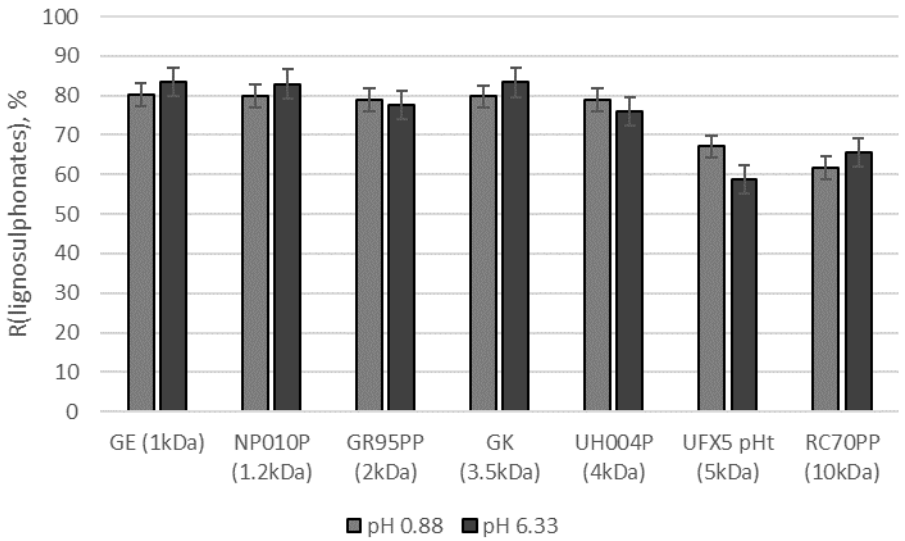

Figure 29. Lignosulphonate retention in filtration experiment with seven different membranes (pH = 0.88 and 6.33, T = 32 °C, p = 1–4 bar, v = 0.8 m s^{-1})

The differences in lignosulphonate retention in relation to temperature showed negligible results also, as can be seen in Figure 30 and Figure 31. Here, as with pH, membrane MWCO seemed to affect the membrane selectivity in terms of lignosulphonate more than the change in feed temperature. All in all, the lignosulphonate retentions at 45 and 60 °C were good (in the range of 80–90 %) with all but UFx5 pHt and RC70PP. It could be concluded that spent liquor temperature had no effect on membrane selectivity in terms of lignosulphonate.

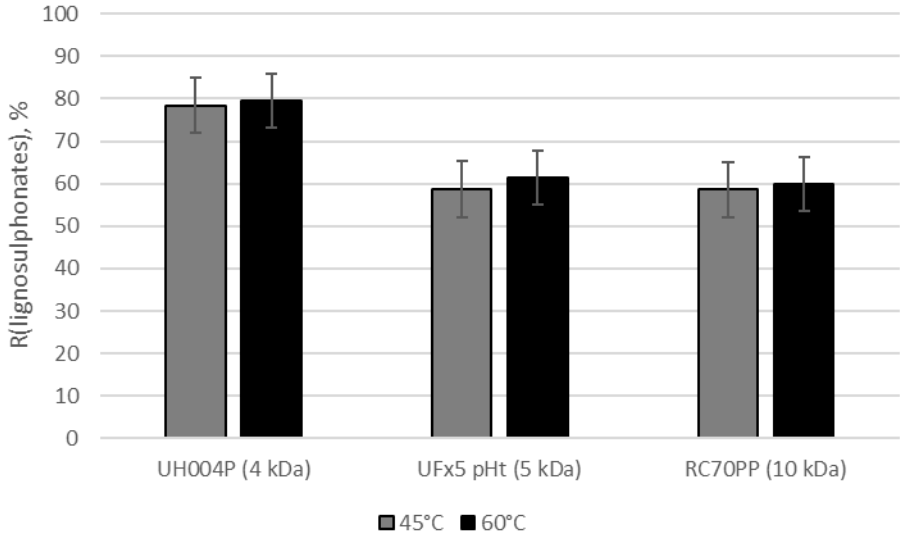

Figure 30. Lignosulphonate retention in filtration experiment with three different membranes (pH = 4.70, T = 45 and 60 °C, p = 1–4 bar, v = 0.8 m s^{-1})

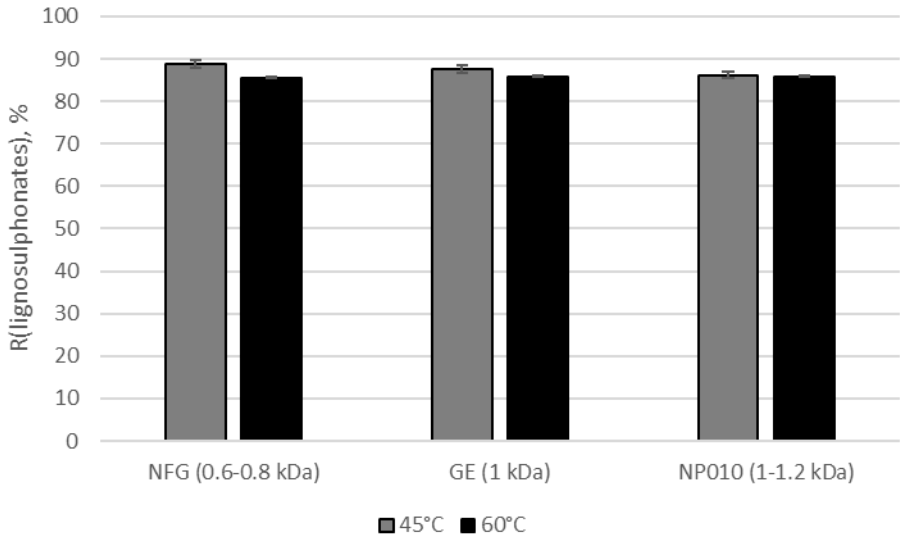

Figure 31. Lignosulphonate retention in filtration experiment with three different membranes (pH = 4.70, T = 45 and 60 °C, p = 4–16 bar, v = 0.8 m s^{-1})

6.3.3 Total sugars retention

The retention factors for total sugars calculated with Equation (1) are shown in Figure 32–Figure 34. An increase in spent liquor pH had a negligible effect on retention of sugars (Figure 32). All the seven membranes showed a retention close to 0 % (the negative readings being most likely due to analytical error) for total sugars i.e., the sugars permeated freely through membranes (which could be expected due to the molecular weight of sugars being so much

lower than the MWCO of the membranes). Due to retention margins being so low it could be concluded that the effect of pH into sugar retention was negligible.

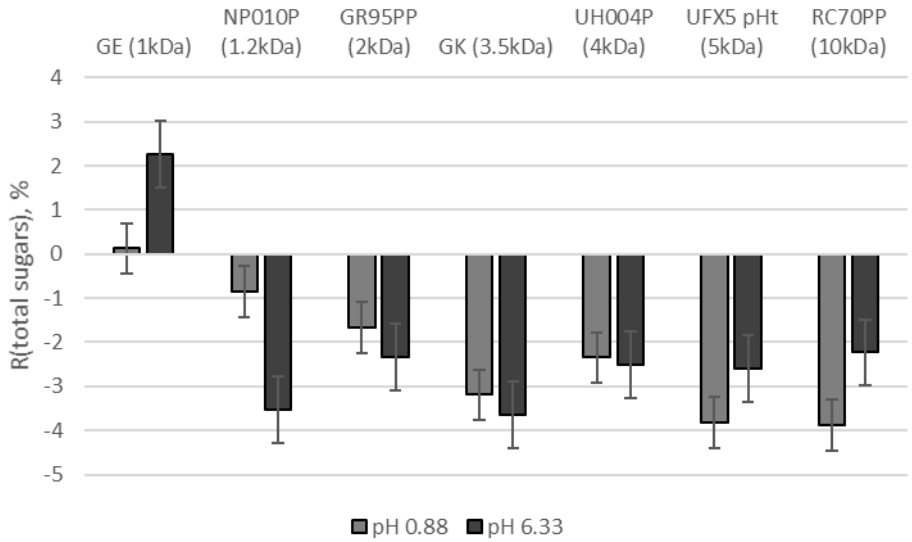

Figure 32. Total sugars retention in filtration experiment with seven different membranes (pH = 0.88 and 6.33, T = 32 °C, p = 1–4 bar, v = 0.8 m s^{-1})

In terms of temperature (Figure 33 and Figure 34), an increase in temperature seemed to favor the permeation of sugars through the membranes with all the six membranes used with filtrations at 45 and 60 °C. An increase in temperature seemed to lead into negative retention factors i.e., concentration of sugars in permeate. The margins were rather small, though, and the negative readings could most likely be explained by analytical error. Due to retention margins being so low it could be concluded that the effect of temperature into sugar retention was negligible.

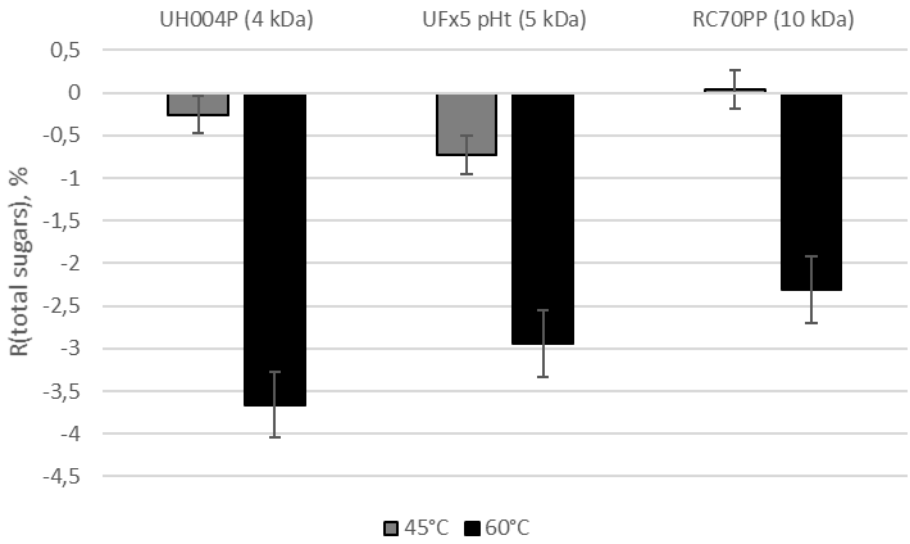

Figure 33. Total sugars retention in filtration experiment with three different membranes (pH = 4.70, T = 45 and 60 °C, p = 1–4 bar, v = 0.8 m s^{-1})

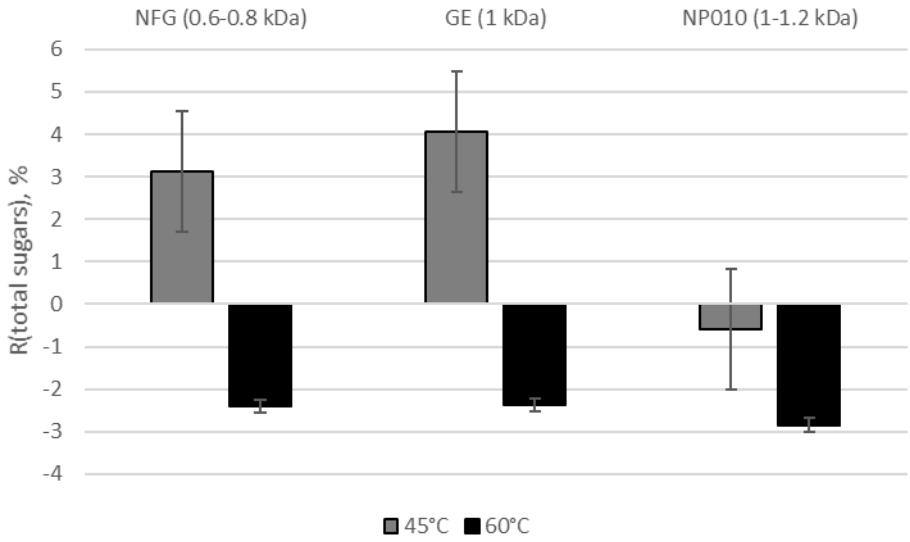

Figure 34. Total sugars retention in filtration experiment with three different membranes (pH = 4.70, T = 45 and 60 °C, p = 4–16 bar, v = 0.8 m s^{-1})

6.3.4 TOC retention

TOC retention is used to measure how well the membrane can remove organic matter from the liquid. Here, pH adjustment of the spent liquor (Figure 35) seemed to have rather inconsistent yet small effect on TOC retention. Here, also, membrane MWCO seemed to affect the membrane selectivity more – the tighter membranes had better retentions than the looser. Yet, due to the margins being well in the range of experimental error it seemed that the effect of pH into TOC retention was negligible.

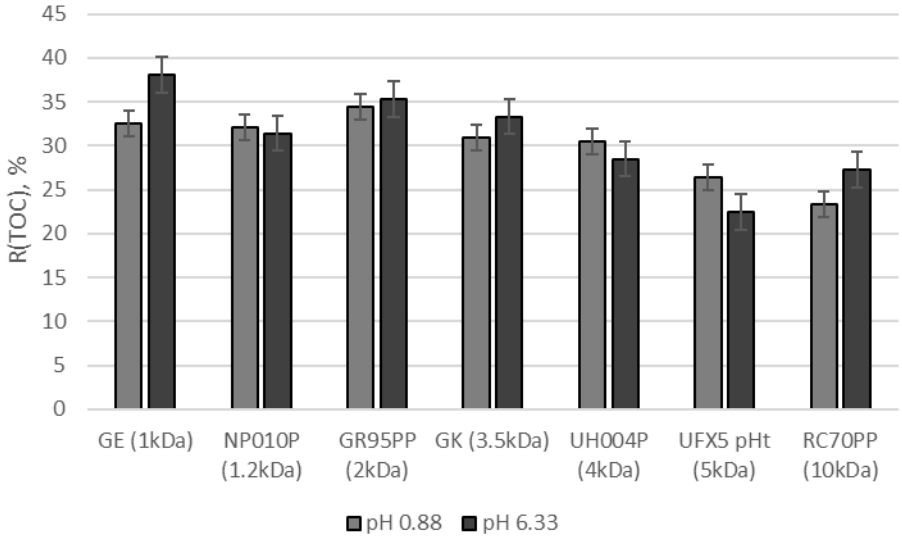

Figure 35. TOC retention in filtration experiment with seven different membranes (pH = 0.88 and 6.33, T = 32 °C, p = 1–4 bar, v = 0.8 m s^{-1})

The effect of temperature on TOC retentions (Figure 36 and Figure 37) seemed to be rather inconsistent also. The membrane MWCO seemed to affect the TOC retentions mostly on a similar way than monitored with the pH i.e., the tighter membranes showed better TOC retentions when compared to the looser ones, with UFx5 pHt being an exception. Due to the margins being well in the range of experimental error it seemed that the effect of temperature into TOC retention was negligible.

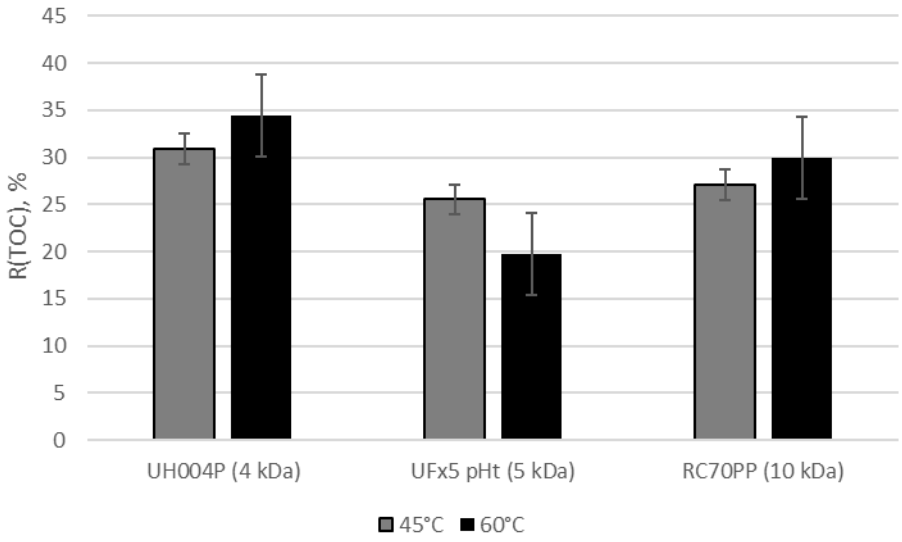

Figure 36. TOC retention in filtration experiment with three different membranes (pH = 4.70, T = 45 and 60 °C, p = 1–4 bar, v = 0.8 m s^{-1})

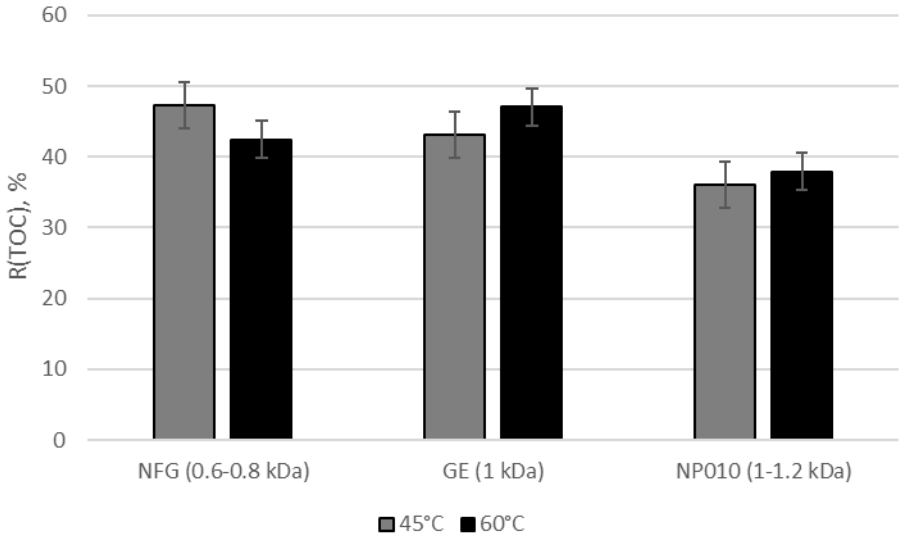

Figure 37. TOC retention in filtration experiment with three different membranes (pH = 4.70, T = 45 and 60 °C, p = 4–16 bar, v = 0.8 m s^{-1})

6.3.5 Conductivity retention

Conductivity retention measures the ability of the membrane to remove salts and organic chemicals affecting the liquid's ability to pass electric current. The more salts and organic chemicals present, the higher the conductivity. The effect of pH adjustment (Figure 38) into conductivity retention was well in the range of experimental error but it seemed that, due to the margins being so small, the effect was negligible.

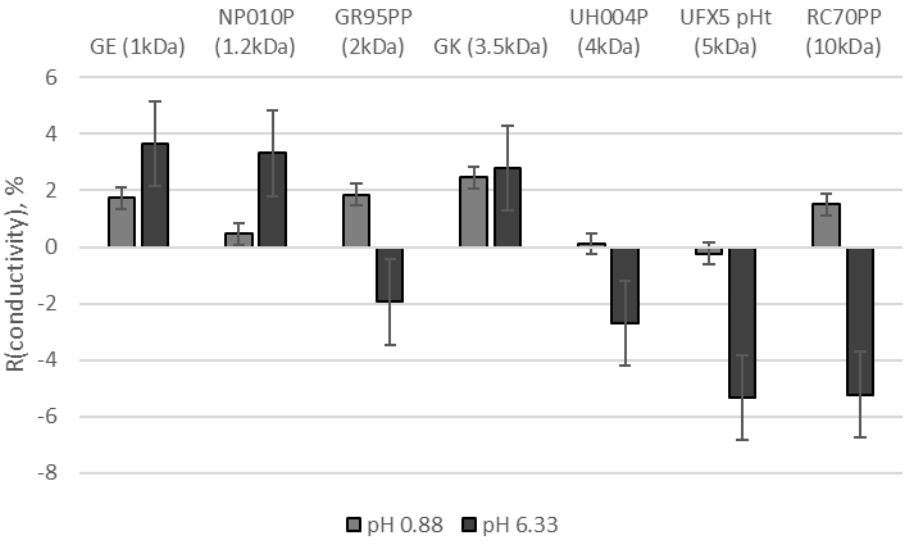

Figure 38. Conductivity retention in filtration experiment with seven different membranes (pH = 0.88 and 6.33, T = 32 °C, p = 1–4 bar, v = 0.8 m s^{-1})

Temperature wise (Figure 39 and Figure 40) the results were also inconsistent in terms of conductivity retention. Here, again, the results are well in the range of analytical error although due to the small margins it seemed that the effect of temperature into conductivity retention was negligible.

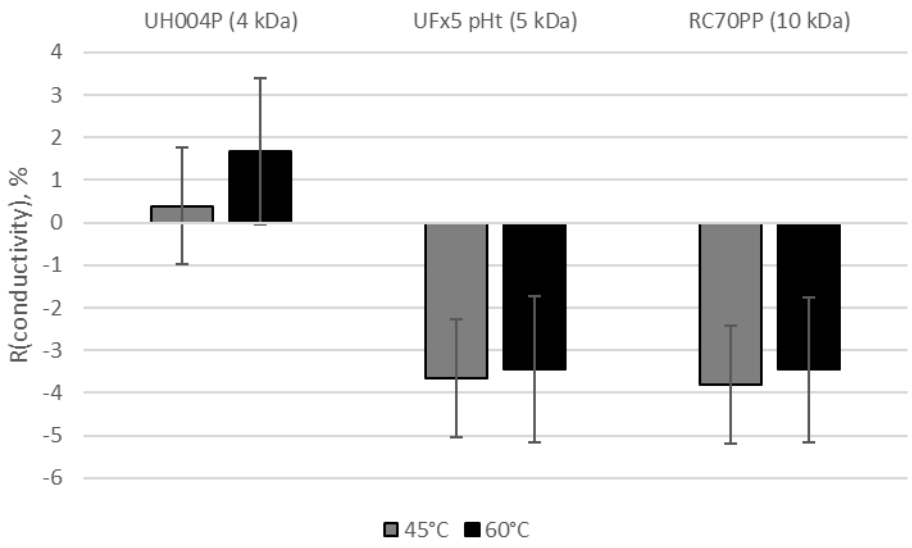

Figure 39. Conductivity retention in filtration experiment with three different membranes (pH = 4.70, T = 45 and 60 °C, p = 1–4 bar, v = 0.8 m s^{-1})

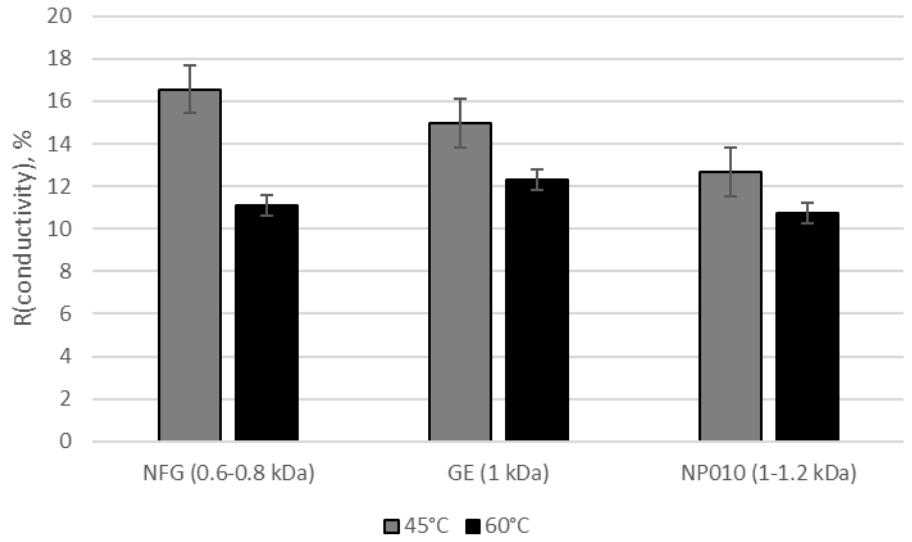

Figure 40. Conductivity retention in filtration experiment with three different membranes (pH = 4.70, T = 45 and 60 °C, p = 4–16 bar, v = 0.8 m s^{-1})

6.3.6 Sample profiles

After analyzing the samples for lignosulphonates and sugars, sample profiles (Table 10–Table 15) were made to better examine the analytical results. Here, DM was analyzed by oven drying the samples at 105 °C until reaching stable weight. The oven dried DM (w/w%) was approx. five percentage points lower than the freeze dried DM (w/w%) probably due to the volatile acids (see Appendix IV) and turned out to be more suitable for the sample profiles compared to freeze dried DM. Lignosulphonate weight-based concentrations were calculated from the volume-based concentrations by using the appropriate densities obtained when preparing the samples for freeze drying i.e., by pipetting 1–2 ml of the samples and weighing them with Precisa H225SM-FR balance. The results were then checked in the last row by subtracting the percentage values of lignosulphonates, total sugars and GLY/AA/LA/EtOH/HMF from DM. The subtractions of the percentage values were in the range of -3.4 to 3.1 % and hence the results could be held rather reliable. The deviations were probably caused by the conversion of lignosulphonate concentrations from volume- to weight-based. Also, a minor deviation was probably caused by ash and other compounds.

A comparison of sample profiles of filtration experiments at pH 0.88 and 6.33, 32 °C, 4 bar, and 0.8 m s^{-1} (Table 10 and Table 11) showed some correlation between membrane MWCO and DM content in permeate even though the results were most likely in the range of experimental error. An increase in pH seemed to have no notable effect on permeation of lignosulphonates and sugars. It seemed that the only difference between these two filtrations, on an analytical point of view, was DM content, which was 2.0–3.2 percentage points higher in pH 6.33. The difference in DM content might be in the range of experimental error and would need further experimenting to be confirmed. This data supports what was seen on R_{obs} comparison.

Table 10. Sample profile (pH = 0.88, T = 32 °C, p = 4 bar, v = 0.8 m s^{-1})

32°C, pH 0.88, 4 bar	Feed	GE (1kDa)	NP010 (1.2kDa)	GR95PP (2kDa)	GK (3.5kDa)	UH004P (4kDa)	UFX5 pHt (5kDa)	RC70PP (10kDa)	Retentate
density, g L^{-1}	1061,1	1050,5	1047,7	1055,7	1056,6	1046,2	1053,9	1059,7	1051,8
DM (oven dried), w/w%	16,8 %	11,7 %	11,5 %	12,2 %	12,1 %	12,1 %	13,7 %	13,9 %	16,9 %
Lignosulphonates, w/w%	9,6 %	1,8 %	1,6 %	1,9 %	1,7 %	1,9 %	2,8 %	3,4 %	9,5 %
Total sugars, w/w%*	9,0 %	8,8 %	8,9 %	9,1 %	9,1 %	9,1 %	9,4 %	9,3 %	9,1 %
Glucose, w/w%*	1,2 %	1,1 %	1,3 %	1,3 %	1,2 %	1,3 %	1,3 %	1,3 %	1,3 %
Xylose, w/w%*	2,0 %	2,0 %	2,0 %	2,0 %	2,1 %	2,0 %	2,1 %	2,0 %	2,0 %
Galactose (approx.), w/w%*	1,2 %	1,2 %	1,2 %	1,2 %	1,2 %	1,2 %	1,3 %	1,3 %	1,2 %
Arabinose, w/w%*	0,5 %	0,5 %	0,5 %	0,6 %	0,6 %	0,6 %	0,5 %	0,5 %	0,5 %
Mannose, w/w%*	4,1 %	3,9 %	3,9 %	4,0 %	4,0 %	3,9 %	4,1 %	4,1 %	4,0 %
GLY, AA, LA, EtOH, HMF, w/w%[1]	1,5 %	1,5 %	1,6 %	1,6 %	1,5 %	1,6 %	1,6 %	1,6 %	1,6 %
Other, w/w%[2]	-3,4 %	-0,3 %	-0,5 %	-0,3 %	-0,2 %	-0,4 %	0,0 %	-0,5 %	-3,2 %
*Analysis by St1 Oy									
[1]Glycerol, acetic acid, levulinic acid, ethanol and hydroxymethylfurfural									
[2]Ash and other compounds									

Table 11. Sample profile (pH = 6.33, T = 32 °C, p = 4 bar, v = 0.8 m s^{-1})

32°C, pH 6.33, 4 bar	Feed	GE (1kDa)	NP010 (1.2kDa)	GR95PP (2kDa)	GK (3.5kDa)	UH004P (4kDa)	UFX5 pHt (5kDa)	RC70PP (10kDa)	Retentate
density, g L^{-1}	1059,6	1045,5	1049,9	1054,2	1052,0	1052,1	1054,7	1062,4	1070,3
DM (oven dried), w/w%	19,6 %	13,9 %	14,3 %	15,1 %	14,2 %	15,3 %	16,7 %	16,2 %	19,5 %
Lignosulphonates, w/w%	9,6 %	1,4 %	1,4 %	2,0 %	1,4 %	2,0 %	3,6 %	3,2 %	9,2 %
Total sugars, w/w%*	8,5 %	8,9 %	8,9 %	8,8 %	8,9 %	8,8 %	8,8 %	8,7 %	8,5 %
Glucose, w/w%*	1,3 %	1,3 %	1,3 %	1,3 %	1,3 %	1,3 %	1,3 %	1,3 %	1,3 %
Xylose, w/w%*	1,8 %	1,9 %	1,9 %	1,9 %	1,9 %	1,9 %	1,9 %	1,9 %	1,8 %
Galactose (approx.) , w/w%*	1,1 %	1,2 %	1,2 %	1,1 %	1,2 %	1,2 %	1,2 %	1,2 %	1,1 %
Arabinose, w/w%*	0,5 %	0,5 %	0,5 %	0,5 %	0,5 %	0,5 %	0,5 %	0,5 %	0,5 %
Mannose, w/w%*	3,8 %	3,9 %	3,9 %	3,9 %	3,9 %	3,9 %	3,9 %	3,8 %	3,8 %
GLY, AA, LA, EtOH, HMF, w/w%[1]	1,4 %	1,5 %	1,6 %	1,5 %	1,5 %	1,3 %	1,4 %	1,4 %	1,4 %
Other, w/w%[2]	0,1 %	2,0 %	2,5 %	2,9 %	2,4 %	3,1 %	2,8 %	2,8 %	0,3 %
*Analysis by St1 Oy									
[1]Glycerol, acetic acid, levulinic acid, ethanol and hydroxymethylfurfural									
[2]Ash and other compounds									

A comparison of DM balance schemes of filtration experiments at pH 4.70, 45 and 60 °C, 4 bar, and 0.8 m s^{-1} (Table 12 and Table 13) showed, also, some correlation between membrane MWCO and DM content in permeate even though the results were most likely in the range of experimental error. An increase in temperature seemed to have no notable effect on permeation lignosulphonates and sugars. Here, also, the differences in DM content might be in the range of experimental error and would need further experimenting to be confirmed. Same as with liquor pH, this data supports what was seen on R_{obs} comparison.

Table 12. Sample profile (pH = 4.70, T = 45 °C, p = 4 bar, v = 0.8 m s^{-1})

45°C, pH 4.70, 4 bar	Feed	UH004P (4 kDa)	UFx5 pHt (5 kDa)	RC70PP (10 kDa)	Retentate
density, g L^{-1}	1065,8	1051,4	1060,1	1057,9	1064,7
DM (oven dried), w/w%	19,0 %	14,8 %	16,4 %	16,2 %	18,9 %
Lignosulphonates, w/w%	8,1 %	1,5 %	3,1 %	3,1 %	8,2 %
Total sugars, w/w%*	9,0 %	8,8 %	8,9 %	8,8 %	8,6 %
Glucose, w/w%*	1,3 %	1,3 %	1,3 %	1,3 %	1,3 %
Xylose, w/w%*	1,9 %	1,9 %	1,9 %	1,9 %	1,9 %
Galactose (approx.) , w/w%*	1,3 %	1,2 %	1,2 %	1,2 %	1,2 %
Arabinose, w/w%*	0,6 %	0,5 %	0,5 %	0,5 %	0,5 %
Mannose, w/w%*	3,9 %	3,8 %	3,9 %	3,8 %	3,8 %
GLY, AA, LA, EtOH, HMF, w/w%[1]	1,8 %	1,9 %	1,7 %	1,8 %	1,8 %
Other, w/w%[2]	0,1 %	2,6 %	2,7 %	2,5 %	0,3 %
*Analysis by St1 Oy					
[1]Glycerol, acetic acid, levulinic acid, ethanol and hydroxymethylfurfural					
[2]Ash and other compounds					

Table 13. Sample profile (pH = 4.70, T = 60 °C, p = 4 bar, v = 0.8 m s^{-1})

60°C, pH 4.70, 4 bar	Feed	UH004P (4 kDa)	UFx5 pHt (5 kDa)	RC70PP (10 kDa)	Retentate
density, g L^{-1}	1067,9	1053,7	1063,7	1061,1	1070,5
DM (oven dried), w/w%	19,7 %	15,3 %	17,2 %	16,9 %	20,1 %
Lignosulphonates, w/w%	8,8 %	1,7 %	3,3 %	3,4 %	9,0 %
Total sugars, w/w%*	8,9 %	9,3 %	9,2 %	9,1 %	9,1 %
Glucose, w/w%*	1,3 %	1,4 %	1,4 %	1,4 %	1,3 %
Xylose, w/w%*	1,9 %	2,0 %	2,0 %	2,0 %	2,0 %
Galactose (approx.) , w/w%*	1,2 %	1,3 %	1,3 %	1,3 %	1,3 %
Arabinose, w/w%*	0,5 %	0,5 %	0,5 %	0,5 %	0,5 %
Mannose, w/w%*	3,9 %	4,1 %	4,0 %	4,0 %	4,0 %
GLY, AA, LA, EtOH, HMF, w/w%[1]	1,4 %	1,5 %	1,4 %	1,4 %	1,4 %
Other, w/w%[2]	0,5 %	2,8 %	3,2 %	3,0 %	0,7 %
*Analysis by St1 Oy					
[1]Glycerol, acetic acid, levulinic acid, ethanol and hydroxymethylfurfural					
[2]Ash and other compounds					

Also, a comparison of DM balance schemes of DSS filtration at pH 4.70, 45 and 60 °C, 16 bar, and 0.8 m s^{-1} (Table 14 and Table 15) showed some correlation between membrane MWCO and DM content in permeate even though the results were most likely in the range of experimental error. An increase in temperature seemed to have no notable effect on permeation lignosulphonates and sugars. Here, also, the differences in DM content might be in the range of experimental error and would need further experimenting to be confirmed. Same as with liquor pH, this data supports what was seen on R_{obs} comparison.

Table 14. Sample profile (pH = 4.70, T = 45 °C, p = 16 bar, v = 0.8 m s^{-1})

45°C, pH 4.70, 16 bar	Feed	NFG (0.6-0.8 kDa)	GE (1 kDa)	NP010 (1-1.2 kDa)	Retentate
density, g L^{-1}	1074,1	1043,7	1041,6	1050,9	1070,4
DM (oven dried), w/w%	20,2 %	11,0 %	11,8 %	13,1 %	20,4 %
Lignosulphonates, w/w%	9,3 %	0,9 %	1,0 %	1,1 %	9,4 %
Total sugars, w/w%*	9,1 %	8,0 %	8,2 %	8,8 %	9,1 %
Glucose, w/w%*	1,3 %	1,1 %	1,2 %	1,3 %	1,3 %
Xylose, w/w%*	1,9 %	2,0 %	1,9 %	2,0 %	1,9 %
Galactose (approx.) , w/w%*	1,3 %	1,0 %	1,1 %	1,2 %	1,3 %
Arabinose, w/w%*	0,5 %	0,5 %	0,5 %	0,5 %	0,5 %
Mannose, w/w%*	4,0 %	3,4 %	3,5 %	3,8 %	4,0 %
GLY, AA, LA, EtOH, HMF, w/w%[1]	1,3 %	1,3 %	1,4 %	1,3 %	1,3 %
Other, w/w%[2]	0,5 %	0,7 %	1,1 %	1,9 %	0,5 %
*Analysis by St1 Oy					
[1]Glycerol, acetic acid, levulinic acid, ethanol and hydroxymethylfurfural					
[2]Ash and other compounds					

Table 15. Sample profile (pH = 4.70, T = 60 °C, p = 16 bar, v = 0.8 m s^{-1})

60°C, pH 4.70, 16 bar	Feed	NFG (0.6-0.8 kDa)	GE (1 kDa)	NP010 (1-1.2 kDa)	Retentate
density, g L^{-1}	1085,9	1055,6	1051,3	1058,1	1087,9
DM (oven dried), w/w%	23,0 %	14,5 %	14,1 %	15,2 %	23,1 %
Lignosulphonates, w/w%	11,1 %	1,3 %	1,2 %	1,3 %	11,1 %
Total sugars, w/w%*	9,9 %	9,9 %	9,8 %	10,1 %	10,0 %
Glucose, w/w%*	1,5 %	1,4 %	1,4 %	1,5 %	1,5 %
Xylose, w/w%*	2,1 %	2,2 %	2,2 %	2,2 %	2,1 %
Galactose (approx.) , w/w%*	1,4 %	1,4 %	1,4 %	1,4 %	1,4 %
Arabinose, w/w%*	0,6 %	0,6 %	0,6 %	0,6 %	0,6 %
Mannose, w/w%*	4,4 %	4,2 %	4,2 %	4,4 %	4,4 %
GLY, AA, LA, EtOH, HMF, w/w%[1]	1,1 %	1,1 %	1,1 %	1,2 %	1,2 %
Other, w/w%[2]	0,9 %	2,2 %	2,0 %	2,6 %	0,8 %
*Analysis by St1 Oy					
[1]Glycerol, acetic acid, levulinic acid, ethanol and hydroxymethylfurfural					
[2]Ash and other compounds					

Rather surprisingly, according to the data presented in (Table 10–Table 15), it seemed that membrane MWCO, liquor pH and liquor temperature didn't affect lignosulphonate and sugar permeability on a notable scale – the permeability of sugars and the retention of lignosulphonates was on somewhat same level with all the membranes. The effects of liquor pH and temperature on the filtration outcome in terms of PWF_r, permeability, and retentions for TOC, conductivity, lignosulphonates, and sugars are summarized in Table 16.

Table 16. Summary of the effects of pH and temperature in filtration of spent organosolv liquor: pure water flux return (PWF_r), permeability, and retention for TOC, conductivity, lignosulphonates (LS), and total sugars

				NFG (0.6–0.8 kDa)	GE (1kDa)	NP010 (1–1.2 kDa)	GR95PP (2kDa)	GK (3.5kDa)	UH004P (4kDa)	UFX5 pHt (5kDa)	RC70PP (10kDa)
T (°C)	pH		p (bar)	TFC PA	CPA	PES	PES	TFC PA	PES	PSU	RCA
32	0,88	PWFr	4		-7,0 %	60,8 %	53,8 %	-2,3 %	7,3 %	4,8 %	10,4 %
32	6,33		4		-29,8 %	29,5 %	22,9 %	-45,6 %	14,9 %	-9,3 %	10,0 %
45	4,70		4						14,3 %	-10,3 %	3,1 %
60	4,70		4						-9,3 %	-19,6 %	-0,8 %
45	4,70		16	16,4 %	4,7 %	38,1 %					
60[1]	4,70		16	3,0 %	6,6 %	19,9 %					
32	0,88	Permeability (kg m^{-2} h^{-1} bar^{-1})	1–4		0,17	0,13	0,41	0,70	0,86	7,21	7,52
32	6,33		1–4		0,20	1,36	3,18	0,94	2,73	8,64	7,11
45	4,70		1–4						3,51	12,73	7,92
60	4,70		1–4						4,25	17,28	10,74
45	4,70		4–16	1,27	0,42	1,80					
60	4,70		4–16	2,35	0,55	1,64					
32	0,88	R(TOC), %	1–4		32,5	32,1	34,4	31,0	30,5	26,4	23,3
32	6,33		1–4		38,1	31,4	35,3	33,3	28,5	22,5	27,3
45	4,70		1–4						30,9	25,5	27,0
60	4,70		1–4						34,4	19,7	29,9
45	4,70		4–16	47,2	43,1	36,1					
60	4,70		4–16	42,5	47,1	38,0					
32	0,88	R(conductivity)[2], %	1–4		1,74	0,46	1,86	2,46	0,11	-0,23	1,51
32	6,33		1–4		3,65	3,32	-1,95	2,78	-2,70	-5,35	-5,22
45	4,70		1–4						0,39	-3,65	-3,81
60	4,70		1–4						1,68	-3,44	-3,45
45	4,70		4–16	16,55	14,97	12,66					
60	4,70		4–16	11,10	12,31	10,74					
32	0,88	R(LS)[2], %	1–4		80,12	79,84	78,89	79,73	78,94	67,11	61,66
32	6,33		1–4		83,47	82,96	77,59	83,37	76,01	58,80	65,58
45	4,70		1–4						78,46	58,77	58,57
60	4,70		1–4						79,63	61,30	59,98
45	4,70		4–16	88,82	87,59	86,13					
60	4,70		4–16	85,63	85,87	85,87					
32	0,88	R(TOT sugars)[2], %	1–4		0,13	-0,86	-1,66	-3,19	-2,34	-3,82	-3,88
32	6,33		1–4		2,27	-3,54	-2,33	-3,64	-2,52	-2,59	-2,23
45	4,70		1–4						-0,26	-0,73	0,04
60	4,70		1–4						-3,66	-2,95	-2,32
45	4,70		4–16	3,12	4,07	-0,59					
60	4,70		4–16	-2,40	-2,36	-2,84					

[1]Compared to PWF after 45°C instead of PWF after additional wash

[2]Median

6.4 Membrane fouling

Membrane fouling was monitored in terms of pure water flux return (PWF_r), calculated with Equation (5), and ATR-FTIR. PWF_r showed that the higher pH reduced fouling with most of the membranes (Figure 41), which is in line with Mänttäri et al., (2002). On the contrary, UH004P seemed to foul more with higher pH and the fouling of RC70PP was of equal scale with both pH values – PWF_r of both UH004P and RC70PP being well in the range of experimental error. With GE and GK, an increase in pH from 0.88 to 6.33 improved the pure water flux 10 and 45 %, respectively. This was probably at least partially due to the differences in membrane characteristics.

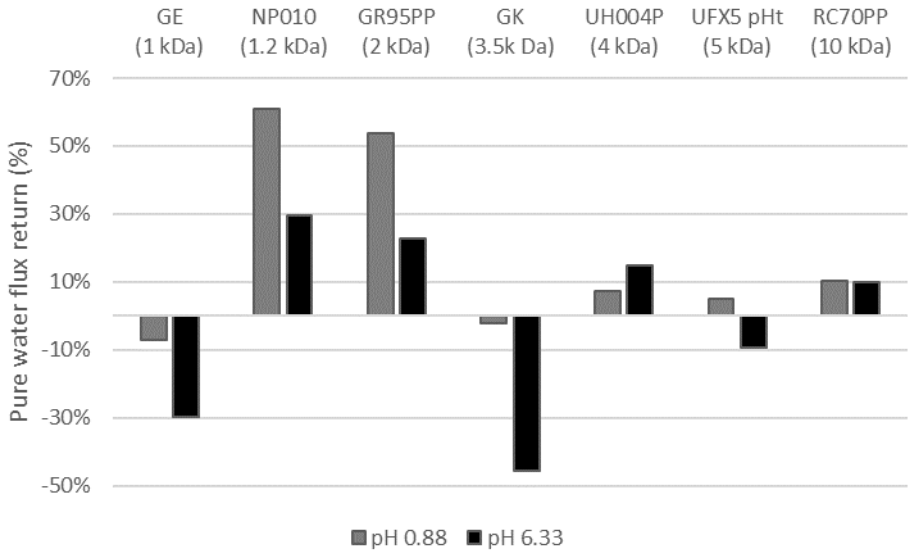

Figure 41. Pure water flux return (pH = 0.88 and 6.33, T = 32 °C, p = 4 bar, v = 0.8 m s^{-1})

The pure water flux returns of filtrations with temperatures of 45 and 60 °C are presented in Figure 42 and Figure 43. Here, an increase in temperature seemed to decrease fouling on membranes of a bigger MWCO (UH004P, UFx5 pHt and RC70PP). The comparison was a little tricky with the tighter membranes (Figure 43) due to additional wash taking place between the filtrations at 45 and 60 °C. Here the pure water flux of NFG, GE and NP010 improved substantially after the wash which is most likely explained by remains of alkaline washing affecting membrane surface charges. Here, the most reasonable way of comparison might take place between the PWF_r at 45 °C and PWF_r at 60 °C (compared to pure water flux after 45 °C i.e., the grey- and the black bar). By doing that it could be concluded that an increase in feed temperature decreased membrane fouling with UH004P, UFx5 pHt, NFG, and NP010 – the results of RC70PP and GE being well in the range of experimental error.

Overall, membrane fouling based on PWF_r seemed more notable with the tighter membranes (Figure 43) compared to the looser ones (Figure 42). It should be noted, though, that the filtration with the tighter membranes took place in higher pressures (4–16 bar instead of 1–4

bar) and hence the data is most probably not directly proportional. The fouling with all the membranes was probably caused by e.g., accumulation of colloids and soluble organic compounds on both the membrane surface and its pores combined with pore blocking in some degree.

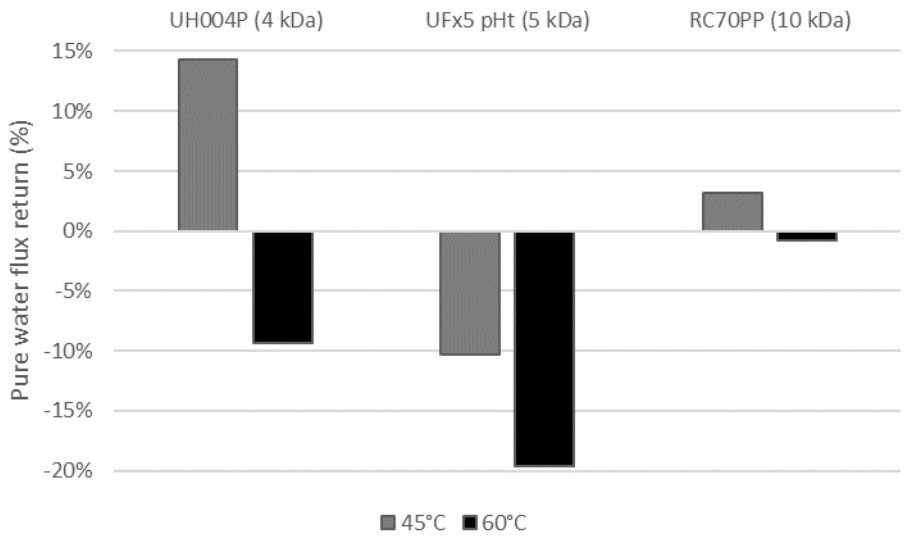

Figure 42. Pure water flux return (pH = 4.70, T = 45 and 60 °C, p = 4 bar, v = 0.8 m s^{-1})

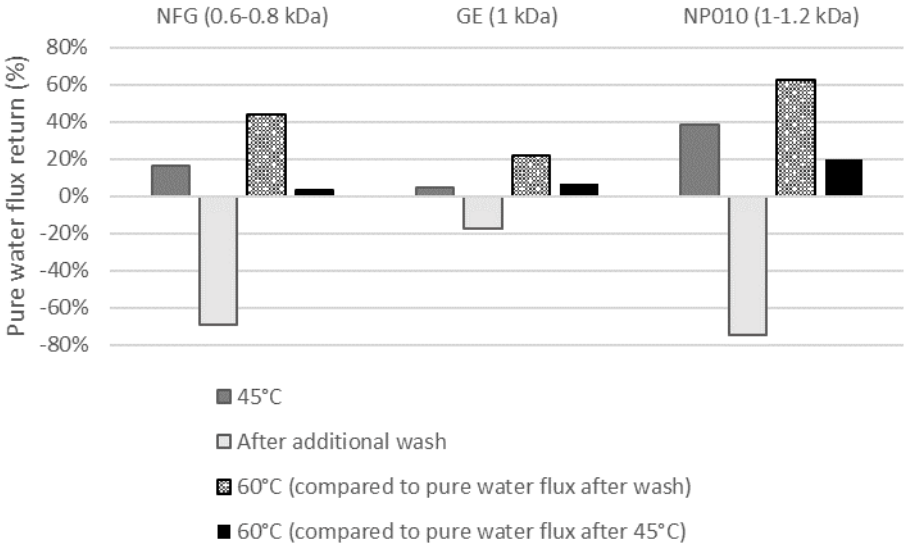

Figure 43. Pure water flux return (pH = 4.70, T = 45 and 60 °C, p = 16 bar, v = 0.8 m s^{-1})

The properties of the feed solution and the characteristics of membrane material affect the outcome of the filtration substantially, and as could be seen in the differences between membrane pure water flux return that is why the selection of the most suitable membrane

material is done experimentally. When it comes to filtration conditions, it seemed that, overall, filtration of the spent liquor with the higher pH and temperature decreased membrane fouling and improved permeate flux.

Membrane fouling was examined not only by comparison of pre- and post-filtration pure water fluxes but also by collecting and comparing the FTIR spectra of the used membranes, unused membranes, and dried spent liquor sample. Figure 44 presents images of three pristine and used membranes merely for observation by eye.

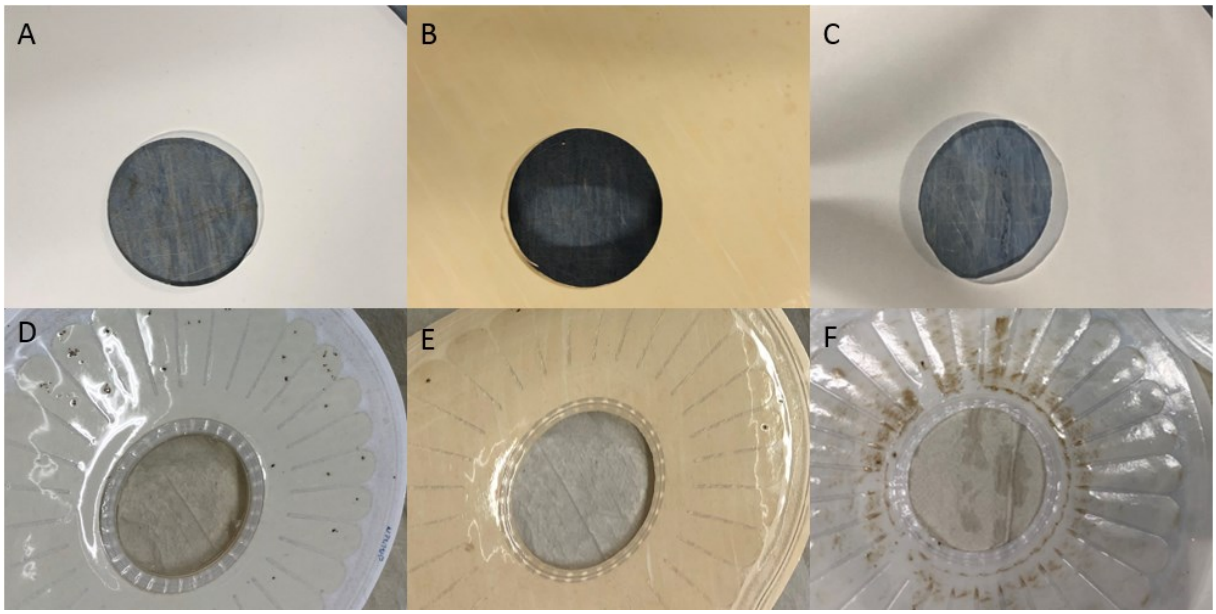

Figure 44. Pristine and fouled membranes after phase 1 filtration experiment at 32 °C, 4 bar and pH 0.88. Membranes A–C represent pristine NP010 (1–1.2 kDa), GE (1kDa) and RC70PP (10kDa) and membranes D–F represent fouled membranes, respectively.

The FTIR spectra were compared to the characteristic bands of glucose and lignosulphonate (Table 17). For FTIR, the membranes were preconditioned in a beaker as presented in analytical methods. Since lignosulphonates tend to cause fouling especially with hydrophobic membranes, as demonstrated by Carlsson et al., (1998), the 1511 cm^{-1} region characteristic for lignosulphonates was taken on focus. More precise images of the membrane FTIR spectra can be found in the Appendix V.

Table 17. Characteristic bands of glucose and lignosulphonate in fourier transfer infrared spectrophotometry (FTIR) (modified from Nybacka, 2016 and Awal & Sain, 2011)

Glucose (Nybacka, 2016)		**Lignosulphonate (Awal & Sain, 2011)**	
Wavenumber (cm $^{-1}$)	Assignment	Wavenumber (cm $^{-1}$)*	Assignment
3350	O–H stretching	3435	O–H stretching
2920	C–H vibration, asymmetric	2924	C–H stretching
2850	C–H vibration, symmetric	1705	C=O stretching (unconjugated)
1450	C–H vibration, bending	1511	Aromatic skeletal vibration
1030	C–O and C–C vibration	1033	Aromatic C–H in-plane deformation
		*Hardwood and softwood, average	

The spectra of dried liquor sample (Figure 45) showed signs of both lignosulphonate and glucose. According to Awal & Sain (2011) and Nybacka (2016) the absorption peaks in the 3350, 2900 and 1030 cm^{-1} area can be due to either lignosulphonate or glucose: the first two peaks representing O–H and C–H stretching vibration, respectively, and the last peak representing either C–O and C–C vibration of glucose or aromatic C–H in-plane deformation of lignosulphonate. According to Kačuráková et al. (2000), absorption peaks at 1035, 1050 and 1070 cm^{-1} (shown as a slight shoulder in Figure 45) are those of glucose, xylose, and mannose, respectively.

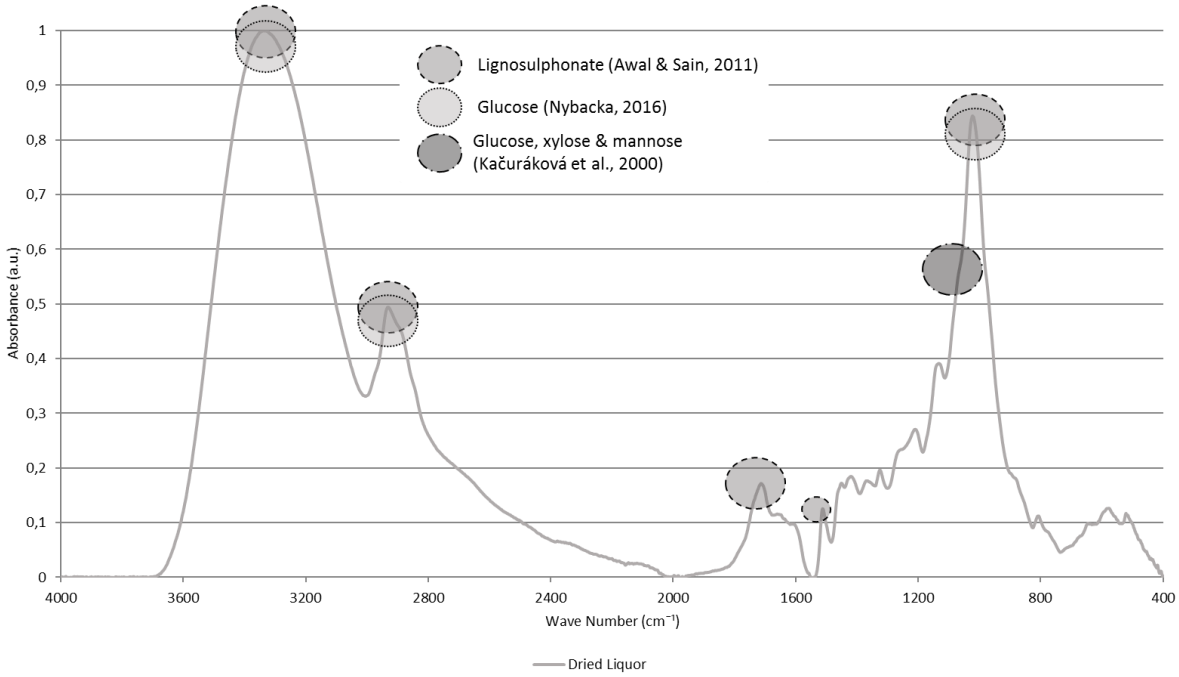

Figure 45. FTIR spectra of dried liquor sample with peaks characteristic to hemicellulose sugars and lignosulphonate

The FTIR spectra of the membranes (Figure 46–Figure 48) showed a rather clear change in the 1511 cm^{-1} region with all but RC70PP (better seen in the bigger images found on Appendix V), indicating fouling caused most likely by lignosulphonates. Due to RC70PP (RCA) being the most hydrophilic of the membranes used in these experiments, the lack of lignosulphonate remains at 1511 cm^{-1} region confirms what was demonstrated by Carlsson et al., (1998): lignosulphonates tend to cause fouling especially on hydrophobic membranes. All in all, each of the PES membranes (UH004P, GR95PP and NP010) and the CPA membrane (GE) showed notable fouling caused by lignosulphonates, whereas from TFC PA membranes (GK and NFG) NFG showed notable fouling and GK fouling of a lesser degree. The fouling of the PSU membrane (UFX5 pHt) was of a lesser degree also.

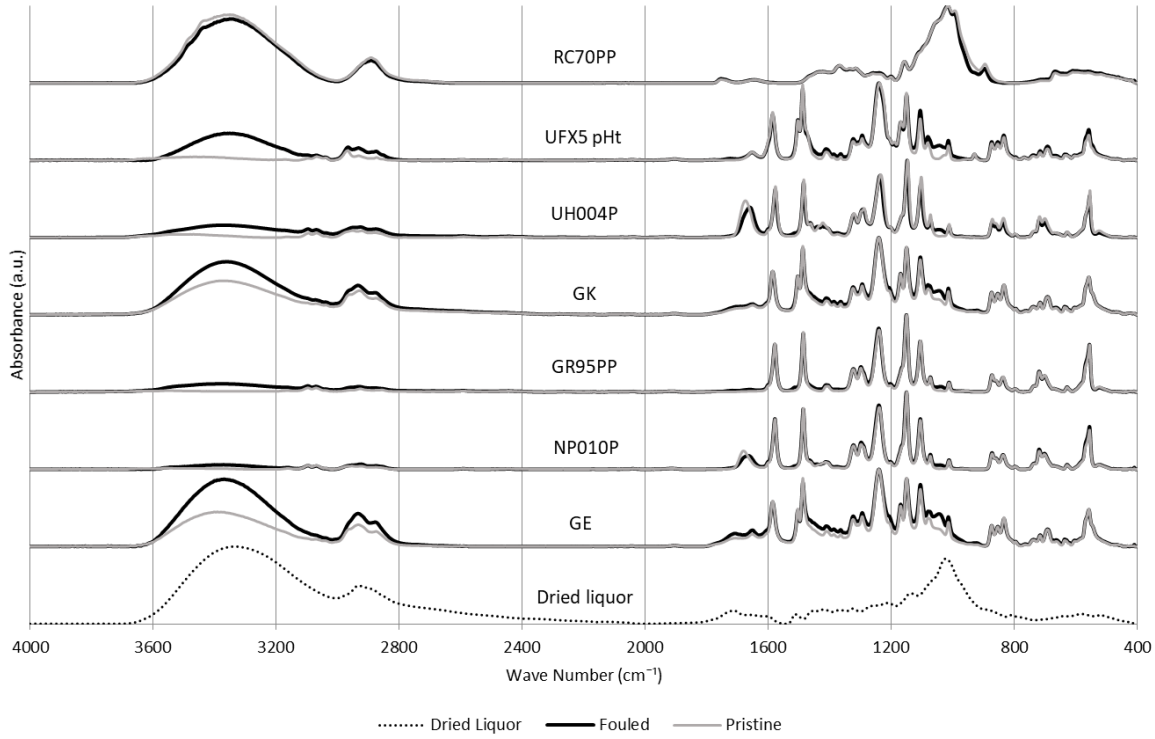

Figure 46. FTIR spectra of the dried liquor sample, fouled-, and membranes (pH = 0.88, T = 32 °C, p = 1–4 bar, v = 0.8 m s^{-1})

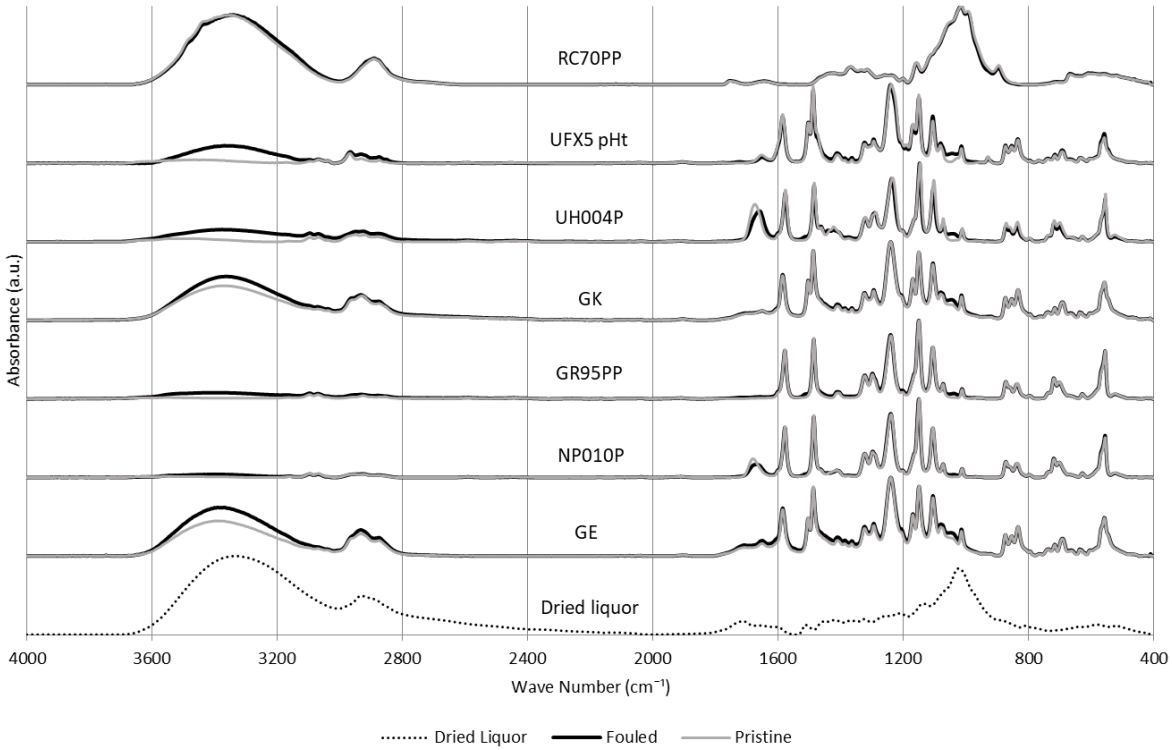

Figure 47. FTIR spectra of the dried liquor sample, fouled-, and membranes (pH = 6.33, T = 32 °C, p = 1–4 bar, v = 0.8 m s^{-1})

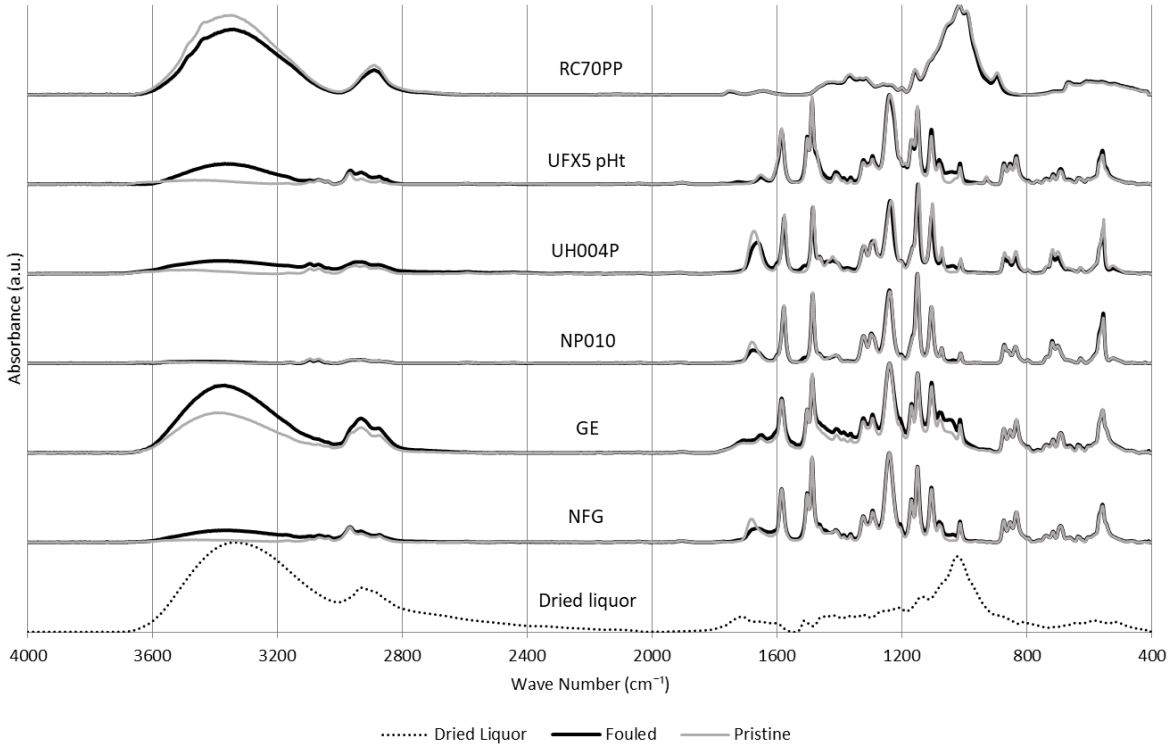

Figure 48. FTIR spectra of the dried liquor sample, fouled-, and pristine membranes (pH = 4.70, T = 45 and 60 °C, p = 1–16 bar, v = 0.8 m s^{-1})

6.5 Production of concentrated lignosulphonate fraction

Lignosulphonates were concentrated with the DSS filter by using three NP010 membranes on a stack. NFG was the membrane of choice, at first, before turning out to be impractical due to the new sheets showing a poor pure water flux. NP010 was chosen due to being of a low MWCO (1–1.2 kDa) and due to GE (1 kDa) being unavailable. Also, the results of filtration experiments with increased pH (Figure 41, p. 54) and increased temperature (Figure 43, p. 55) showed promising results while keeping in mind that the concentration experiment was to take place in similar conditions in terms of pH (4.59) and temperature (60 °C). Additionally, the flux of NP010 was the second to the best (NFG) in earlier experiment (Figure 24, p. 37) and the fouling – even though the worst at a glance (Figure 26, p. 39) – was actually rather close to NFG and GE.

The concentration experiment was taken further by DDF i.e., by adding water to the feed tank between the filtration cycles. The experiments were carried out at 60 °C, pH 4.59 and 16 bar with a cross-flow velocity of 0.8 m s^{-1}. Pure water flux was measured at 32 °C before membrane filtration and after DDF. Measuring the pure water flux after membrane filtration was ruled out as being impossible to carry out due to the very small volume of the liquor – flushing the filtration system causes a loss of liquor and even without the loss of liquor it was expected that the experiment might be rather hard to carry out successfully. The analytical results of the DSS concentration are shown in Table 18.

Table 18. Analytical results of lignosulphonate concentration with membrane filtration and discontinuous diafiltration (DDF) with a stack of three NP010 membranes (pH 4.59, T = 60 °C, p = 16 bar, v = 0.8 m s^{-1})

	DSS concentration			DDF 1			DDF 2		
NP010, 60 °C, pH 4.59, 16 bar	Start Retentate	End Retentate	End Permeate Cumulative	Start Retentate	End Retentate	End Permeate Cumulative	Start Retentate	End Retentate	End Permeate Cumulative
pH	4,59	4,41	4,56	4,48	4,30	4,53	4,35	4,19	4,57
Conductivity (mS cm^{-1})	12,7	13,2	11,2	11,8	14,0	8,7	9,9	13,0	5,5
Brix (%)	22,9	42,1	16,7	20,1	37,5	9,9	17,0	30,5	5,2
TOC (g L^{-1})	53,6	86,6	37,6	49,1	119,8	20,6	43,9	97,8	11,8
DM (w/w%)	22,6	44,9	18,3	17,9	16,6	11,1	13,7	8,7	5,6
DM (g L^{-1})	240,8	505,3	193,9	188,8	341,2	113,8	141,4	254,6	56,8
Total sugars (St1 Oy, g kg^{-1})[1]	86,9	108,5	100,3	49,9	58,4	53,6	26,4	28,2	25,8
Other (St1 Oy, g kg^{-1})[2]	14,4	9,5	12,2	4,3	5,8	5,4	2,6	3,8	2,2
Lignosulphonates (g L^{-1})	98,0	257,6	14,9	120,6	307,1	10,0	133,2	286,0	7,0
R(TOC), %			29,9			58,0			73,0
R(conductivity), %			12,0			25,7			43,9
R(lignosulphonates), %			84,8			91,7			94,7
R(sugars), %			-15,3			-7,3			2,2

[1]Total sugars = Glucose, Xylose, Galactose (approx.), Arabinose, Mannose

[2]Other i.e., glycerol, acetic acid, levulinic acid, ethanol and hydroxymethylfurfural

The concentration experiment was continued for as long as possible i.e., until the feed pump started to have major problems with keeping the flowrate constant causing the filtration pressure started to deviate largely. Rather linear drop in the permeate flux could be seen. This was most likely caused by increasing liquor concentration, and a combination of adsorption, pore blocking, and gel layer formation. The permeate flux in lignosulphonate concentration experiment plotted against mass reduction factor (MRF), calculated with Equation (7), can be seen in Figure 49.

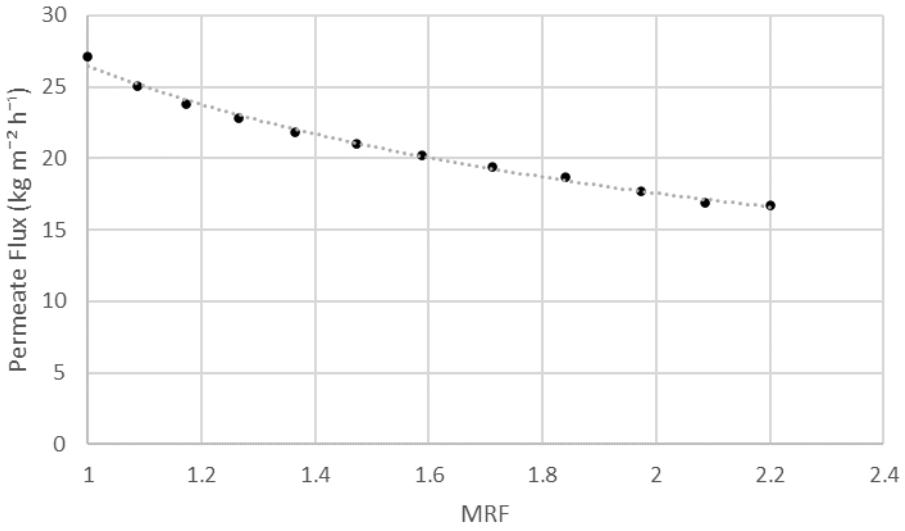

Figure 49. Permeate flux in lignosulphonate concentration with a stack of three NP010 membranes and mass reduction factor of 1.09–2.24 (pH 4.59, T = 60 °C, p = 16 bar, v = 0.8 m s^{-1}, t = 113 min)

According to analysis, lignosulphonate concentration experiment seemed to have been rather successful. The concentration of lignosulphonates was increased from 98 g L^{-1} to 258 g L^{-1} with membrane filtration, and up to 307 g L^{-1} and 286 g L^{-1} with DDF I and DDF II, respectively. The mass reduction factors were 2.24, 1.65 and 1.41 with membrane filtration, DDF I and DDF II, respectively. In total, from the beginning of membrane filtration until the end of DDF II the *MRF* was 1.61. As can be seen in Figure 50, the second DDF was not as successful as the first one in terms of lignosulphonate concentration. This was due to the challenges with the feed pump caused by low volume of the liquor. All in all, production of concentrated lignosulphonate fraction seemed to have been very successful should the conclusions be drawn based on lignosulphonate concentration only.

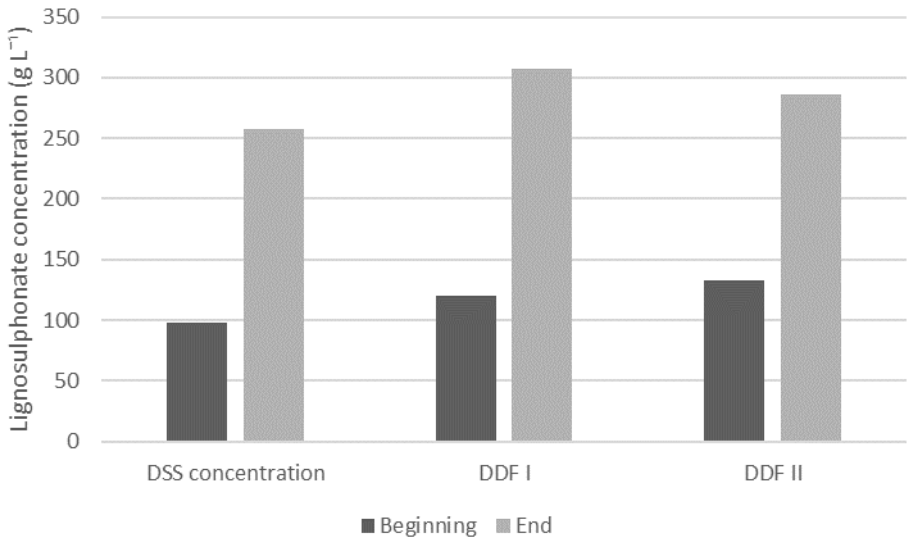

Figure 50. Production of concentrated lignosulphonate fraction with membrane filtration and discontinuous diafiltration (DDF) (pH 4.59, T = 60 °C, p = 16 bar, v = 0.8 m s^{-1})

A mass balance of the production of concentrated lignosulphonate fraction with membrane filtration and DDF was made (Figure 51). Based on the analysis only (in italics), the amount of lignosulphonates seemed to have increased from 563 g at the beginning to 1014 g at the end. Due to the input of the system having to, obviously, match the output, the results had to be corrected for the error resulting most likely from LS analytics. Here, the amounts of LS and sugars (inside the boxes) were kept unchanged at the beginning (DSS beginning), and for the rest the amounts were calculated on a percentage based comparison.

The analytical error resulted most likely from: (1) lignosulphonate concentration conversion from g L^{-1} to g kg^{-1}, based on sample densities obtained for each sample individually while weighing 1 ml of the wet sample in DM analysis, (2) analytical error in sugar analysis, and (3) the volume of the samples taken (340 ml in total) being omitted from the mass balance. The analytical results of the concentration experiment can be seen in Appendix IV.

The mass balance reveals that not enough water could be removed from the feed into permeate on either of the diafiltrations. In the first DDF the mass of added water was 2619 g while the mass of water removed was only 2098 g. In the second DDF the numbers were 2119 and 1568 g, respectively. Besides omitting the volume of samples taken this is explained by the fact that the total volume of the liquor was very low which led into feed pump malfunction sooner than expected i.e., it was impossible to continue the filtrations long enough to remove the desired amount of water.

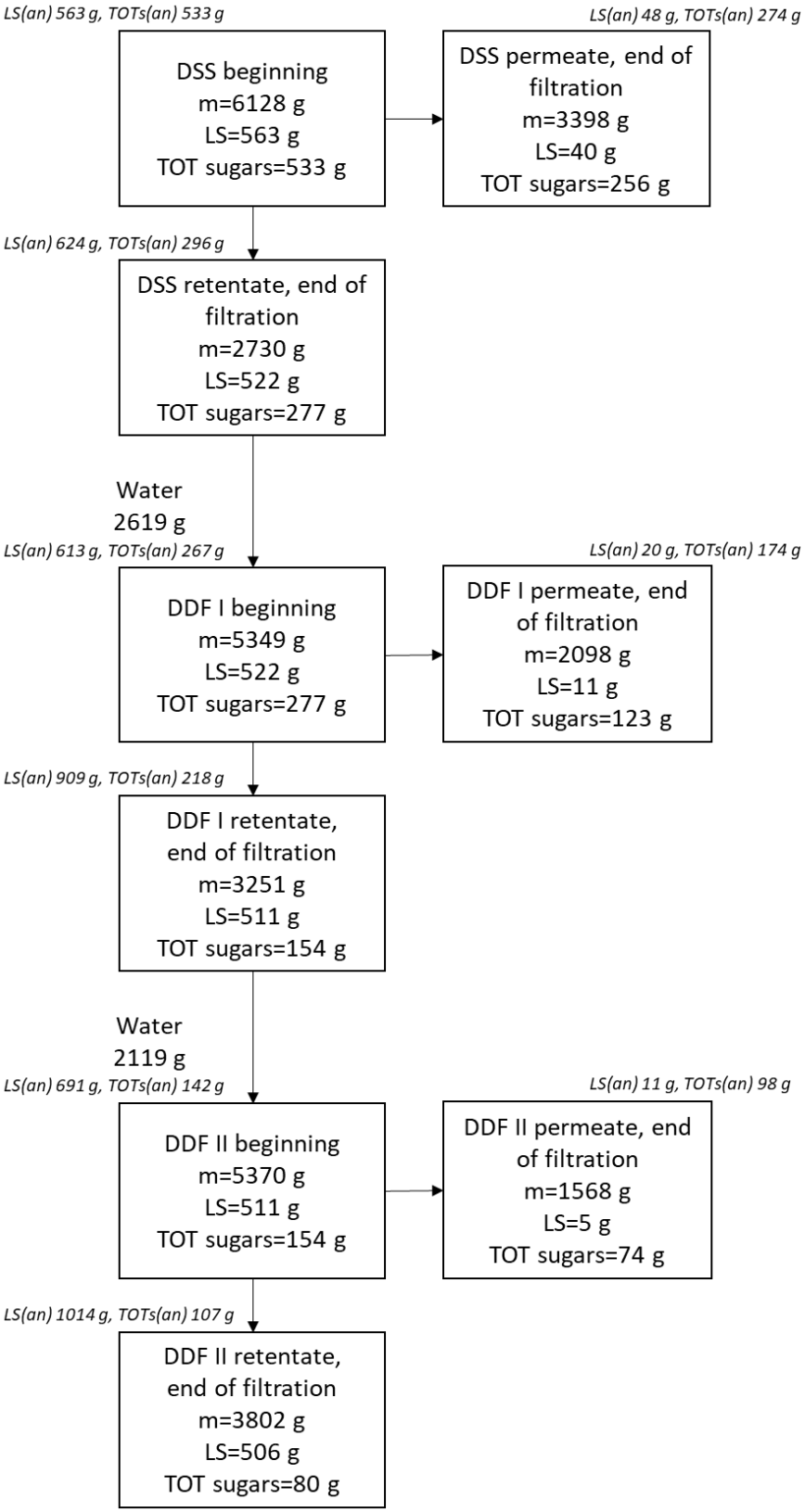

Figure 51. Production of concentrated lignosulphonate fraction with membrane filtration and discontinuous diafiltration (DDF) (pH 4.59, T = 60 °C, p = 16 bar, v = 0.8 m s^{-1}): mass balance. LS(an) = lignosulphonate based on analysis, TOTs(an) = total sugar based on analysis, LS = lignosulphonate (corrected), TOT sugars = total sugars (corrected).

Pure water flux was measured before filtration and after diafiltration to monitor membrane fouling. As can be seen in Figure 52 and Figure 53, the PWF_r was of somewhat equal scale with all the NP010 membrane pairs. A reduction of over 70 % (Figure 53) in the pure water flux is a clear indicator of membranes having become heavily fouled, although while experimenting with concentrated liquor the result was rather expected. In an industrial point of view, use of several filtration units with different MWCOs in series is highly recommended to avoid excessive fouling in production of concentrated lignosulphonate stream.

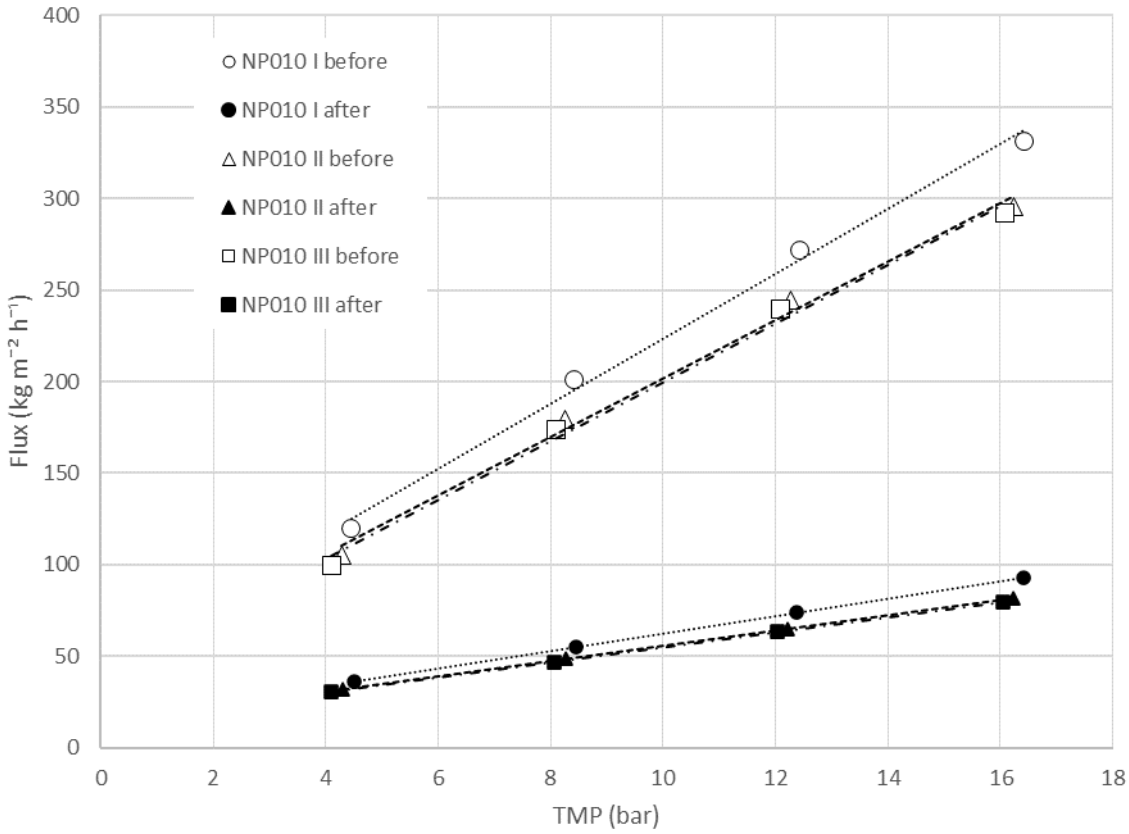

Figure 52. Pure water flux as a function of *TMP* with NP010 before membrane filtration and after discontinuous diafiltration (pH 4.59, T = 60 °C, p = 16 bar, v = 0.8 m s^{-1})

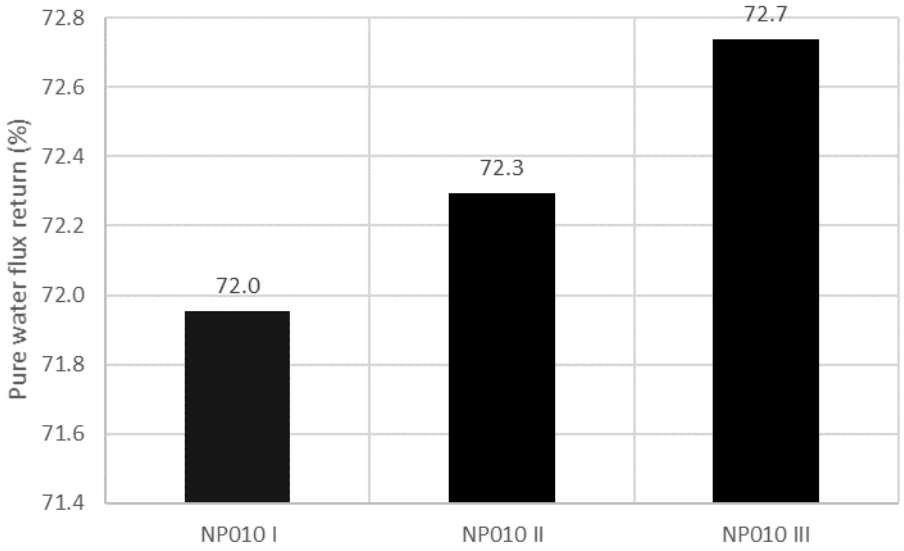

Figure 53. Pure water flux return in membrane filtration and discontinuous diafiltration experiment with a stack of three NP010 membrane pairs (pH 4.59, T = 60 °C, p = 16 bar, v = 0.8 m s^{-1})

7 CONCLUSIONS

In this thesis, membrane separation of lignosulphonates and hemicellulose sugars containing spent organosolv liquor were studied. The filtration experiments were carried out by using DSS LabStak® M20-0.72 cross-flow test unit. Membranes from Alfa Laval, Nadir, GE membranes/Suez, and Synder Filtration with MWCO ranging from 0.6–0.8 to 10 kDa were used. Alfa Laval membranes were GR95PP (2 kDa, PES), UFX5 pHt (4 kDa, PSU), and RC70PP (10 kDa, RCA), Nadir membranes were NP010 (1.2 kDa, PES), and UH004P (4 kDa, PES), GE membranes/Suez membranes were GE (1 kDa, CPA) and GK (3.5 kDa, TFC PA), and Synder Filtration membrane was NFG (0.6–0.8 kDa, TFC PA). Membrane performance was monitored in terms of permeability and selectivity (R_{obs} of lignosulphonates (LS), total sugars, TOC, and conductivity), and membrane fouling was monitored via PWF_r and ATR-FTIR. Cross-flow velocity of 0.8 m s^{-1} was used at all the experiments.

Demonstrating the effect of membrane MWCO in membrane permeability, permeabilities of 17.3 and 10.7 kg m^{-2} h^{-1} bar^{-1} (pH = 4.70, T = 60 °C, p = 1–4 bar) were achieved with the two loosest membranes, UFx5 pHt and RC70PP, respectively, whereas the permeabilities of the two tightest membranes, NFG and GE, were 2.3 and 0.6 kg m^{-2} h^{-1} bar^{-1}, respectively. Under these conditions R_{obs} of LS with UFx5 pHt and RC70PP were in the range of 60 %, while R_{obs} in the range of 85 % was achieved with NFG and GE, demonstrating the trade-off between membrane permeability and selectivity.

The effect of pH into membrane permeability was rather significant with PES membranes (NP010, GR95PP and UH004P) which showed increases of 982, 674 and 216 % in permeability when spent liquor pH was increased from 0.88 to 6.33 at 32 °C and 1–4 bar. With other membranes (GE, GK, UFx5 pHt, and RC70PP) the effect of pH into permeability ranged from -5 to 35 %. The effect of pH in R_{obs} of LS, total sugars, TOC, and conductivity was negligible with all the membranes.

Membrane permeability increased by up to 84 % with the tightest membrane, NFG (0.6–0.8 kDa, TFC PA), when spent liquor temperature was increased from 45 to 60 °C, at pH 4.70, and 4–16 bar. With GE and NP010 the permeability changed by 33 and -9 %, respectively, at 4–16 bar. With membranes of MWCO 4, 5 and 10 kDa (UH004p, UFX5 pHt, and RC70PP) the permeability increased by 21, 36 and 36 %, respectively, at pH 4.70, and 1–4 bar. Alike pH, the effect of temperature in R_{obs} of LS, total sugars, TOC, and conductivity was negligible with all the membranes.

Membrane fouling was monitored in terms of pure water flux return (PWF_r). PWF_r was calculated from the pure water fluxes measured before- and after filtration. Here, increasing the spent liquor pH from 0.88 to 6.33 showed promising results with all the membranes (GE, NP010, GR95PP, GK, UH004P, UFX5 pHt, and RC70PP), but variance between the membranes was notable most likely due to the differences in membrane characteristics. At pH 0.88 (32 °C, 1–4 bar) the pure water fluxes of NP010 and GR95PP decreased by 60 and 55 %, respectively, whereas at pH 6.33 (32 °C, 1–4 bar) the decreases were 30 and 25 %, respectively. With GE and GK, on the other hand, a minor improvement of pure water flux was monitored at pH 0.88 (32 °C, 1–4 bar) whereas at 6.33 (32 °C, 1–4 bar) the pure water fluxes of GE and

GK improved by 30 and 45 %, respectively. This was probably due to e.g., changes in membrane surface charges and/or due to the foulants causing membranes to become more hydrophilic. To verify the latter, further experiments with contact angle measurements are suggested.

The effect of temperature into membrane fouling was studied by using six different membranes. The experiments with NFG, GE and NP010 were carried out at 45 and 60 °C, pH 4.70 and 4–16 bar, whereas UH004P, UFX5 pHt and RC70PP were subjected to spent liquor at 45 and 60 °C, pH 4.70 and 1–4 bar. In terms of PWF_r, GE and RC70PP showed negligible change whereas the fluxes of UH004P and UFX5 pHt were strongly favored by the higher temperature, with PWF_r of UH004P increasing by 25, and PWF_r of UFX5 pHt increasing by10 percentage points at 45 and 60 °C, respectively. The corresponding PWF_r values for UH004P and UFX5 at 60 °C were -10 and -20 % i.e., the pure water fluxes increased. This was probably due to the reasons mentioned at the previous chapter.

Membrane fouling caused by LS (pH = 0.88 and 6.33, T = 32 °C, p = 1–4 bar) was further monitored with attenuated total reflection fourier transform infrared spectroscopy (ATR-FTIR). Here, 1511 cm^{-1} region characteristic for LS was taken on focus. RC70PP showed no fouling caused by LS, whereas some fouling could be seen on GK and UFX5 pHt. With GE, NP010, GR95PP, and UH004P fouling caused by LS was notable. The LS-related fouling with NFG (pH = 4.70, T = 60 °C, p = 4–16 bar) was also notable. The effect of spent liquor pH seemed to have the most notable effect on fouling caused by LS on GK, UH004P and UFX5 pHt, which had more traces of LS at pH 0.88 compared to 6.33. With the rest of the membranes the LS traces were of equal scale at both pH values. An increase in temperature, on the other hand, seemed to lead into more traces of LS in all the membranes (except for RC70PP which showed no traces of LS) that were subjected to higher filtration temperatures.

A concentrated LS fraction was produced with membrane filtration and discontinuous diafiltration (DDF). A stack of three NP010 membranes was used, and the experiment was carried out at pH 4.59, 60 °C, 16 bar. LS concentration was improved from 98 g L^{-1} to 258 g L^{-1} with membrane filtration, and further up to 307 g L^{-1} and 286 g L^{-1} with DDF I and DDF II, respectively, concluding the viability of LS concentration with membrane filtration. The mass reduction factors (*MRF*) were 2.24, 1.65 and 1.41 with membrane filtration, DDF I and DDF II, respectively. The lower *MRF* in DDF I and DDF II compared to membrane filtration were due to the low amount of spent liquor causing the feed pump to fail maintaining a steady flow i.e., it was impossible to carry out with the DDF experiments long enough to remove all the added water from the process. In total, from the beginning of membrane filtration until the end of DDF II the *MRF* was 1.61.

Overall, increasing the spent organosolv liquor pH and temperature seemed to be favorable for the filtration process in terms of permeability. The permeability of PES membranes (NP010, GR95PP and UH004P) benefited the most from the increased pH, whereas variance of the effect of increased temperature into permeability was rather big among the membranes. As expected, the membrane MWCO played a major role in permeability and the selectivity (in general, permeabilities were better with the loose membranes, and selectivity was better with the tight

membranes) demonstrating the trade-off between permeability and selectivity. In terms of R_{obs} (TOC, conductivity, LS, and sugars) the effects of pH and temperature were mostly negligible.

In factory-scale filtration, as discussed in the literature part, a spiral wound element might be, in general, preferred over hollow fiber and tubular due to the lesser CAPEX and OPEX. Here, increasing the liquor pH is beneficial for not only the permeability but also for the module lifetime. This is due to the membrane envelope adhesives being less resistant to extreme pH values than the membranes. However, more experimenting with the spent organosolv liquor filtration is needed to better determine the best membrane material and operating conditions, keeping an eye on the effect of the cost of e.g., chemicals and heating into OPEX. Also, the volumetric flow of the feed and the sought-after purity of the final LS and sugar products determine the boundaries for the process design. The filtration process could consist of several UF and NF units in series if the sought-after purity of the final products is a determining factor.

REFERENCES

Agrimi, G. et al. (2012) 'Process development and metabolic engineering for bioethanol production from lignocellulosic biomass' in *Biorefinery from biomass to chemicals and fuels*. [Online]. Berlin: Walter de Gruyter. https://doi.org/10.1515/9783110260281

Ajo, P. et al. (2018) Hospital Wastewater Treatment with Pilot-Scale Pulsed Corona Discharge for Removal of Pharmaceutical Residues. [Online] 6 (2), A1–A1. https://doi.org/10.1016/j.jece.2018.02.007

Alfa Laval n.d.a Alfa Laval UF flat sheet membranes. Accessed 19.8.2021 at https://www.alfalaval.com/globalassets/documents/products/separation/membranes/flat-sheet-membranes/uf-flat-sheet-membranes_200000311-1-en-gb.pdf

Alfa Laval (n.d.b) Alfa Laval UF-pHt flat sheet membranes. Accessed 24.9.2021 at https://www.alfalaval.com/products/separation/membranes/flat-sheet-membranes/uf-flat-sheet/

Alfa Laval (n.d.c) Flat sheet membranes for ultrafiltration. Accessed 24.9.2021 at https://www.yumpu.com/en/document/view/35945757/kyflat-sheet-membranes-for-ultrafiltration-alfa-laval

Alfa Laval (n.d.d) Alfa Laval UF flat sheet membranes. Accessed 24.9.2021 at https://www.alfalaval.com/products/separation/membranes/flat-sheet-membranes/uf-flat-sheet/

Alriols, M. G. et al. (2010) Combined organosolv and ultrafiltration lignocellulosic biorefinery process. Chemical engineering journal (Lausanne, Switzerland: 1996). [Online] 157 (1), 113–120. https://doi.org/10.1016/j.cej.2009.10.058

Arato, C. et al. (2005) The lignol approach to biorefining of woody biomass to produce ethanol and chemicals. Applied biochemistry and biotechnology. [Online] 123 (1), 871–882.

Aro, T. and Fatehi, P. (2017) Production and Application of Lignosulfonates and Sulfonated Lignin. ChemSusChem. [Online] 10 (9), 1861–1877. https://doi.org/10.1002/cssc.201700082

Awal, A. and Sain, M. (2011) Spectroscopic studies and evaluation of thermorheological properties of softwood and hardwood lignin. Journal of applied polymer science. [Online] 122 (2), 956–963. https://doi.org/10.1002/app.34211

Bajpai, P. (2016) *Pretreatment of Lignocellulosic Biomass for Biofuel Production*. 1st ed. 2016. [Online]. Singapore: Springer Singapore. https://doi.org/10.1007/978-981-10-0687-6

Basma et al. (2016) 'Qualitative and Quantitative Analysis of Lignins from Different Sources and Isolation Methods for an Application as a Biobased Chemical Resource and Polymeric Material', in Vaz Jr. S. (eds) *Analytical Techniques and Methods for Biomass*. Springer, Cham. https://doi-org.ezproxy.cc.lut.fi/10.1007/978-3-319-41414-0_2

Bergman, R. (2007) *Reverse osmosis and nanofiltration (2nd Edition)*. [Online] Denver, Colorado: American Water Works Association. Accessed 30.7.2021 at https://app.knovel.com/hotlink/toc/id:kpRONMWSP1/reverse-osmosis-nanofiltration/reverse-osmosis-nanofiltration

Bhattacharya, P. et al. (2005) Studies on ultrafiltration of spent sulfite liquor using various membranes for the recovery of lignosulphonates. Desalination. [Online] 174 (3), 287–297. https://doi.org/10.1016/j.desal.2004.09.017

Bhave, R. R. (2014) 'Chapter 9 - Cross-Flow Filtration', in Fermentation and Biochemical Engineering Handbook. Third Edition [Online]. Elsevier Inc. pp. 149–180. https://doi.org/10.1016/B978-1-4557-2553-3.00009-X

Bing et al., (2016) 'Preparation and applications of the hollow fiber ultrafiltration membrane' in Ramirez, J. *Ultrafiltration*. [Online] Hauppauge: Nova Science Publishers, Incorporated.

Bordonal, R. de O. et al. (2018) Sustainability of sugarcane production in Brazil. A review. Agronomy for sustainable development. [Online] 38 (2), 1–23. https://doi.org/10.1007/s13593-018-0490-x

Borregaard (n.d.) Biopolymer functionalities. Accessed 24.8.2021 at https://www.borregaard.com/product-areas/lignin-biopolymers/biopolymer-functionalities/

Brosse, N. et al. (2017) 'Organosolv Process' in Wagemann, K. and Tippkötter, N. (eds) *Biorefineries (1st edition)*. [Online]. Cham: Springer International Publishing, pp. 153–176. https://doi-org.ezproxy.cc.lut.fi/10.1007/10_2016_61

Butylina, S. (2007) Effect of physico-chemical conditions and operating parameters on flux and retention of different components in ultrafiltration and nanofiltration fractionation of sweet whey. http://urn.fi/URN:ISBN:978-952-214-379-2

Cao, Y. et al. (2019) Advances in lignin valorization towards bio-based chemicals and fuels: Lignin biorefinery. Bioresource technology. [Online] 291121878–121878. https://doi.org/10.1016/j.biortech.2019.121878

Carlsson, D. et al. (1998) A surface spectroscopic study of membranes fouled by pulp mill effluent. Journal of membrane science. [Online] 142 (1), 1–11. https://doi.org/10.1016/S0376-7388(97)00305-0

Cheng, W. et al. (2018) Selective removal of divalent cations by polyelectrolyte multilayer nanofiltration membrane: Role of polyelectrolyte charge, ion size, and ionic strength. Journal of membrane science. [Online] 55998–106. https://doi.org/10.1016/j.memsci.2018.04.052

Cheryan, M. and Kuo, K. P. (1984). Hollow fibers and spiral wound modules for ultrafiltration of whey: energy consumption and performance. *Journal of Dairy Science*, *67*(7), 1406-1413.

Childress, A. E. and Elimelech, M. (1996) Effect of solution chemistry on the surface charge of polymeric reverse osmosis and nanofiltration membranes. Journal of membrane science. [Online] 119 (2), 253–268. https://doi.org/10.1016/0376-7388(96)00127-5

Damar, I. et al. (2020) Concentration of whey proteins by ultrafiltration: Comparative evaluation of process effectiveness based on physicochemical properties of membranes. International dairy journal. [Online] 111104823–. https://doi.org/10.1016/j.idairyj.2020.104823

De Wild, P. J. et al. (2014) Lignin pyrolysis for profitable lignocellulosic biorefineries. Biofuels, bioproducts and biorefining. [Online] 8 (5), 645–657. https://doi.org/10.1002/bbb.1474

DuPont (2021) FilmTec™ Membranes. Accessed 28.3.2022 at https://www.dupont.com/content/dam/dupont/amer/us/en/water-solutions/public/documents/en/45-D01529-en.pdf

Excel off the Grid (2020) Interpolate with Excel. Accessed 6.10.2021 at https://excelofftheGrid.com/interpolate-values-using-the-forecast-function/

Fengel, D. and Wegener, G. (1989) Wood chemistry, ultrastructure, reactions. Reprint 2011. [Online]. Berlin: Walter de Gruyter. https://doi.org/10.1515/9783110839654

Fernández-Rodríguez, J. et al. (2015) Spent sulphite liquor fractionation into lignosulphonates and fermentable sugars by ultrafiltration. Separation and purification technology. [Online] 152172–179. https://doi.org/10.1016/j.seppur.2015.08.017

Field, R. et al. (1995) Critical flux concept for microfiltration fouling. Journal of membrane science. [Online] 100 (3), 259–272. https://doi.org/10.1016/0376-7388(94)00265-Z

Galkin, M. V. and Samec, J. S. M. (2016) Lignin Valorization through Catalytic Lignocellulose Fractionation: A Fundamental Platform for the Future Biorefinery. ChemSusChem. [Online] 9 (13), 1544–1558. https://doi.org/10.1002/cssc.201600237

Gautam, R. et al. (2015) Review of multidimensional data processing approaches for Raman and infrared spectroscopy. *EPJ Techniques and Instrumentation*. [Online] 2(1), 1–38. https://doi.org/10.1140/epjti/s40485-015-0018-6

Gillgren, T. et al. (2017) Comparison of laccase-catalyzed cross-linking of organosolv lignin and lignosulfonates. International journal of biological macromolecules. [Online] 105 (Pt 1), 438–446. https://doi.org/10.1016/j.ijbiomac.2017.07.061

Joensson, B., Grundberg, H. and Gustafsson, A., Domsjoe Fabriker AB, (2016). *Lignosulfonate of a certain quality and method of preparation of lignosulfonate of a certain quality*. U.S. Patent 9,447,131.

Lenntech (n.d.) Diafiltration. Accessed 13.1.2022 at https://www.lenntech.com/processes/diafiltration.htm

Lewis, M. J. (1996) 'Diafiltration' in Grandison, A. S. & Lewis, M. J. (eds) *Separation processes in the food and biotechnology industries – Principles and Applications*. Cambridge, England: Woodhead Publishing.

Heinze, T. et al. (2018) Cellulose Derivatives Synthesis, Structure, and Properties. [Online]. Cham: Springer International Publishing. https://doi.org/10.1007/978-3-319-73168-1

Hong, N. and Qiu, X. (2020) Structure–Adsorption Behavior–Dispersion Property Relationship of Alkyl Chain Cross-Linked Lignosulfonate with Different Molecular Weights. ACS omega. [Online] 5 (10), 4836–4843. https://doi.org/10.1021/acsomega.9b03535

Hongzhang, C. (2015) '3 - Lignocellulose biorefinery feedstock engineering', in *Lignocellulose Biorefinery Engineering*. [Online]. Elsevier Ltd. pp. 37–86. https://doi.org/10.1016/B978-0-08-100135-6.00003-X

Iakovlev, M. and van Heiningen, A. (2011). SO2-ethanol-water (SEW) pulping: I. Lignin determination in pulps and liquors. *Journal of wood chemistry and technology*. [Online] *31*(3), 233-249. http://dx.doi.org/10.1080/02773813.2010.523161

Iakovlev, M. and van Heiningen, A. (2012) Efficient Fractionation of Spruce by SO2-Ethanol-Water Treatment: Closed Mass Balances for Carbohydrates and Sulfur. ChemSusChem. [Online] 5 (8), 1625–1637. https://doi.org/10.1002/cssc.201100600

Iakovlev, M. et al. (2020) Sulfur dioxide-ethanol-water fractionation platform for conversion of recycled wood to sugars, lignin and lignosulfonates. Bioresource technology. [Online] 300122652–122652. https://doi.org/10.1016/j.biortech.2019.122652

Kačuráková, M. et al. (2000) FT-IR study of plant cell wall model compounds: pectic polysaccharides and hemicelluloses. Carbohydrate polymers. [Online] 43 (2), 195–203. https://doi.org/10.1016/S0144-8617(00)00151-X

Kaya, Y. et al. (2009) Nanofiltration of Cleaning-in-Place (CIP) wastewater in a detergent plant: Effects of pH, temperature and transmembrane pressure on flux behavior. Separation and purification technology. [Online] 65 (2), 117–129. https://doi.org/10.1016/j.seppur.2008.10.034

Koivula, E. et al. (2011) Evaluation of various pretreatment methods to manage fouling in ultrafiltration of wood hydrolysates. Separation and purification technology. [Online] 8350–56. https://doi.org/10.1016/j.seppur.2011.09.006

Kubota, N. et al. (2008) 'Microfiltration and Ultrafiltration', in *Advanced Membrane Technology and Applications*. [Online]. Hoboken, NJ, USA: John Wiley & Sons, Inc. pp. 101–129. https://doi.org/10.1002/9780470276280.ch5

Kucera, J. (2015) *Reverse osmosis: industrial processes and applications (2nd edition)*. [Online] Hoboken, New Jersey: Scrivener Publishing.

Kumar, A. (2012) 'Fundamentals of Membrane Processes', in *Membrane Technology and Environmental Applications*. [Online]. American Society of Civil Engineers (ASCE). pp. 75–95.

Lahti, J. (2009) Nanosuodatuskalvojen alkalikestävyys. Accessed 20.10.2021 at http://urn.fi/URN:NBN:fi-fe200902241197

Lai, Y.-Z. (2017) 'Wood and Wood Products' in Kent, J. A. et al. (ed.) *Handbook of Industrial Chemistry and Biotechnology (13th edition)*. [Online]. Cham: Springer International Publishing. https://doi.org/10.1007/978-3-319-52287-6

Laurichesse, S. and Avérous, L. (2014) Chemical modification of lignins: Towards biobased polymers. Progress in polymer science. [Online] 39 (7), 1266–1290. https://doi.org/10.1016/j.progpolymsci.2013.11.004

Lee, R. A. et al. (2013) UV–Vis as quantification tool for solubilized lignin following a single-shot steam process. Bioresource technology. [Online] 144658–663. https://doi.org/10.1016/j.biortech.2013.06.045

Lehmann&Voss&Co. (n.d.) Cross-Flow-Membrane-Modules. Accessed 5.4.2022 at https://www.lehvoss-filtration.de/fr/products/filtration-modules/

Lewis, M. (1996) 'Chapter 4 - Ultrafiltration', in *Separation Processes in the Food and Biotechnology Industries*. [Online]. Elsevier Ltd. pp. 97–139. https://doi.org/10.1016/B978-1-85573-287-2.50007-1

Lipnizki, F. (2006) Membrane applications in the pulp and paper industry: Experience on lab, pilot and industrial scale. Desalination. [Online] 199 (1), 159–160.

Løhre, C. et al. (2017) Organosolv extraction of softwood combined with lignin-to-liquid-solvolysis as a semi-continuous percolation reactor. Biomass & bioenergy. [Online] 99147–155. https://doi.org/10.1016/j.biombioe.2017.02.014

Magina, S. et al. (2021) Lignosulfonate-Based Polyurethane Adhesives. *Materials*. [Online] 14(22), 7072–. https://doi.org/10.3390/ma14227072

Mann+Hummel (2021a) Nadir NP010 P Nanofiltration Membrane. Accessed 24.9.2021 at https://www.microdyn-nadir.com/flat-sheet-membrane-data-sheets/

Mann+Hummel (2021b) Nadir UH004 P Ultrafiltration Membrane. Accessed 24.9.2021 at https://www.microdyn-nadir.com/flat-sheet-membrane-data-sheets/

Marson, G. V. et al. (2021) Ultrafiltration performance of spent brewer's yeast protein hydrolysate: Impact of pH and membrane material on fouling. *Journal of food engineering*. [Online] 302110569–. https://doi.org/10.1016/j.jfoodeng.2021.110569

Matsakas, L. et al. (2018) A novel hybrid organosolv: steam explosion method for the efficient fractionation and pretreatment of birch biomass. Biotechnology for biofuels. [Online] 11 (1), 160–160. https://doi.org/10.1186/s13068-018-1163-3

McKeen, L. W. (2012) Permeability properties of plastics and elastomers. 3rd ed. Waltham [Mass: William Andrew, an imprint of Elsevier.

MSR (2021) Hollow Fiber Membrane Filters: Advantages in Backpacking Water Filters. Accessed 22.12.2021 at https://www.msrgear.com/blog/hollow-fiber-membrane-advantages-backpacking-water-filters/

Mulder, M. (1996) *Basic principles of membrane technology*. [Online] Dordrecht: Kluwer Academic Publishers.

Muro, C. et al. (2012) 'Membrane Separation Process in Wastewater Treatment of Food Industry' in *Food Industrial Processes – Methods and Equipment*. [Online]. InTech. Accessed 29.7.2021 at http://www.intechopen.com/books/foodindustrial-processes-methods-and-equipment/membrane-separation-process-in-wastewater-treatment-offood-industry

Mussatto, S. I. and Dragone, G. M. (2016) 'Biomass Pretreatment, Biorefineries, and Potential Products for a Bioeconomy Development' in *Biomass fractionation technologies for a lignocellulosic feedstock based biorefinery*. [Online]. Elsevier Ltd. pp. 1–22.

Nybacka, L. (2016) FTIR spectroscopy of glucose. Accessed 15.12.2021 at http://urn.kb.se/resolve?urn=urn:nbn:se:uu:diva-306952

Mänttäri, M. et al. (2002) Comparison of nanofiltration and tight ultrafiltration membranes in the filtration of paper mill process water. Desalination. [Online] 149 (1), 131–136. https://doi.org/10.1016/S0011-9164(02)00744-0

Mänttäri, M. et al. (2004) NF270, a new membrane having promising characteristics and being suitable for treatment of dilute effluents from the paper industry. Journal of membrane science. [Online] 242 (1), 107–116. https://doi.org/10.1016/j.memsci.2003.08.032

Nicolini, J. V. et al. (2016) Selective rejection of ions and correlation with surface properties of nanofiltration membranes. Separation and purification technology. [Online] 171238–247. https://doi.org/10.1016/j.seppur.2016.07.042

Ochando-Pulido, J. M. and Stoller, M. (2015) 'The Boundary Flux', in *Boundary Flux Handbook - A Comprehensive Database of Critical and Threshold Flux Values for Membrane Practitioners*. [Online]. Elsevier Inc. pp. 7–18. https://doi.org/10.1016/B978-0-12-801589-6.00002-4

Olsson, M. R. et al. (2006) Exporting lignin or power from heat-integrated kraft pulp mills: A techno-economic comparison using model mills. Nordic pulp & paper research. [Online] 21 (4), 476–484.

Pan, X. et al. (2005) Biorefining of softwoods using ethanol organosolv pulping: Preliminary evaluation of process streams for manufacture of fuel-grade ethanol and co-products. Biotechnology and bioengineering. [Online] 90 (4), 473–481. https://doi.org/10.1002/bit.20453
Pearce, G. (2007) Introduction to membranes: Membrane selection. Filtration & separation. [Online] 44 (3), 35–37. https://doi.org/10.1016/S0015-1882(07)70083-6

Porter, M. C. (1990) *Handbook of industrial membrane technology*. [Online]. Park Ridge, N.J., U.S.A: Noyes Publications.

Pulido, J. M. O. (2017) 'Optimized ultrafiltration membrane module control during two-phase olive mill wastewater purification' in *Ultrafiltration: methods, applications and insights*. [Online]. New York: Nova Publishers. pp 113–127.

Pylkkänen, V. et al. (2015). Flexible pretreatment technology supports production of biobased co-products at pulp and paper mills. *TAPPI JOURNAL*, *14*(3), 179-184. Accessed 10.07.2021 at https://imisrise.tappi.org/TAPPI/Products/15/MAR/15MAR179.aspx

Ragauskas, A. J. and Huang, F. (2013) 'Chemical Pretreatment Techniques for Biofuels and Biorefineries from Softwood', in *Pretreatment Techniques for Biofuels and Biorefineries*. [Online]. Berlin, Heidelberg: Springer Berlin Heidelberg. pp. 151–179.

Restolho, J. A. et al. (2009) Sugars and lignosulphonates recovery from eucalyptus spent sulphite liquor by membrane processes. Biomass & bioenergy. [Online] 33 (11), 1558–1566. https://doi.org/10.1016/j.biombioe.2009.07.022

Rowell, R. M. et al. (2005) 'Cell wall chemistry', in *Handbook of Wood Chemistry and Wood Composites*. [Online]. Ebook Central. pp. 35–74.

Rudolph, G. (2021) *Investigations on Membrane Fouling and Cleaning in Ultrafiltration Process in Lignocellulosic Biorefineries*. Chemical Engineering, Lund University. Accessed 14.12.2021 at https://lucris.lub.lu.se/ws/portalfiles/portal/98299537/Gregor_Rudolph_WEBB.pdf

Rudolph-Schöpping, G., Schagerlöf, H., Jönsson, A-S. and Lipnizki, F. (2022) Membrane Fouling Studied by QCM-D - Insights on Irreversible Fouling When Treating Process Water from Thermomechanical Pulping. http://dx.doi.org/10.2139/ssrn.4036638

Saha, B. C. (2003) Hemicellulose bioconversion. Journal of industrial microbiology & biotechnology. [Online] 30 (5), 279–291. https://doi.org/10.1007/s10295-003-0049-x

Sandru, M. (2016) 'Fixed Carrier Membrane', in *Encyclopedia of Membranes*. [Online]. Berlin, Heidelberg: Springer Berlin Heidelberg. pp. 776–777.

Sathitsuksanoh, N. et al. (2010) '4 - Solvent fractionation of lignocellulosic biomass', in *Bioalcohol production – biochemical conversion of lignocellulosic biomass*. [Online]. Woodhead Publishing. pp. 122–140. Accessed 22.7.2021 at https://app.knovel.com/hotlink/toc/id:kpBPBCLB01/bioalcohol-production/bioalcohol-production

Shui, T. et al. (2016) Highly efficient organosolv fractionation of cornstalk into cellulose and lignin in organic acids. Bioresource technology. [Online] 218953–961.

Singh, R. (2014) *Membrane Technology and Engineering for Water Purification: Application, Systems Design and Operation (2nd edition)*. Oxford: Elsevier Science & Technology. [Online]

Sjostrom, E. and Haglund, P. (1964). Spectrophotometric determination of the dissolution of lignin during sulfite cooking. *Tappi*, *47*(5), 286-291.

Sparks, T. and Chase, G. (2016) *Filters and filtration handbook (6th Edition)*. Oxford, England: Butterworth-Heinemann. Accessed 12.8.2021 at https://app.knovel.com/hotlink/pdf/id:kt010R0OE1/filters-filtration-handbook

Stade, S. et al. (2013) Reversible and irreversible compaction of ultrafiltration membranes. *Separation and purification technology*. [Online] 118127–134. https://doi.org/10.1016/j.seppur.2013.06.039

Stade, S. et al. (2015) Compaction and its effect on retention of ultrafiltration membranes at different temperatures. *Separation and purification technology*. [Online] 151211–217. https://doi.org/10.1016/j.seppur.2015.07.034

Sterlitech (n.d.a) UF Flat-Sheet Performance Comparison by Manufacturer: Suez (GE). Accessed 24.9.2021 at https://www.sterlitech.com/ge-osmonics-flat-sheet-membrane-ge-composite-pa-uf-cf016-5-pk.html

Sterlitech (n.d.b) Synder Flat Sheet Membrane. Accessed 2.12.2021 at https://www.sterlitech.com/synder-flat-sheet-membrane-nfg-pa-tfc-nf-cf016-5-pk.html

Strand, E. (2016) Enhancement of ultrafiltration process by pretreatment in recovery of hemicelluloses from wood extracts. Lappeenranta University of Technology.

Sun, Y. and Cheng, J. (2002) Hydrolysis of lignocellulosic materials for ethanol production: a review. Bioresource Technology. [Online] 83 (1), 1–11.

Synder Filtration (n.d.a) Hollow Fiber Membranes. Accessed 22.12.2021 at https://membrane.page/learning-center/articles/module-configurations-process/hollow-fiber-membranes/

Synder Filtration (n.d.b) Spiral-Wound Membrane. Accessed 22.12.2021 at https://membrane.page/learning-center/articles/module-configurations-process/spiral-wound-membranes/

Synder Filtration (n.d.c) Tubular Membranes. Accessed 25.3.2022 at https://synderfiltration.com/learning-center/articles/module-configurations-process/tubular-membranes/

Tikka, P. and Virkola, N-E. (1986) *Method for the rapid determination of the concentrations of lignin, monosaccharides and organic acids in process solutions from sulphite digestion*, USA Patent US4718979A [Online]. Accessed 12.1.2022 at https://patentimages.storage.googleapis.com/49/1c/c7/4e055604517c5e/US4718979.pdf

Tres, M. V. et al. (2010) Characterization of polymeric membranes used in vegetable oil/organic solvents separation. Journal of membrane science. [Online] 362 (1), 495–500. https://doi.org/10.1016/j.memsci.2010.07.011

Wang, Z. et al. (2007) Experimental study on treatment of electroplating wastewater by nanofiltration. Journal of membrane science. [Online] 305 (1), 185–195. https://doi.org/10.1016/j.memsci.2007.08.011

Wagner (2001) Membrane filtration handbook: Practical tips and hints (Vol. 129). [Online]. Cambridge: Osmonics. Accessed 21.9.2021 at https://bigbrandwater.com/assets/library/ge/ge-membranefiltrationhandbook.pdf

Weng, Y.-H. et al. (2010) Separation of furans and carboxylic acids from sugars in dilute acid rice straw hydrolyzates by nanofiltration. Bioresource technology. [Online] 101 (13), 4889–4894. https://doi.org/10.1016/j.biortech.2009.11.090

Wenten, I. G. and Ganesha, J. (1996). Ultrafiltration in water treatment and its evaluation as pre-treatment for reverse osmosis system. *Institut Teknologi Bandung*.

Xu, C. and Ferdosian, F. (2017) Conversion of Lignin into Bio-Based Chemicals and Materials. [Online]. Berlin, Heidelberg: Springer Berlin Heidelberg. https://doi.org/10.1007/978-3-662-54959-9

Xu, P. et al. (2006) Effect of membrane fouling on transport of organic contaminants in NF/RO membrane applications. Journal of membrane science. [Online] 279 (1), 165–175. https://doi.org/10.1016/j.memsci.2005.12.001

Yammine, S., Rabagliato, R., Vitrac, X., Peuchot, M.M. and Ghidossi, R. (2019) Selecting ultrafiltration membranes for fractionation of high added value compounds from grape pomace extracts. Oeno One, 53(3), pp.487-497.

Zhao, X. et al. (2017) Organosolv fractionating pre-treatment of lignocellulosic biomass for efficient enzymatic saccharification: chemistry, kinetics, and substrate structures. Biofuels, bioproducts and biorefining. [Online] 11 (3), 567–590. https://doi.org/10.1002/bbb.1768

Zhang et al. (2012). 'The Values of Membrane Science and Technology: Introduction and Overview', in *Membrane technology and environmental applications*. [Online]. Reston, VA: American Society of Civil Engineers. pp. 1–40. Accessed at 12.8.2021 at https://app.knovel.com/hotlink/pdf/id:kt00ASW1D1/membrane-technology-environmental/references

Zhang, H. et al. (2017) Color reduction of sulfonated eucalyptus kraft lignin. International journal of biological macromolecules. [Online] 97201–208. https://doi.org/10.1016/j.ijbiomac.2017.01.031

Zhou, H. et al. (2013) Lignosulfonate to Enhance Enzymatic Saccharification of Lignocelluloses: Role of Molecular Weight and Substrate Lignin. *Industrial & engineering Chemistry Research*. [Online] 52 (25), 8464–8470. https://doi.org/10.1021/ie401085k

Zhou, Z. et al. (2021) 'Deconstruction of Lignocellulose Recalcitrance by Organosolv Fractionating Pretreatment for Enzymatic Hydrolysis', in Emerging Technologies for Biorefineries, Biofuels, and Value-Added Commodities. [Online]. Cham: Springer International Publishing. pp. 23–56. https://doi.org/10.1007/978-3-030-65584-6_2

APPENDIX I (1/3) UV-Vis calibration spectra and calibration curves

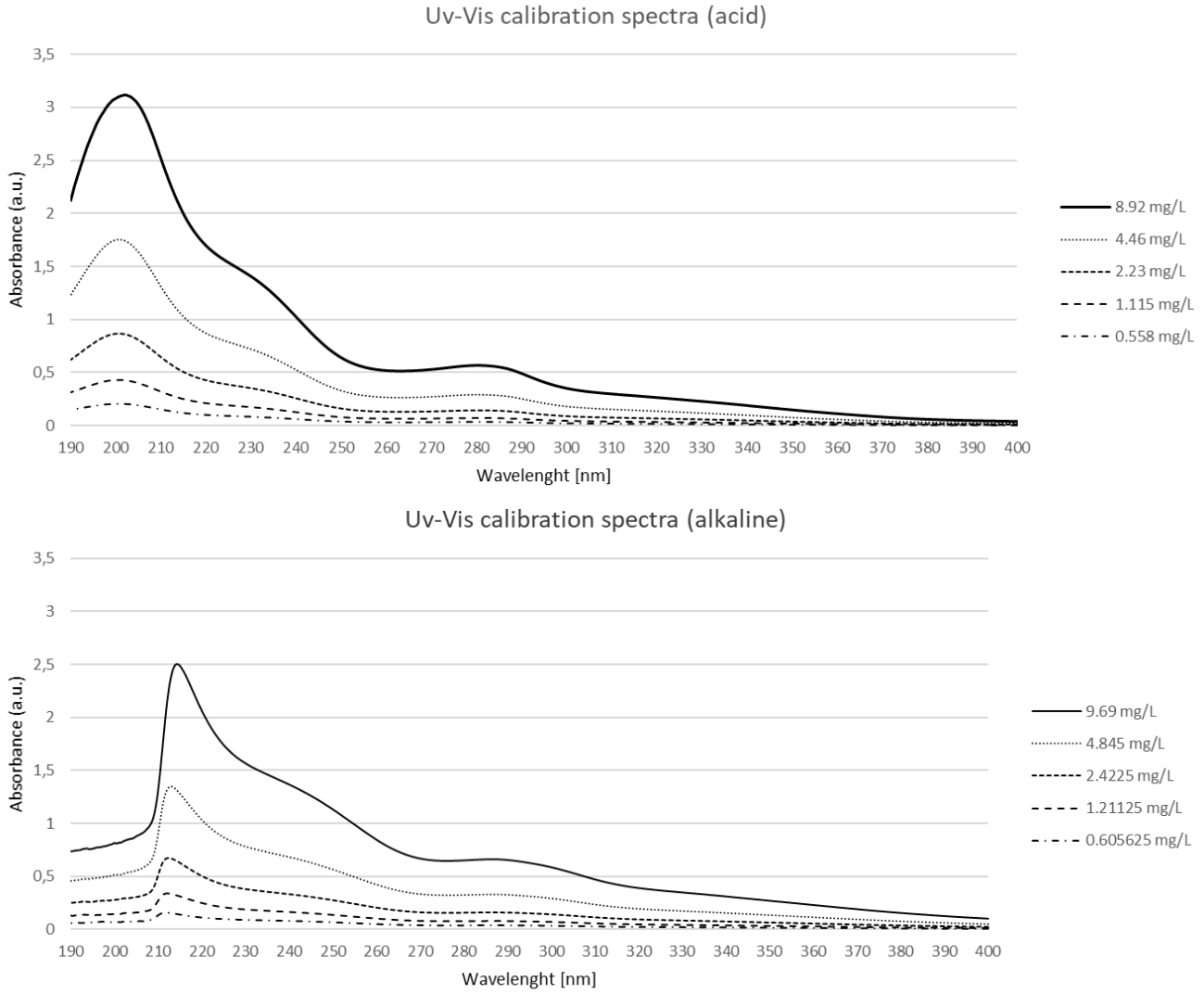

APPENDIX I (2/3) UV-Vis calibration spectra and calibration curves

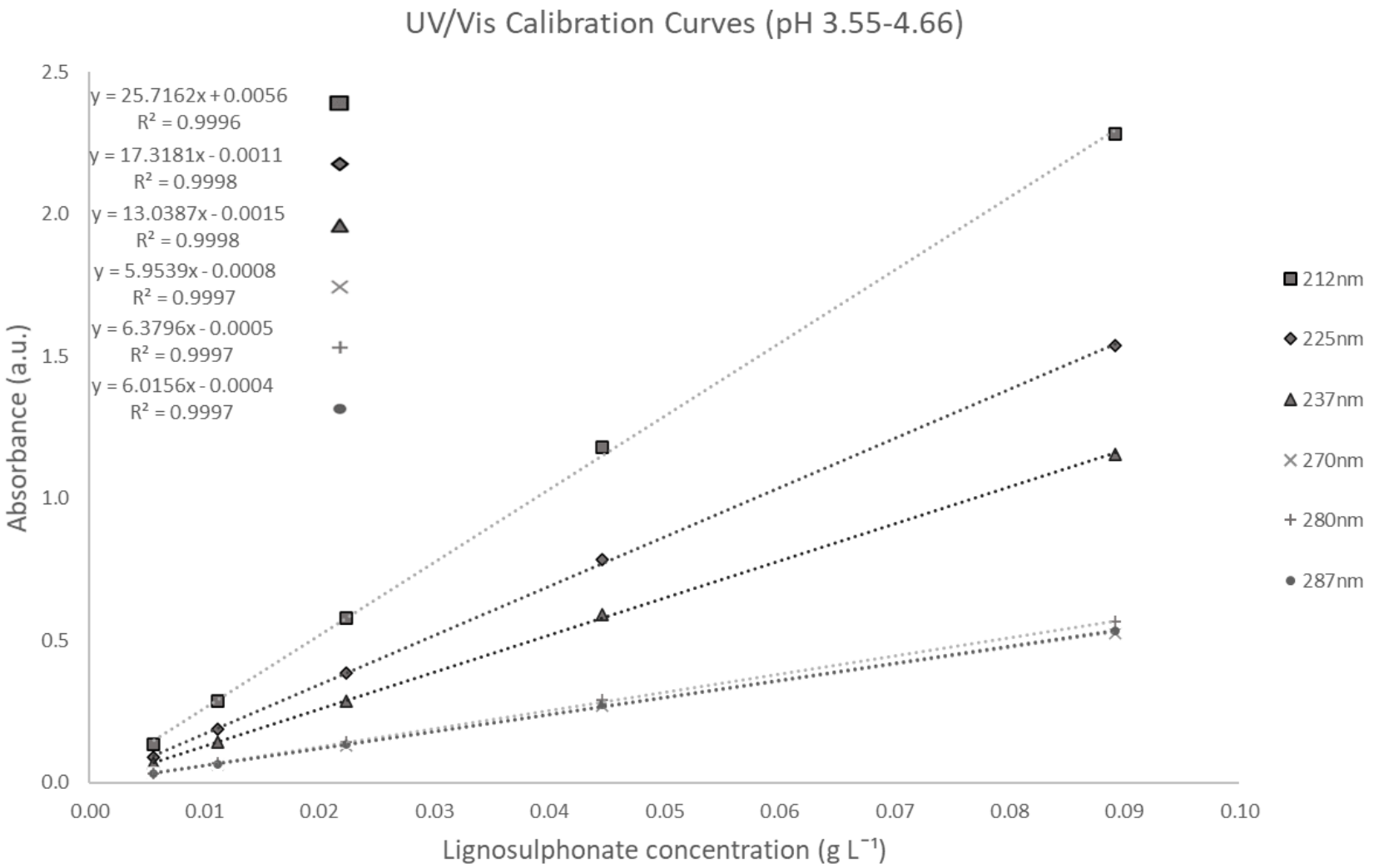

APPENDIX I (3/3) UV-Vis calibration spectra and calibration curves

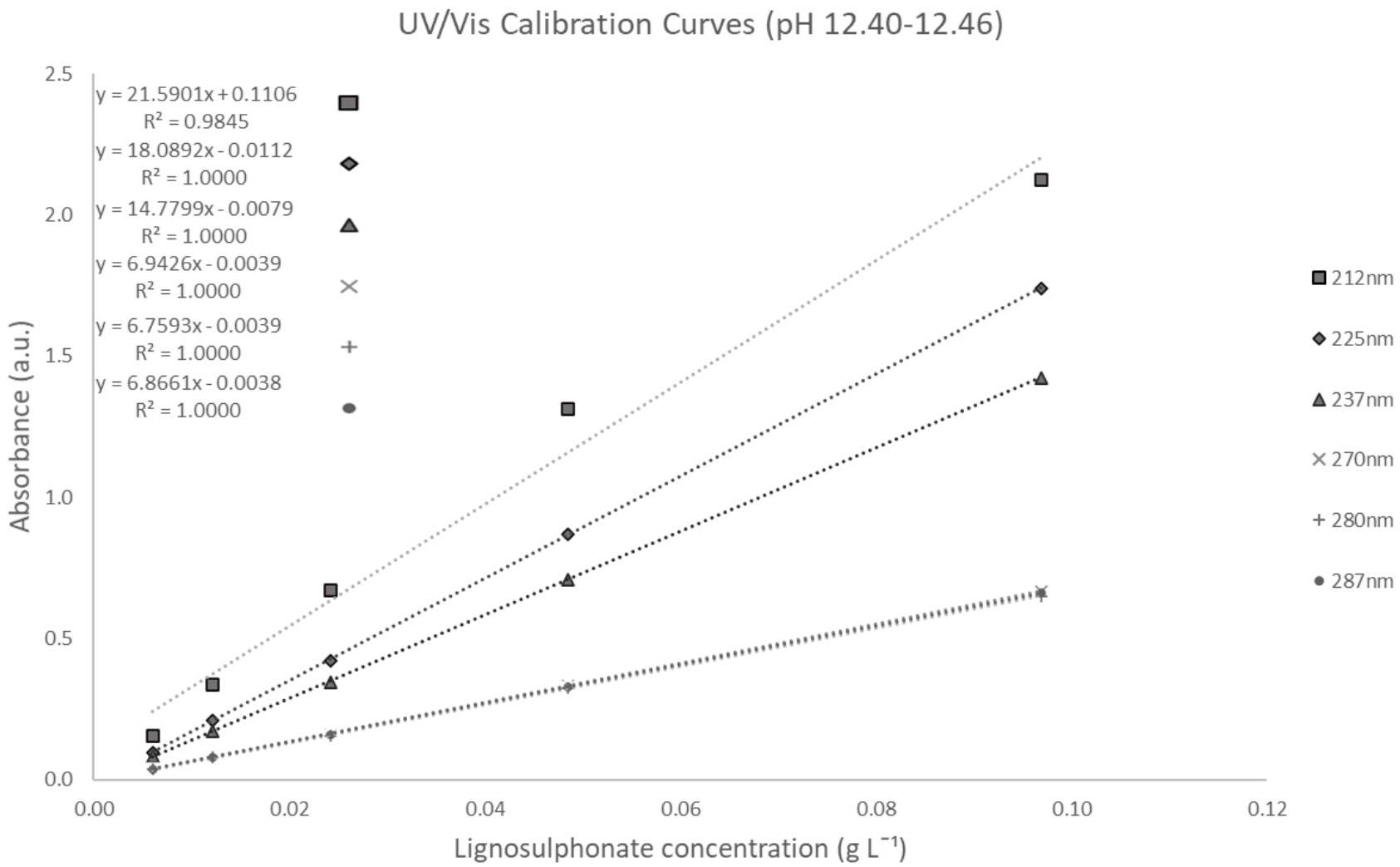

APPENDIX II (1/1) Titration of the hydrolyzed sample with 1M NaOH

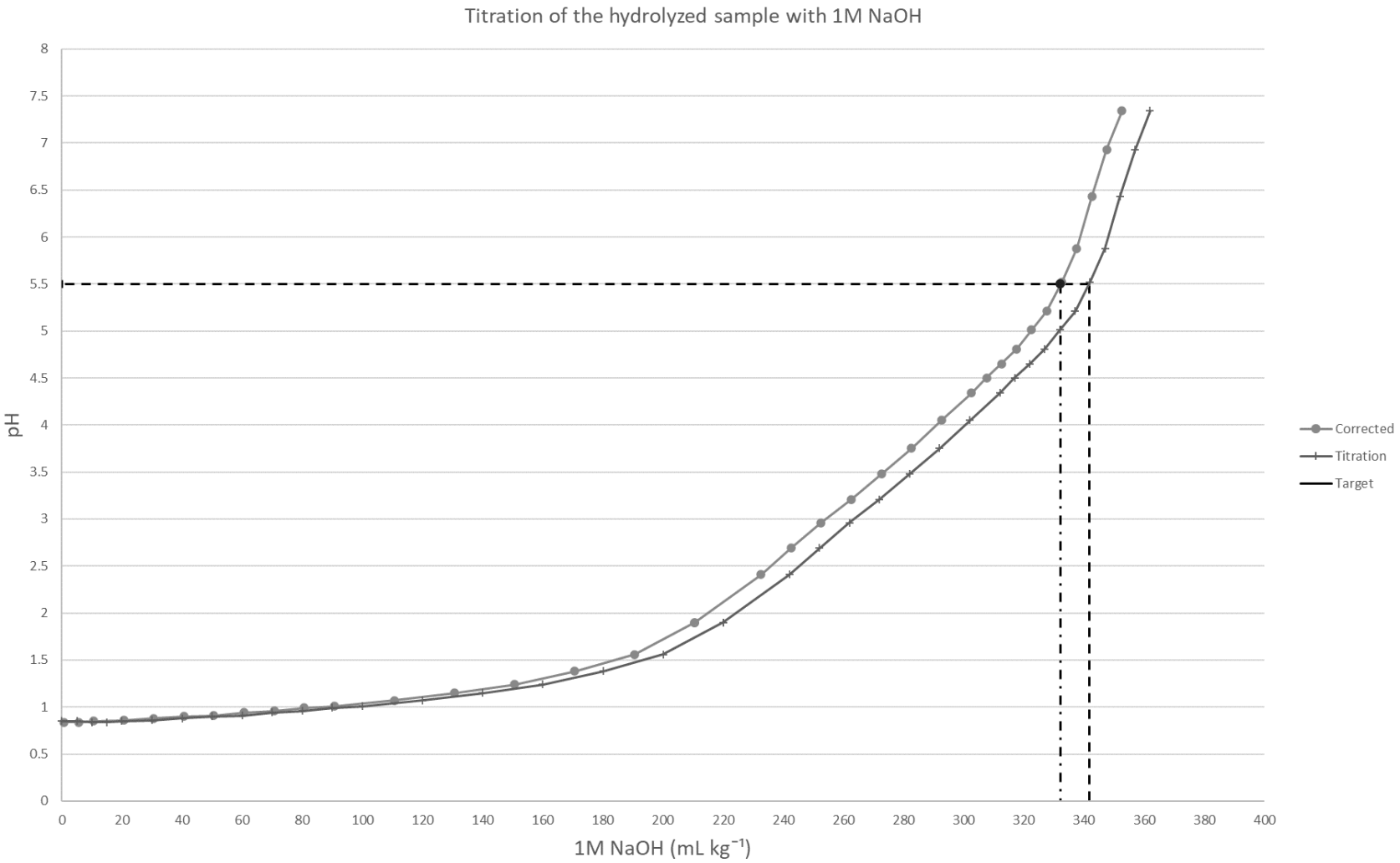

APPENDIX III (1/3) Results of the pure water flux measurements

pH	pH = 0.88, T = 32°C	p (bar)	GE (1kDa)	NP010 (1.2kDa)	GR95PP (2kDa)	GK (3.5kDa)	UH004P (4kDa)	UFX5 pHt (5kDa)	RC70PP (10kDa)
0,88	Pure water flux before filtration (kg m^{-2} h^{-1})	1	3,38	40,58	36,83	8,88	12,96	40,00	70,33
		2	4,58	55,50	52,58	13,13	20,29	64,79	113,75
		3	5,79	70,71	67,13	17,67	27,46	89,04	155,21
		4	7,17	85,00	80,54	21,96	34,58	113,50	193,67
	Pure water flux after filtration (kg m^{-2} h^{-1})	1	3,50	14,13	15,33	8,79	11,50	37,75	66,71
		2	4,88	20,83	22,71	13,21	18,25	61,96	103,79
		3	6,21	26,92	30,04	18,00	25,08	84,96	140,58
		4	7,67	33,29	37,25	22,46	32,04	108,00	173,50
	PWFr	1	-3,70 %	65,20 %	58,37 %	0,94 %	11,25 %	5,63 %	5,15 %
		2	-6,36 %	62,46 %	56,81 %	-0,63 %	10,06 %	4,37 %	8,75 %
		3	-7,19 %	61,93 %	55,25 %	-1,89 %	8,65 %	4,59 %	9,42 %
		4	-6,98 %	60,83 %	53,75 %	-2,28 %	7,35 %	4,85 %	10,41 %
6,33	Pure water flux before filtration (kg m^{-2} h^{-1})	1	3,67	38,75	47,96	8,50	12,75	41,25	101,67
		2	4,83	51,33	64,67	12,46	19,13	63,54	143,08
		3	6,04	63,67	81,38	16,46	25,83	87,17	179,92
		4	7,00	75,25	96,08	20,29	32,33	109,42	208,88
	Pure water flux after filtration (kg m^{-2} h^{-1})	1	4,42	24,79	34,33	12,00	10,13	44,17	88,00
		2	6,00	34,54	48,54	17,92	15,83	69,83	121,46
		3	7,54	44,04	61,83	23,79	21,67	95,17	157,08
		4	9,08	53,04	74,04	29,54	27,50	119,63	187,92
	PWFr	1	-20,45 %	36,02 %	28,41 %	-41,18 %	20,59 %	-7,07 %	13,44 %
		2	-24,14 %	32,71 %	24,94 %	-43,81 %	17,21 %	-9,90 %	15,11 %
		3	-24,83 %	30,82 %	24,01 %	-44,56 %	16,13 %	-9,18 %	12,69 %
		4	-29,76 %	29,51 %	22,94 %	-45,59 %	14,95 %	-9,33 %	10,03 %

APPENDIX III (2/3) Results of the pure water flux measurements

pH	T = 45 and 60°C	p (bar)	UH004P (4 kDa)	UFx5 pHt (5 kDa)	RC70PP (10 kDa)
4,70	Pure water flux before filtration (kg m^{-2} h^{-1})	1	13,46	40,54	98,75
		2	20,67	64,71	120,83
		3	28,38	90,38	177,08
		4	35,88	115,13	205,29
	Pure water flux after filtration at 45°C (kg m^{-2} h^{-1})	2	17,79	73,38	127,04
		4	30,75	127,00	198,88
	PWFr	2	13,91 %	-13,39 %	-5,14 %
		4	14,29 %	-10,31 %	3,13 %
	Pure water flux after filtration at 60°C (kg m^{-2} h^{-1})	2	19,75	88,58	119,75
		4	33,63	151,88	200,42
	PWFr	2	-11,01 %	-20,73 %	5,74 %
		4	-9,35 %	-19,59 %	-0,78 %

APPENDIX III (3/3) Results of the pure water flux measurements

pH	T = 45 and 60°C	p (bar)	NFG (0.6-0.8 kDa)	GE (1 kDa)	NP010 (1-1.2 kDa)
4,70	Pure water flux before filtration (kg m^{-2} h^{-1})	4	75,75	7,17	76,79
		8	136,25	13,00	139,42
		12	192,17	19,04	192,17
		16	240,75	24,67	232,67
	Pure water flux after filtration at 45°C (kg m^{-2} h^{-1})	8	108,00	12,54	76,21
		16	201,33	23,50	144,00
	PWFr	8	20,73 %	3,53 %	45,34 %
		16	16,37 %	4,73 %	38,11 %
	Pure water flux after additional wash (kg m^{-2} h^{-1})	8	205,50	15,08	167,83
		16	341,08	27,58	251,58
	PWFr	8	-90,28 %	-20,27 %	-120,23 %
		16	-69,41 %	-17,38 %	-74,71 %
	Pure water flux after filtration at 60°C (kg m^{-2} h^{-1})	8	101,29	11,17	46,71
		16	191,04	21,67	93,96
	PWFr	8	50,71 %	25,97 %	72,17 %
		16	43,99 %	21,45 %	62,65 %

APPENDIX IV (1/5) Results of the analysis

	Brix (%), (±0.2)				Total sugars (g kg^{-1})				pH				Conductivity (mS cm^{-1})			
pH 0.88, 32°C	1 bar	2 bar	3 bar	4 bar	1 bar	2 bar	3 bar	4 bar	1 bar	2 bar	3 bar	4 bar	1 bar	2 bar	3 bar	4 bar
Feed	21,8	22,2	22,6	22,9	87,7	-	-	89,9	0,88	0,92	0,88	0,87	43,1	41,7	42,9	43,2
GE (1kDa)	16,0	15,8	15,6	15,3	89,7	-	-	87,6	0,90	0,99	0,92	0,91	42,1	42,3	42,4	42,1
NP010P (1.2kDa)	16,0	15,8	15,5	15,3	90,4	-	-	88,8	0,95	0,92	0,95	0,91	42,7	42,3	42,8	42,9
GR95PP (2kDa)	16,4	16,2	16,1	15,9	89,7	-	-	90,9	0,95	0,91	0,90	0,91	41,3	42,5	42,1	42,4
GK (3.5kDa)	16,4	16,2	16,0	15,9	91,9	-	-	91,4	0,96	0,92	0,92	0,91	41,5	41,2	41,1	42,7
UH004P (4kDa)	16,9	16,3	16,0	15,8	91,1	-	-	90,7	0,91	0,94	0,90	0,91	42,0	42,4	43,2	42,8
UFX5 pHt (5kDa)	15,4	17,8	17,8	17,8	90,9	-	-	93,5	0,94	0,99	0,87	0,91	42,9	42,8	43,3	41,5
RC70PP (10kDa)	17,9	17,9	18,1	18,1	91,1	-	-	93,4	0,94	0,96	0,88	0,90	42,0	43,7	42,5	42,3
Retentate	21,9	22,2	22,6	22,9	88,1	-	-	90,7	0,96	0,93	0,89	0,89	43,5	43,2	43,7	43,8

	DM, freeze dried (w/w%)				DM (g L^{-1})				Lignosulphonates (g L^{-1})				TOC (g L^{-1})			
pH 0.88, 32°C	1 bar	2 bar	3 bar	4 bar	1 bar	2 bar	3 bar	4 bar	1 bar	2 bar	3 bar	4 bar	1 bar	2 bar	3 bar	4 bar
Feed	21,0	20,9	21,3	21,6	221,8	220,2	224,4	229,0	81,6	88,6	77,4	102,2	76,6	63,4	56,6	80,7
GE (1kDa)	17,0	16,6	16,1	16,1	178,7	174,8	167,9	168,6	18,0	16,5	16,4	18,7	48,2	45,7	45,0	47,8
NP010P (1.2kDa)	17,1	17,4	16,9	16,1	177,8	182,1	175,4	168,3	17,5	17,6	15,8	17,2	48,0	46,7	41,4	46,9
GR95PP (2kDa)	17,1	16,7	17,0	16,7	180,9	176,5	178,2	175,9	19,6	17,4	17,4	19,7	50,8	43,8	36,7	51,0
GK (3.5kDa)	17,2	17,5	17,0	16,7	180,3	185,1	181,5	176,5	18,4	17,6	16,0	18,2	51,8	46,3	39,8	46,4
UH004P (4kDa)	17,2	17,1	16,8	16,7	179,2	179,2	176,5	174,5	19,0	18,0	16,8	19,5	52,3	44,8	40,2	50,2
UFX5 pHt (5kDa)	18,3	19,4	19,5	18,8	191,7	203,6	207,1	197,3	29,4	27,2	27,2	29,5	52,2	47,7	47,4	58,1
RC70PP (10kDa)	19,6	18,6	18,9	19,1	206,1	195,3	199,4	202,9	33,6	31,0	35,1	36,3	50,8	52,2	53,1	57,2
Retentate	21,0	21,1	21,5	21,6	222,2	223,3	228,5	227,7	84,1	79,2	99,4	99,7	59,5	56,2	78,5	75,4

	Brix (%), (±0.2)				Total sugars (g kg^{-1})				pH				Conductivity (mS cm^{-1})			
pH 6.33, 32°C	1 bar	2 bar	3 bar	4 bar	1 bar	2 bar	3 bar	4 bar	1 bar	2 bar	3 bar	4 bar	1 bar	2 bar	3 bar	4 bar
Feed	22,0	22,4	22,7	23,1	83,7	-	-	85,1	6,33	6,41	6,39	6,37	11,5	12,0	12,3	12,1
GE (1kDa)	14,0	15,8	15,6	15,4	76,2	-	-	88,8	6,28	6,27	6,27	6,26	11,3	11,7	11,7	11,5
NP010P (1.2kDa)	16,3	16,1	16,0	15,8	86,2	-	-	88,6	6,29	6,27	6,25	6,24	12,1	11,8	11,7	11,1
GR95PP (2kDa)	16,9	16,9	16,8	16,7	85,0	-	-	87,8	6,32	6,28	6,26	6,24	12,4	12,3	11,9	12,3
GK (3.5kDa)	16,3	16,1	15,9	15,8	86,4	-	-	88,6	6,23	6,27	6,28	6,25	11,4	11,8	11,8	11,5
UH004P (4kDa)	17,1	17,0	17,0	17,0	85,2	-	-	87,9	6,30	6,28	6,26	6,23	12,5	12,3	12,5	12,5
UFX5 pHt (5kDa)	18,6	18,5	18,8	18,8	85,1	-	-	88,1	6,35	6,33	6,35	6,30	12,5	12,6	12,8	12,8
RC70PP (10kDa)	18,0	18,0	18,1	18,1	85,7	-	-	86,9	6,33	6,32	6,30	6,28	12,8	12,6	12,8	12,8
Retentate	22,1	22,4	22,8	23,2	82,9	-	-	85,1	6,44	6,44	6,39	6,36	12,1	12,1	12,4	12,4

	DM, freeze dried (w/w%)				DM (g L^{-1})				Lignosulphonates (g L^{-1})				TOC (g L^{-1})			
pH 6.33, 32°C	1 bar	2 bar	3 bar	4 bar	1 bar	2 bar	3 bar	4 bar	1 bar	2 bar	3 bar	4 bar	1 bar	2 bar	3 bar	4 bar
Feed	20,8	21,2	21,3	21,8	221,0	222,5	228,2	230,7	93,9	98,3	97,5	101,7	70,8	76,8	72,0	74,9
GE (1kDa)	15,2	17,5	16,3	16,3	159,1	182,4	169,7	170,2	15,7	16,8	16,0	14,7	41,0	45,7	50,8	48,2
NP010P (1.2kDa)	18,6	17,6	16,6	16,5	195,2	184,8	172,9	173,1	19,2	17,1	16,3	14,5	52,9	51,1	50,8	42,6
GR95PP (2kDa)	18,2	19,3	17,2	17,6	191,8	201,7	180,5	185,2	24,0	22,1	21,8	20,7	46,3	49,2	44,0	56,4
GK (3.5kDa)	17,4	17,8	16,6	17,8	182,0	189,4	172,9	186,8	18,5	16,8	15,7	14,9	52,3	46,0	46,8	51,2
UH004P (4kDa)	17,2	18,2	17,6	17,7	180,6	190,9	184,0	185,8	25,5	23,6	23,4	21,4	51,7	48,1	56,1	52,4
UFX5 pHt (5kDa)	19,0	19,2	18,9	19,0	199,7	202,2	199,2	200,4	40,6	40,6	40,0	38,5	55,0	57,9	60,0	57,9
RC70PP (10kDa)	18,7	18,7	18,7	18,5	202,8	197,1	196,9	196,5	34,1	33,7	33,6	34,3	53,9	52,1	58,5	51,8
Retentate	20,9	21,6	21,4	22,0	221,2	227,4	227,4	235,7	94,2	93,4	99,9	98,7	71,0	61,1	74,7	79,2

APPENDIX IV (3/5) Results of the analysis

	Brix (%), (±0.2)				Total sugars (g kg^{-1})				pH				Conductivity (mS cm^{-1})				DM, freeze dried (w/w%)				DM (g L^{-1})				Lignosulphonates (g L^{-1})				TOC (g L^{-1})			
45°C	1 bar	2 bar	3 bar	4 bar	1 bar	2 bar	3 bar	4 bar	1 bar	2 bar	3 bar	4 bar	1 bar	2 bar	3 bar	4 bar	1 bar	2 bar	3 bar	4 bar	1 bar	2 bar	3 bar	4 bar	1 bar	2 bar	3 bar	4 bar	1 bar	2 bar	3 bar	4 bar
Feed	22,1	22,2	22,2	22,4	85,7	-	-	90,0	4,7	4,7	4,7	4,7	12,5	12,7	12,8	12,9	21,7	21,1	22,3	21,5	231,2	224,7	237,9	229,2	84,8	83,3	84,2	85,9	69,9	67,5	74,4	75,4
UH004P (4 kDa)	17,4	17,1	16,9	16,7	88,2	-	-	87,8	4,7	4,7	4,7	4,7	12,9	12,7	12,6	12,5	18,4	17,5	17,7	17,5	194,8	184,4	186,9	184,3	20,3	18,7	17,3	16,2	49,5	51,5	50,1	38,7
UFx5 pHt (5 kDa)	18,8	18,8	18,7	18,6	87,9	-	-	88,9	4,7	4,7	4,7	4,7	13,1	13,1	13,3	13,3	18,8	18,8	19,0	19,1	199,0	199,1	201,3	202,2	35,7	34,7	34,3	32,9	47,5	47,9	58,2	58,7
RC70PP (10 kDa)	18,7	18,6	18,6	18,3	87,9	-	-	87,6	4,7	4,7	4,7	4,7	13,2	13,2	13,3	13,2	19,9	19,4	19,1	19,3	211,3	204,8	202,3	204,7	36,5	34,8	34,6	32,7	54,1	57,2	50,9	48,2
Retentate	22,1	22,3	22,3	22,4	88,3	-	-	86,2	4,7	4,7	4,7	4,7	12,9	12,8	12,7	13,0	21,0	21,2	21,3	21,4	223,3	225,4	227,4	228,4	84,7	86,7	86,0	87,8	72,2	77,8	71,3	78,2
60°C	1 bar	2 bar	3 bar	4 bar	1 bar	2 bar	3 bar	4 bar	1 bar	2 bar	3 bar	4 bar	1 bar	2 bar	3 bar	4 bar	1 bar	2 bar	3 bar	4 bar	1 bar	2 bar	3 bar	4 bar	1 bar	2 bar	3 bar	4 bar	1 bar	2 bar	3 bar	4 bar
Feed	22,6	22,9	23,1	23,2	87,8	-	-	89,5	4,7	4,7	4,7	4,7	13,0	13,1	13,1	13,2	22,1	22,5	21,7	22,1	235,2	240,1	232,1	236,1	85,9	91,9	92,9	93,7	72,4	70,0	73,2	66,1
UH004P (4 kDa)	17,5	17,3	17,3	17,1	90,9	-	-	92,8	4,7	4,7	4,7	4,7	13,1	12,9	12,8	12,7	18,2	18,1	17,7	17,6	192,7	191,4	187,3	185,4	21,2	18,7	18,9	17,6	46,8	52,2	46,3	44,0
UFx5 pHt (5 kDa)	19,0	19,2	19,2	19,2	90,3	-	-	92,2	4,7	4,7	4,7	4,7	13,4	13,5	13,5	13,7	19,7	20,2	19,1	19,4	208,3	214,9	203,0	206,5	37,2	35,9	35,6	35,3	59,4	57,0	55,1	52,3
RC70PP (10 kDa)	19,0	19,0	19,1	19,0	89,9	-	-	91,4	4,7	4,7	4,7	4,7	13,5	13,5	13,6	13,6	20,5	19,3	19,3	19,4	216,5	205,1	205,1	206,1	35,8	35,9	38,1	35,9	49,7	50,0	48,5	52,3
Retentate	22,6	23,0	23,3	23,4	87,7	-	-	90,7	4,7	4,7	4,7	4,7	13,0	13,1	13,2	13,3	21,5	21,8	22,2	22,7	229,6	233,0	236,8	242,8	89,7	93,3	95,1	95,8	72,4	59,9	70,4	74,6

APPENDIX IV (4/5) Results of the analysis

	Brix (%), (±0.2)				Total sugars (g kg^{-1})				pH				Conductivity (mS cm^{-1})				DM, freeze dried (w/w%)				DM (g L^{-1})				Lignosulphonates (g L^{-1})				TOC (g L^{-1})			
45°C	4 bar	8 bar	12 bar	16 bar	4 bar	8 bar	12 bar	16 bar	4 bar	8 bar	12 bar	16 bar	4 bar	8 bar	12 bar	16 bar	4 bar	8 bar	12 bar	16 bar	4 bar	8 bar	12 bar	16 bar	4 bar	8 bar	12 bar	16 bar	4 bar	8 bar	12 bar	16 bar
Feed	22,8	23,4	23,5	23,7	87,4	-	-	90,8	4,7	4,6	4,6	4,7	12,7	13,0	13,0	13,2	23,1	22,8	22,6	23,9	247,1	243,4	243,0	256,5	93,8	92,2	95,3	99,9	66,2	73,8	72,7	67,2
NFG (0.6-0.8 kDa)	15,8	14,7	13,4	12,5	91,9	-	-	80,5	4,8	4,8	4,8	4,8	12,2	11,1	10,6	10,1	16,8	15,8	14,5	13,5	176,8	165,8	151,0	140,9	14,2	11,3	9,6	8,9	44,6	40,6	36,7	33,4
GE (1 kDa)	15,7	15,1	14,1	13,2	88,4	-	-	82,4	4,8	4,7	4,8	4,8	12,0	11,4	10,7	10,2	16,5	16,4	14,4	14,2	173,1	172,1	150,5	148,3	16,2	13,0	10,0	10,7	44,8	43,6	32,2	36,8
NP010 (1-1.2 kDa)	16,4	15,7	15,0	14,5	91,3	-	-	87,8	4,7	4,8	4,7	4,7	12,3	11,7	11,0	10,6	17,5	16,7	15,8	15,7	184,7	175,4	165,3	164,9	16,1	13,5	12,5	11,3	46,0	46,5	45,2	43,6
Retentate	22,9	23,3	23,6	23,8	88,4	-	-	90,6	4,7	4,6	4,7	4,7	13,0	13,0	13,2	13,2	21,8	22,6	23,4	22,7	232,6	243,0	251,2	243,4	95,0	95,7	98,0	100,8	65,8	69,9	75,7	77,1
60°C	4 bar	8 bar	12 bar	16 bar	4 bar	8 bar	12 bar	16 bar	4 bar	8 bar	12 bar	16 bar	4 bar	8 bar	12 bar	16 bar	4 bar	8 bar	12 bar	16 bar	4 bar	8 bar	12 bar	16 bar	4 bar	8 bar	12 bar	16 bar	4 bar	8 bar	12 bar	16 bar
Feed	24,3	25,2	25,9	26,8	92,4	-	-	99,4	4,6	4,6	4,6	4,6	13,5	13,7	13,7	13,9	23,0	24,6	26,1	27,7	248,2	265,2	282,1	300,5	100,9	109,9	105,6	120,5	74,7	76,3	84,9	84,1
NFG (0.6-0.8 kDa)	17,4	16,8	16,3	15,9	96,9	-	-	99,3	4,7	4,7	4,7	4,7	13,0	12,4	11,9	11,6	18,7	18,7	16,9	16,9	198,5	198,1	177,8	178,9	19,0	15,9	15,0	13,6	55,3	42,8	50,1	45,9
GE (1 kDa)	17,5	16,7	16,1	15,7	98,4	-	-	97,6	4,7	4,7	4,7	4,7	13,0	12,2	11,8	11,4	18,5	18,3	17,3	16,5	196,7	192,9	182,1	173,3	21,1	15,7	14,8	12,9	48,6	37,1	46,1	43,3
NP010 (1-1.2 kDa)	17,6	17,1	16,8	16,6	96,5	-	-	100,7	4,7	4,7	4,7	4,7	13,1	12,5	12,0	11,6	18,8	18,8	17,0	16,6	199,1	199,3	179,7	175,5	19,7	15,9	14,5	14,1	49,6	49,0	50,9	46,7
Retentate	24,5	25,6	26,1	26,9	92,9	-	-	100,1	4,6	4,7	4,6	4,6	13,5	13,8	13,7	14,0	24,6	26,0	26,8	27,7	264,6	280,6	290,4	301,1	104,4	110,8	118,3	121,3	77,1	68,7	84,5	90,5

APPENDIX IV (5/5) Results of the analysis

	DSS concentration			DDF 1			DDF 2		
NP010, 60°C, pH 4.59, 16bar	Start Retentate	End Retentate	End Permeate Cumulative	Start Retentate	End Retentate	End Permeate Cumulative	Start Retentate	End Retentate	End Permeate Cumulative
pH	4.59	4.41	4.56	4.48	4.30	4.53	4.35	4.19	4.57
Conductivity (mS cm^{-1})	12.7	13.2	11.2	11.8	14.0	8.7	9.9	13.0	5.5
Brix (%)	22.9	42.1	16.7	20.1	37.5	9.9	17.0	30.5	5.2
TOC (g L^{-1})	53.6	86.6	37.6	49.1	119.8	20.6	43.9	97.8	11.8
DM (w/w%)	22.6	44.9	18.3	17.9	16.6	11.1	13.7	8.7	5.6
DM (g L^{-1})	240.8	505.3	193.9	188.8	341.2	113.8	141.4	254.6	56.8
Total sugars (St1 Oy, g kg^{-1})[1]	86.9	108.5	100.3	49.9	58.4	53.6	26.4	28.2	25.8
Other (St1 Oy, g kg^{-1})[2]	14.4	9.5	12.2	4.3	5.8	5.4	2.6	3.8	2.2
Lignosulphonates (g L^{-1})	98.0	257.6	14.9	120.6	307.1	10.0	133.2	286.0	7.0
Density (g L^{-1})	1067.42	1126.51	1057.51	1052.43	1097.97	1028.63	1034.66	1072.42	1009.24

[1]Total sugars = Glucose, Xylose, Galactose (approx.), Arabinose, Mannose

[2]Other i.e., glycerol, acetic acid, levulinic acid, ethanol and hydroxymethylfurfural

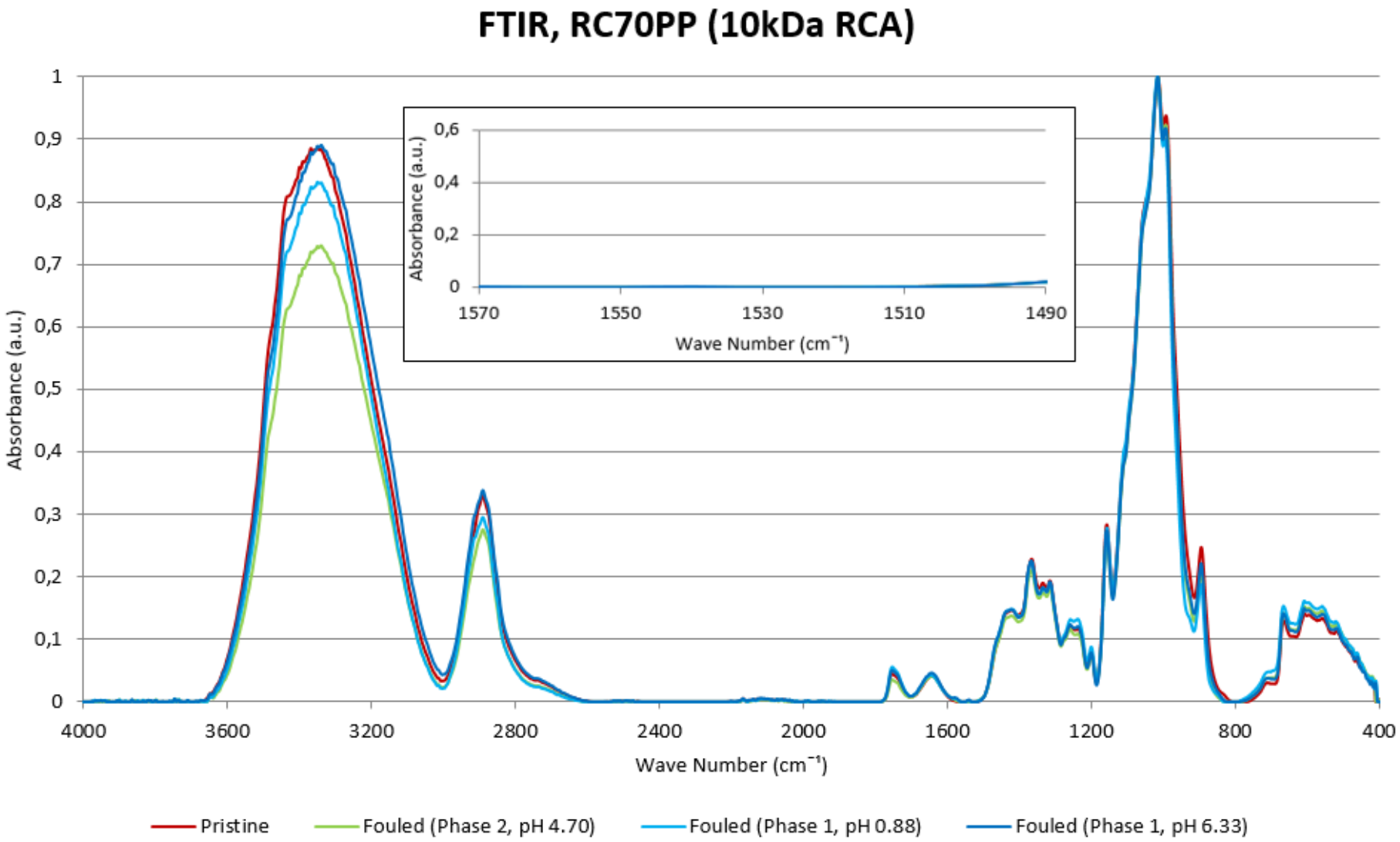
FTIR, RC70PP (10kDa RCA)
Absorbance (a.u.)
Wave Number (cm⁻¹)
1
0,9
0,8
0,7
0,6
0,5
0,4
0,3
0,2
0,1
0
4000
3600
3200
2800
2400
2000
1600
1200
800
400
0,6
0,4
0,2
0
1570
1550
1530
1510
1490
Pristine
Fouled (Phase 2, pH 4.70)
Fouled (Phase 1, pH 0.88)
Fouled (Phase 1, pH 6.33)

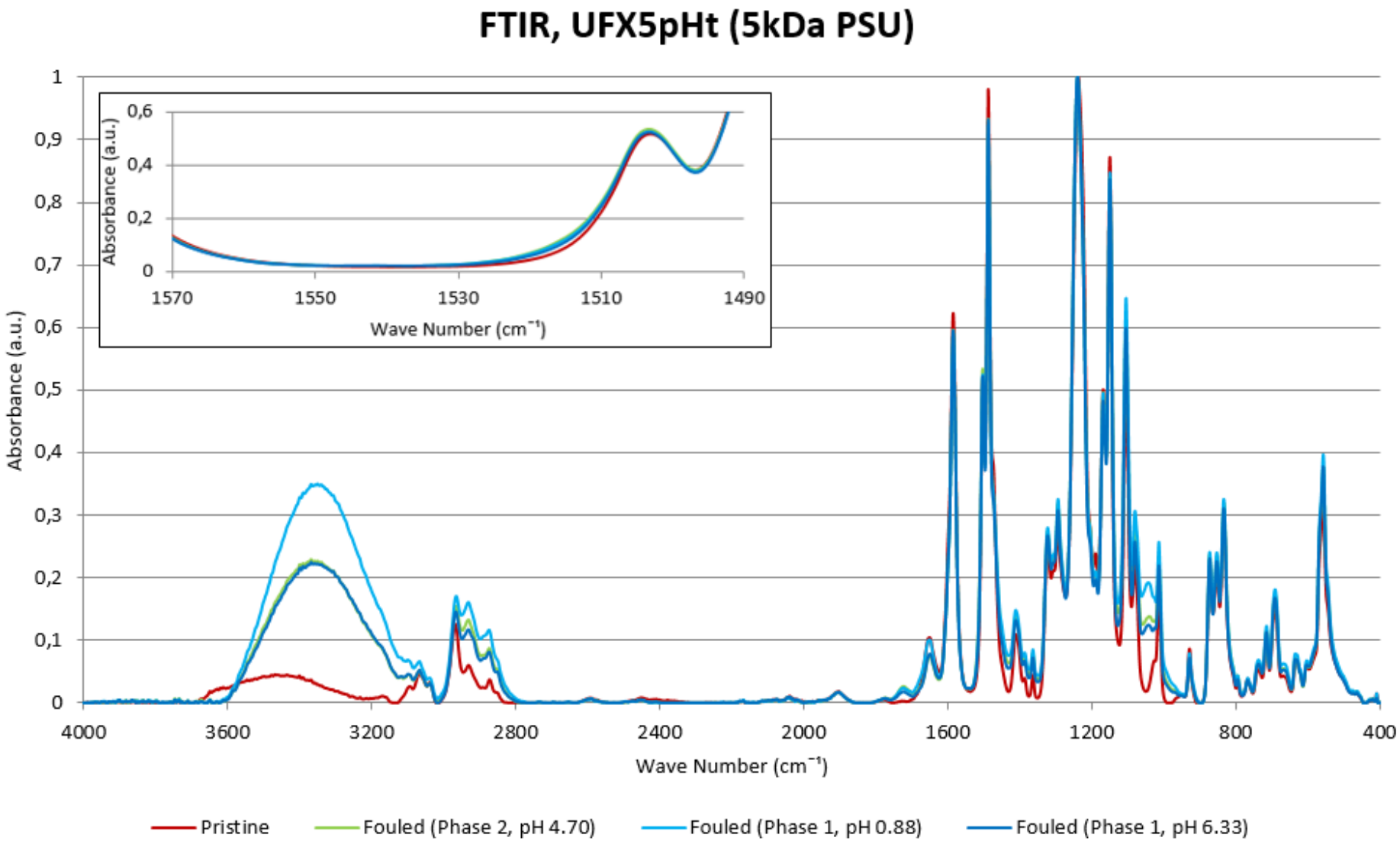
FTIR, UFX5pHt (5kDa PSU)
Absorbance (a.u.)
Wave Number (cm⁻¹)
4000
3600
3200
2800
2400
2000
1600
1200
800
400
0
0,1
0,2
0,3
0,4
0,5
0,6
0,7
0,8
0,9
1
Absorbance (a.u.)
Wave Number (cm⁻¹)
1570
1550
1530
1510
1490
0
0,2
0,4
0,6
Pristine
Fouled (Phase 2, pH 4.70)
Fouled (Phase 1, pH 0.88)
Fouled (Phase 1, pH 6.33)

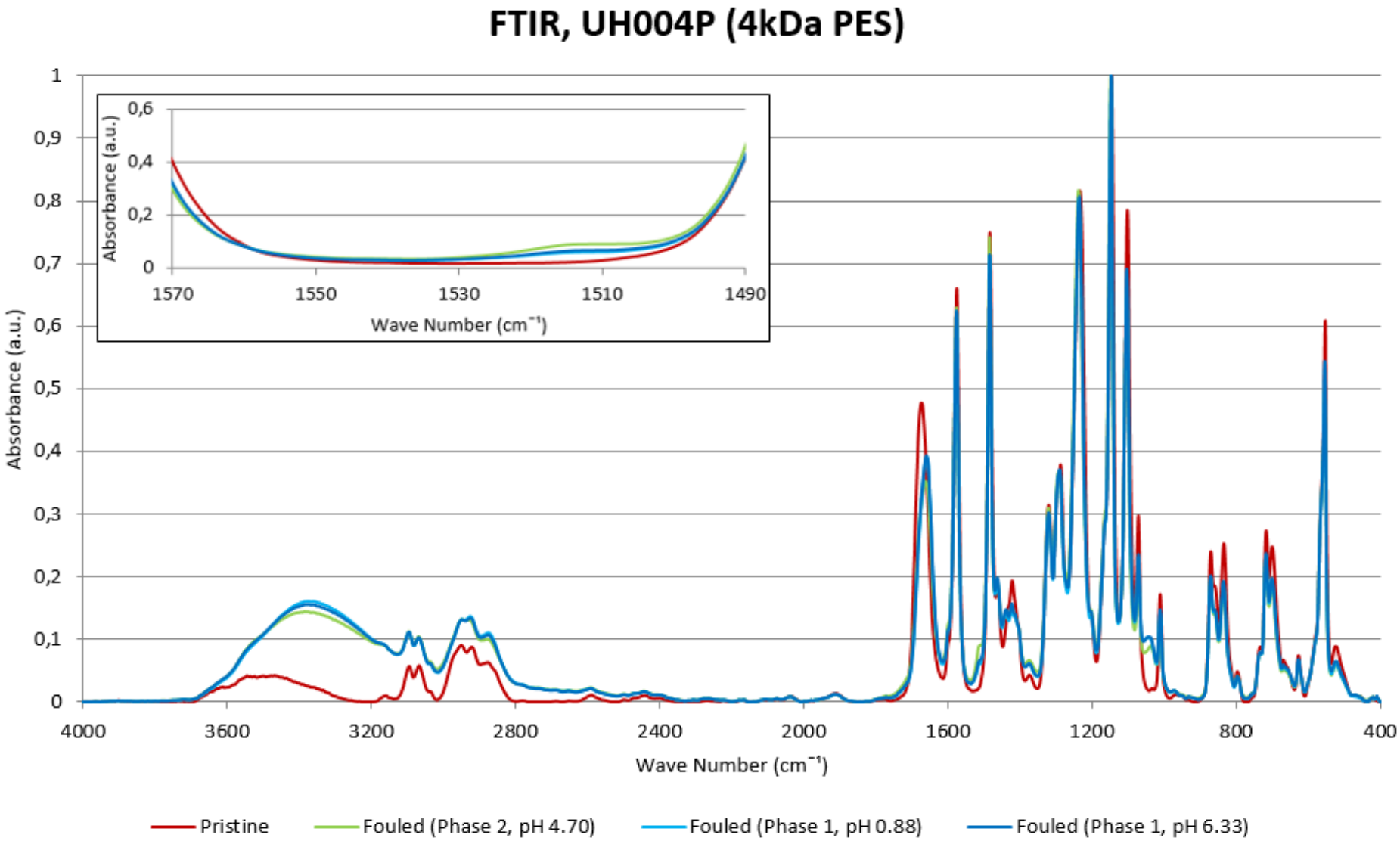
FTIR, UH004P (4kDa PES)
Absorbance (a.u.)
Wave Number (cm⁻¹)
1
0,9
0,8
0,7
0,6
0,5
0,4
0,3
0,2
0,1
0
4000
3600
3200
2800
2400
2000
1600
1200
800
400
0,6
0,4
0,2
0
1570
1550
1530
1510
1490
Pristine
Fouled (Phase 2, pH 4.70)
Fouled (Phase 1, pH 0.88)
Fouled (Phase 1, pH 6.33)

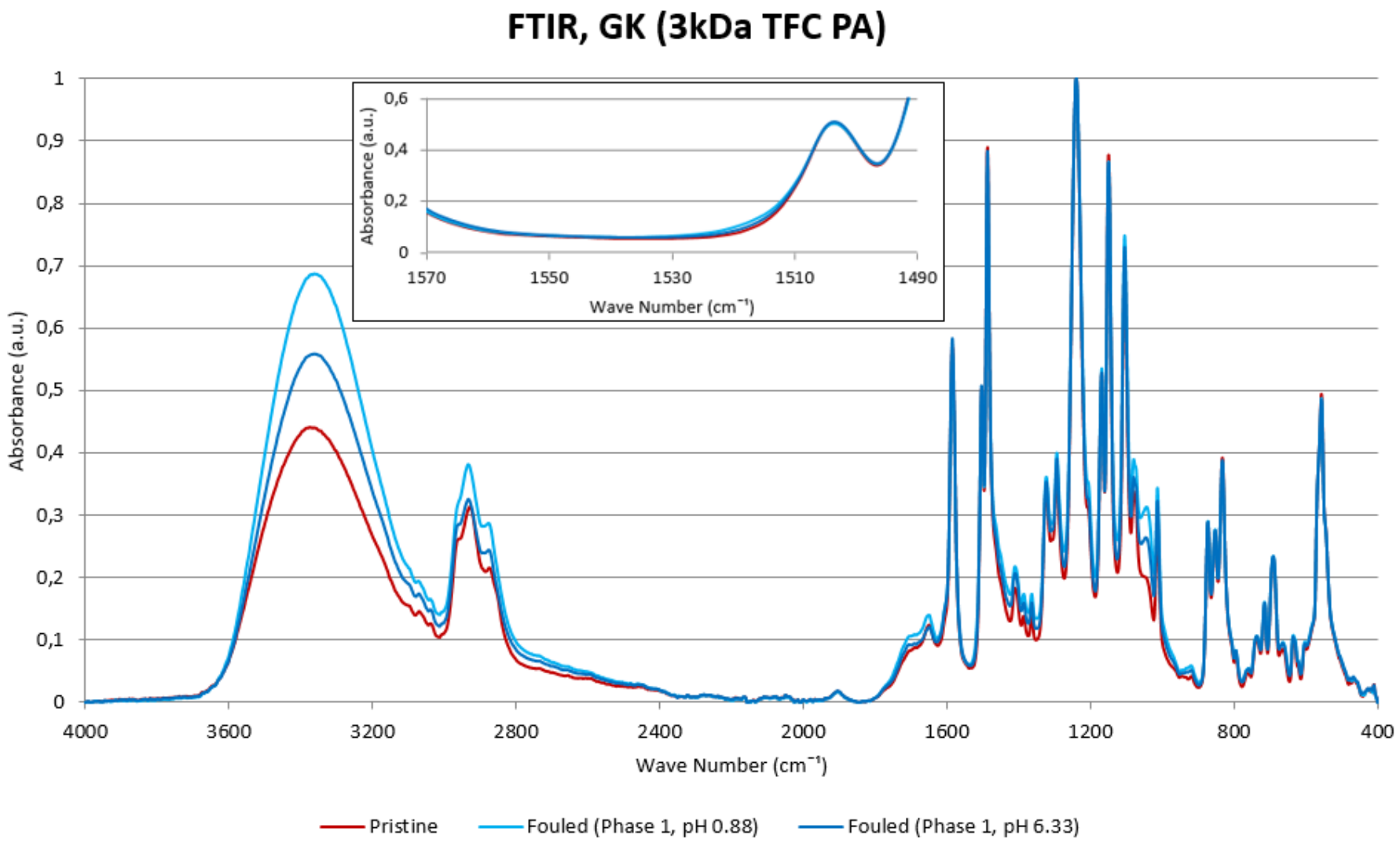
FTIR, GK (3kDa TFC PA)
Absorbance (a.u.)
Wave Number (cm⁻¹)
1
0,9
0,8
0,7
0,6
0,5
0,4
0,3
0,2
0,1
0
4000
3600
3200
2800
2400
2000
1600
1200
800
400
0,6
0,4
0,2
0
1570
1550
1530
1510
1490
Pristine
Fouled (Phase 1, pH 0.88)
Fouled (Phase 1, pH 6.33)

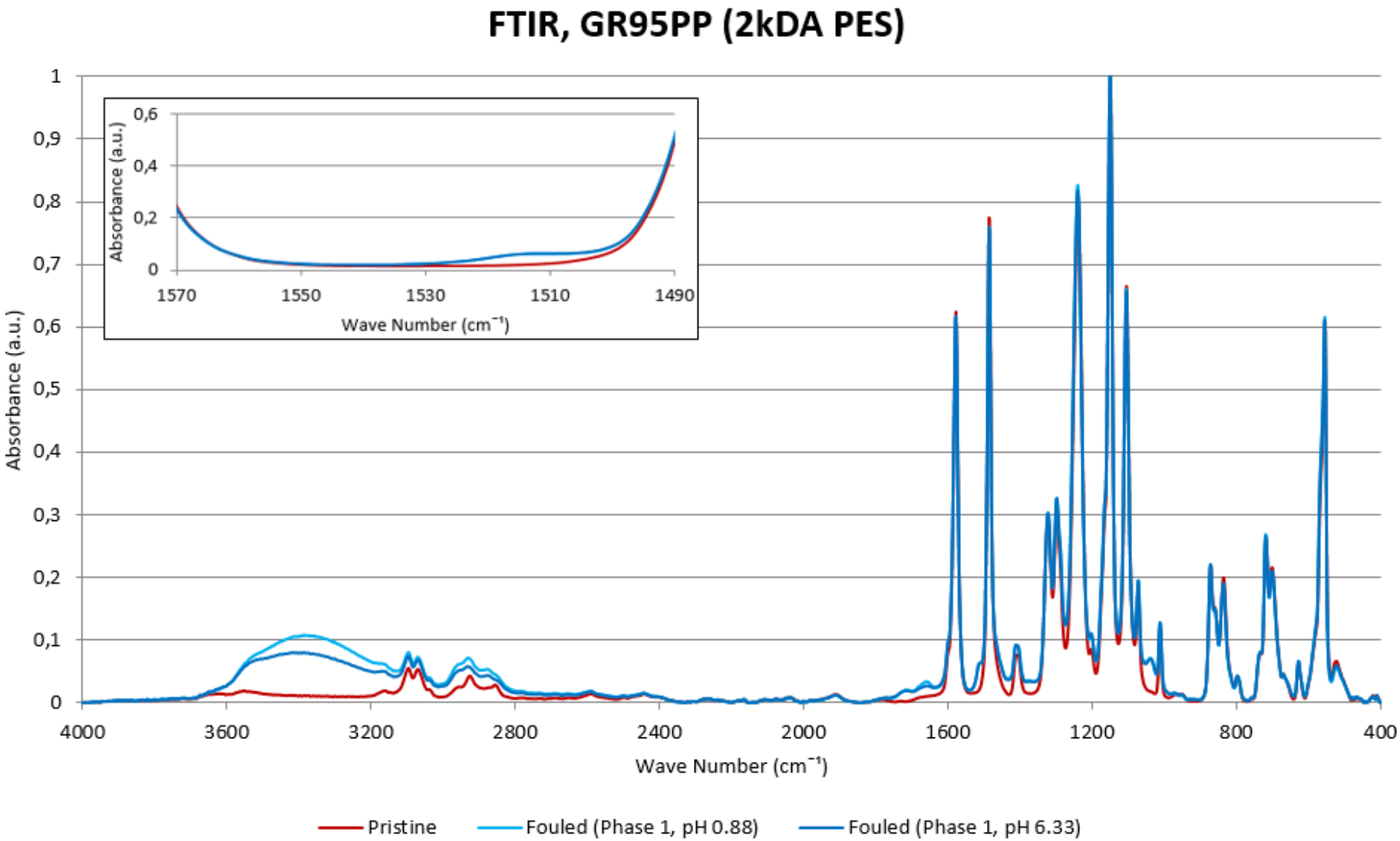
FTIR, GR95PP (2kDA PES)
Absorbance (a.u.)
Wave Number (cm⁻¹)
Absorbance (a.u.)
Wave Number (cm⁻¹)
Pristine
Fouled (Phase 1, pH 0.88)
Fouled (Phase 1, pH 6.33)

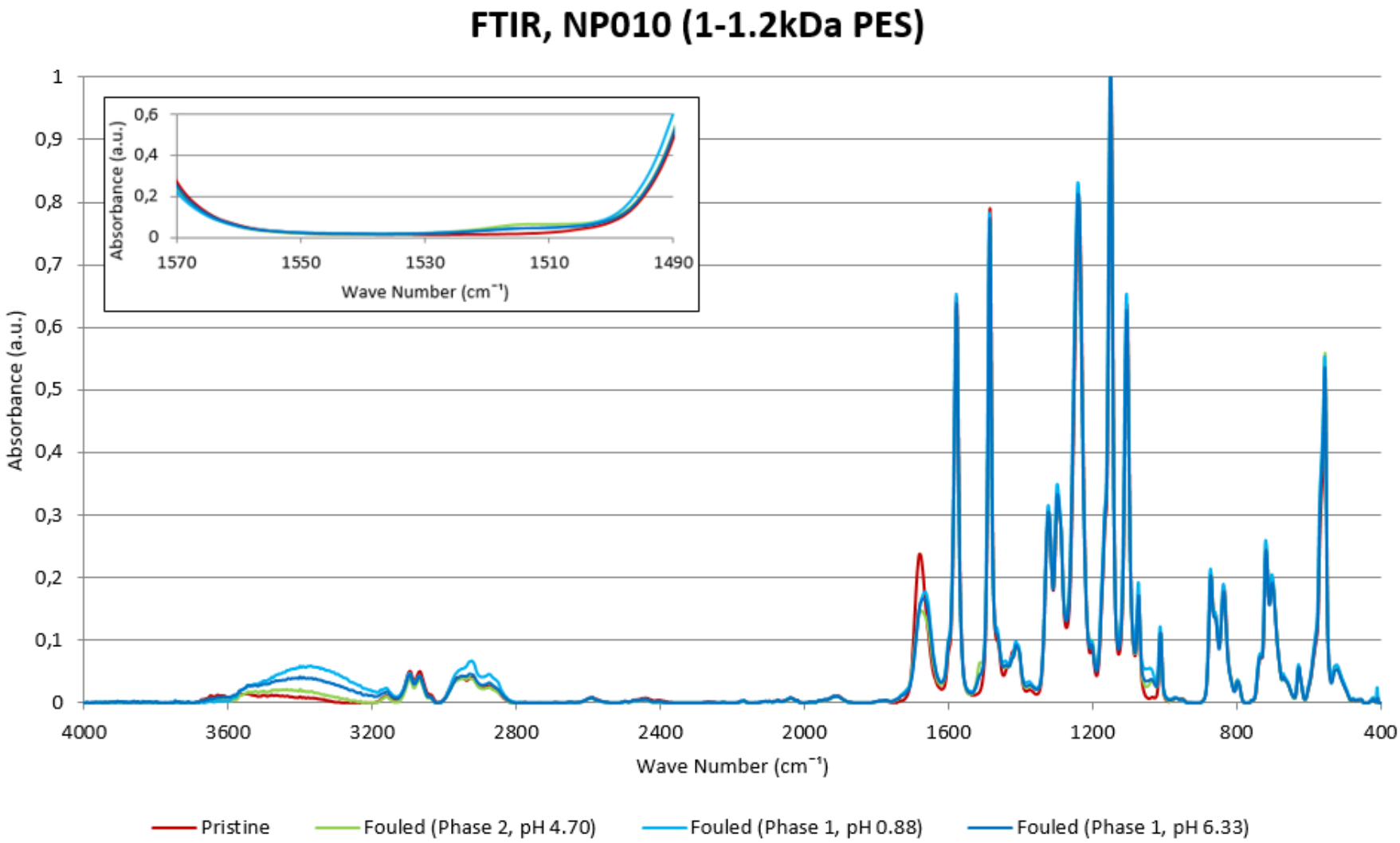
FTIR, NP010 (1-1.2kDa PES)
Absorbance (a.u.)
Wave Number (cm⁻¹)
Pristine
Fouled (Phase 2, pH 4.70)
Fouled (Phase 1, pH 0.88)
Fouled (Phase 1, pH 6.33)

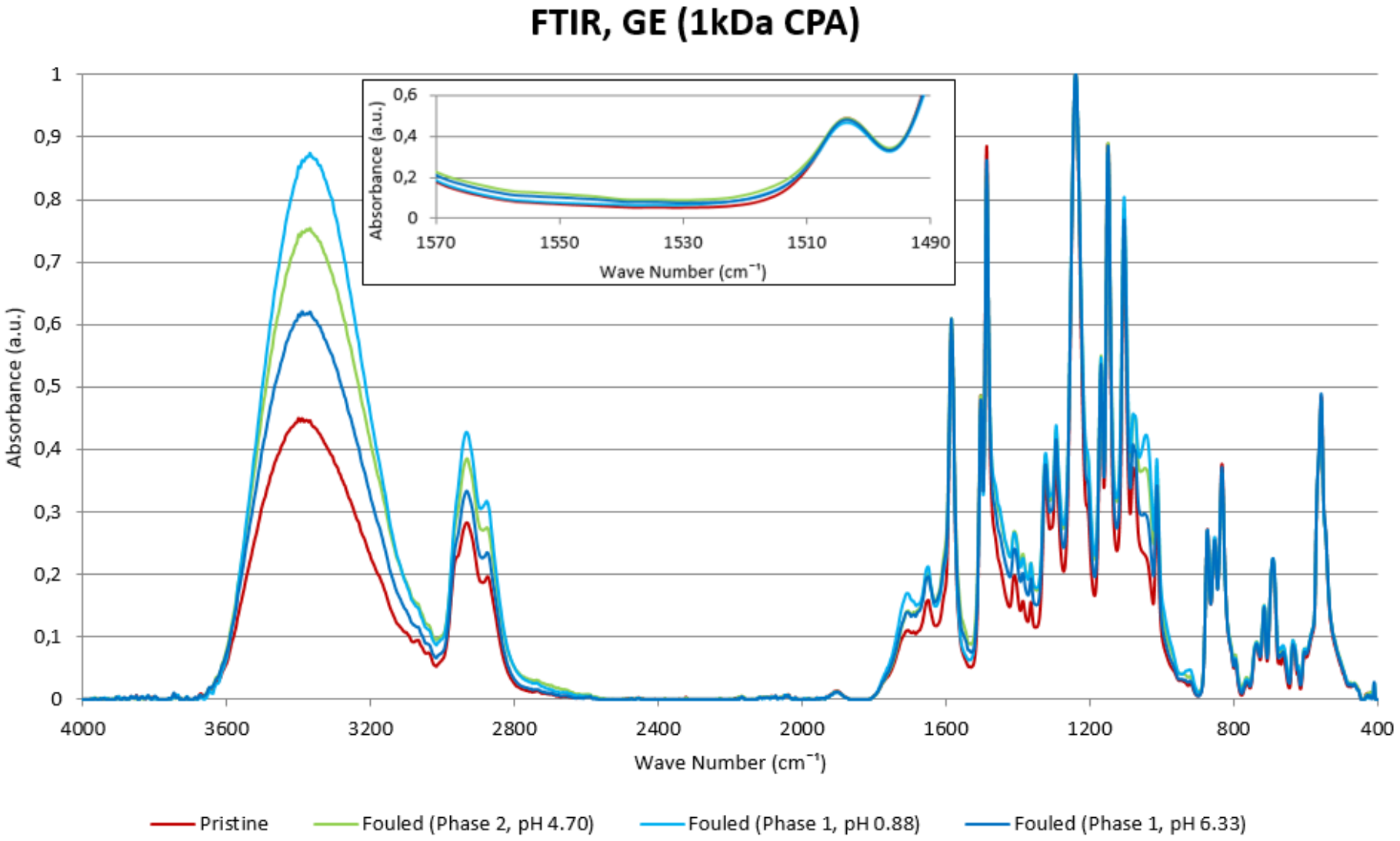
FTIR, GE (1kDa CPA)
Absorbance (a.u.)
Wave Number (cm⁻¹)
1
0,9
0,8
0,7
0,6
0,5
0,4
0,3
0,2
0,1
0
4000
3600
3200
2800
2400
2000
1600
1200
800
400
0,6
0,4
0,2
0
1570
1550
1530
1510
1490
Pristine
Fouled (Phase 2, pH 4.70)
Fouled (Phase 1, pH 0.88)
Fouled (Phase 1, pH 6.33)

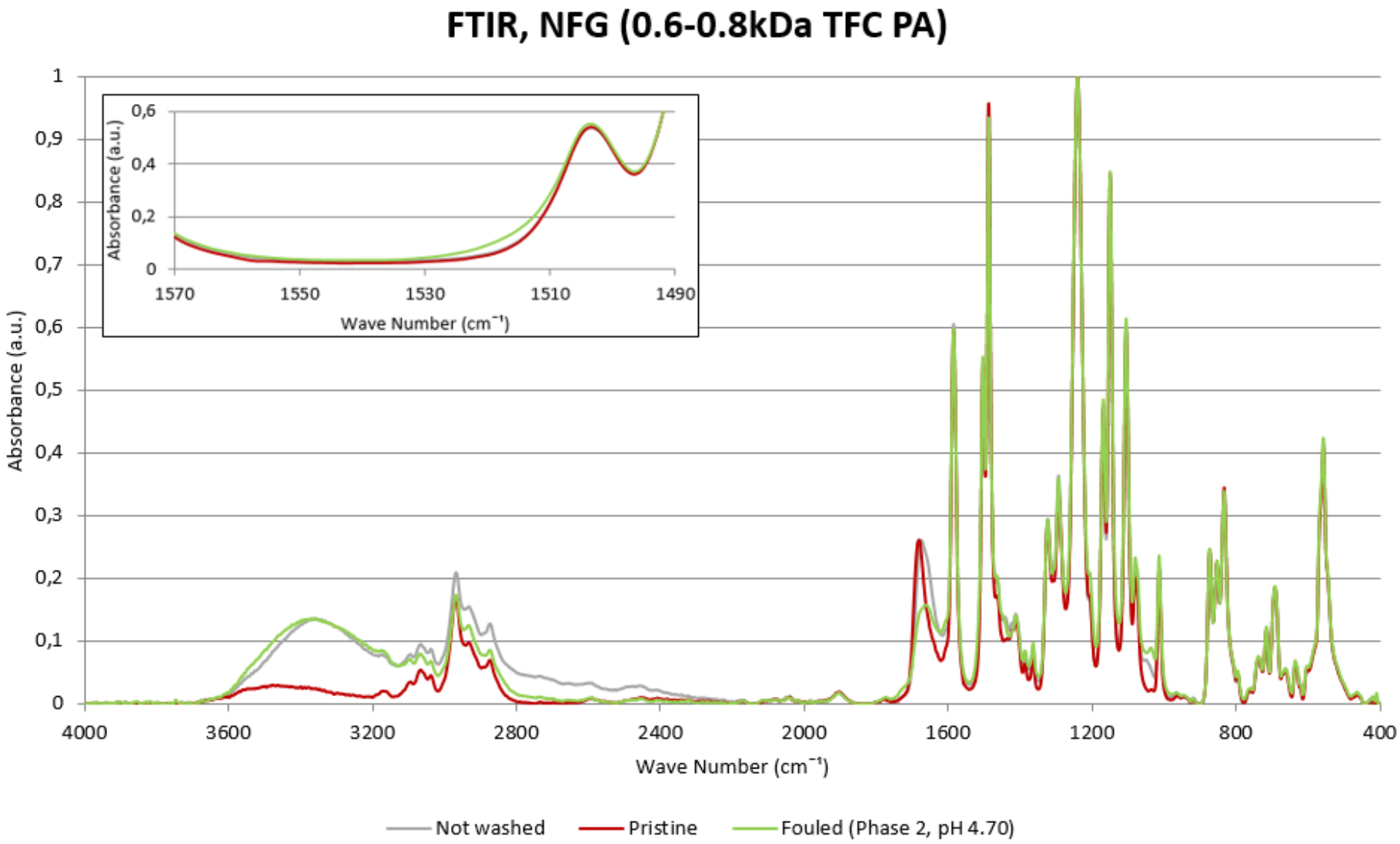
FTIR, NFG (0.6-0.8kDa TFC PA)
Absorbance (a.u.)
Wave Number (cm⁻¹)
4000
3600
3200
2800
2400
2000
1600
1200
800
400
0
0,1
0,2
0,3
0,4
0,5
0,6
0,7
0,8
0,9
1
Absorbance (a.u.)
Wave Number (cm⁻¹)
1570
1550
1530
1510
1490
0
0,2
0,4
0,6
Not washed
Pristine
Fouled (Phase 2, pH 4.70)